The Effect of Interferon-Lambda 3 on Human T-Cell Polarization and Activation

By

Xinyun Liu

A thesis submitted to the Faculty of Graduate Studies of the University of Manitoba

in Partial Fulfilment of the Requirements of the Degree of

MASTER OF SCIENCE

Department of Immunology

Max Rady College of Medicine

Rady Faculty of Health Sciences

University of Manitoba

Winnipeg, Manitoba, Canada

ABSTRACT

Type III interferons (IFNs) are one of the core IFNs that directly inhibit viral replication, and their function specifically acts on mucosal epithelial cells and certain immune cells. We recently showed that additional human, but not mouse, immune cell types express *IFNLR1* mRNA (including T cells) and respond to IFN-λ3 stimulation. T cells are critical members of our adaptive immune system, where CD4+ T cells promote the effector functions of other immune cells, and CD8+ T cells directly kill altered cells. CD4+ T cells can differentiate into distinct T helper (Th) subtypes. We previously showed IFN-λ3 inhibited Th2 cytokine induction in influenza vaccine-stimulated peripheral blood mononuclear cells (PBMCs), but the inhibitory mechanisms were unknown. Since Th2 cytokines are associated with allergic diseases and inflammation, such as Th2-endotype allergic asthma, a better understanding of the interplay between type III IFNs and T cell polarization could aid in the development of future therapies. Little is known about the levels of IFN-λR1 on CD8+ T cells and how CD8+ T cells respond to IFN-λs with or without the presence of T cell receptor (TCR) stimulation.

To reveal the distribution of IFN-λR1 on T cells, we screened several antibodies and identified a candidate that can specifically and efficiently bind IFN-λR1. Using the newly identified antibody, we detected unique IFN-λR component IFN-λR1 at protein levels on total human CD4+ T cells and CD8+ T cells as well as different subsets. The percentage of CD8+ T cells expressing IFN-λR1 on the surface (about 10%) was higher than CD4+ T cells (about 2%) at the steady state ($p < 0.05$). The other component of IFN-λR, IL-10RB, was expressed on almost 100% of CD4+ and CD8+ T cells.

In the context of TCR stimulation, IFN-λR1 levels on human T cells were significantly increased over 1-3 days within whole PBMC as well as purified CD4+ and CD8+ T cell cultures *in vitro*. Through testing multiple TCR signalling inhibitors, we identified multiple signalling intermediates that likely contribute to IFN-λR1 upregulation on T cells after TCR stimulation.

Lastly, we demonstrated that IFN-λ3 downregulated IL-13 production in whole PBMCs during TCR stimulation and also during longer-term naïve CD4+ T cell Th2 polarization. For CD8+ T cells, using RNA sequencing transcriptome analyses, we showed that without TCR stimulation, IFN-λ3 inhibited protein synthesis and activated antiviral genes. When comparing

transcriptome changes after TCR stimulation, with or without IFN-λ3, we found multiple pathways altered upon IFN-λ3 addition with some overlap to when IFN-λ3 was added alone to CD8+ T cells.

Overall, this body of work has demonstrated that human T cells can directly respond to IFN-λ3, although the subset of T cell and activation state dramatically alter the magnitude of IFN-λ responsiveness due to the different surface levels of IFN-λR1. This means that although some T cells (e.g. naïve CD4+ T cells) are poor responders at rest, IFN-λ can directly influence Th2 and CD8+ T cell responses during an infection or periods of chronic inflammation that we wouldn't have expected if we only studied T cells at steady state. Through the greater understanding of IFN-λ immunoregulatory pathways, IFN-λ3 could be an ideal future immunotherapy going beyond just promoting antiviral pathways and instead targeting specific immune cell types, including T cells, with fewer side effects compared to other IFNs.

ACKNOWLEDGEMENTS

To begin with, I would like to express my sincere gratitude to my supervisor, Dr. Deanna M. Santer, for her constant and influential support, guidance, encouragement, and patience throughout the course of this research and thesis writing. It was my great pleasure to be a Santer lab member, and I will always appreciate the experience I had. Dr. Santer's profound knowledge of immunology, dedication to research, and enthusiasm for resolving questions have been invaluable inspirations to me. I was also trained to be more detail-oriented, as well as make plans to track and ensure progress is made on time; those are the required virtues of being an independent scientist, and I learned those from Dr. Santer. Thank you for being an awesome mentor and teacher, allowing me to progress in both research and career development.

I extend my heartfelt gratitude to my advisory committee members, Dr. Thomas T. Murooka and Dr. Neeloffer Mookherjee, for their constructive feedback and insightful comments and suggestions, which have helped shape this research project into where it is. Dr. Murooka opened the door of Immunology for me a few years ago; his guidance and support fostered my interest in research and made me want to proceed with graduate studies. Dr. Mookherjee also supported me a lot along the way; Dr. Hemshekhar Mahadevappa from the Mookherjee lab provided vital support to aid my project in going further. All my committee members provided a generous amount of support, helping me proceed to my next stage of graduate studies and my PhD application.

I would also like to thank Dr. Heather Armstrong and Dr. Santer; together, they provided us with a collaborative sister lab environment and guidance for our career success. I would also like to thank Dr. Cedric Tremblay for his support and humour, which made my experiments shorter and easier.

It was my great pleasure to be a Santer lab member and grow together with everyone here. Olamide Ogungbola, as the "co-founder" of the lab, thank you, Lami, for providing me with numberless help and support. Without you, my project would stop at stage one as I need you as a phlebotomist to get blood and as a friend for life, LOL. You also helped me recruit donors with no spare effort. I will always appreciate that, as well as so many other things. Ouyang Jing (Maggie), I appreciate your support; your strong scientific background and experience inspired me so many times. Testimony Olumade, I really enjoyed the interactions with you, and it is certainly impossible

to finish my project without your help; you contributed to all the figures I have for RNA sequencing. Thank you, Vi Diep Vu, for your help in maintaining a well-prepared lab space. Also, to all current and previous lab members, including summer students, it was my great pleasure to have gotten to know each of you and become friends with you all.

I would like to extend my gratitude to all the Armstrong lab members, including Richard Miller, who also helped to be a phlebotomist, and Hana Olof, who cared for and donated blood for my project so many times. I would also like to thank all the Murooka lab current and past members: Marina Costa Fujishima, Paul Lopez, Seun Ajibola, and Morgan Taverner. Thank you all for being extremely supportive. We witnessed growth and lots of shining moments in each other's lives.

I want to acknowledge all the faculty, staff, technicians, and students who made up this prosperous department; you all made my last three years and two summers invaluable. It was my great pleasure serving the graduate students in the department as a member of the student representatives for two years; thank other representatives Fola Olayinka-Adefemi, Seun Ajibola, Courtney Marshall, Padmanie Ramotar, and Heqing Ma; together we had lots of great memories. Thank you, Angela Peloquin and Silvia Panameno; I cannot thank you enough for your support along the way. Dr. Christine Zhang, thank you for your efforts in maintaining the vital equipment and your helpful guidance!

To my family members: Wen Liu, Quanfeng Zheng, Xinrui Zheng, and Jashua Adams; my partner, Xinhao Tang; our dogs Rourou, Peppie, Charlie, and Lucas; and our cats Pickles and Achu. I could not have reached this stage without all of you standing by my side. To my dear friends: Yi Cui, Yuwei Zhang, Shuo Feng, Bo Wang, Wenyu Chen, Jingmei Pei, Carrie, Trent, and Stefan.

I thank the funding agencies that supported my research: Rady Faculty of Health Sciences Graduate Studentship, Research Manitoba, Natural Sciences and Engineering Research Council of Canada (NSERC), and the University of Manitoba. As the department's vampire, I thank all the blood donors; every single piece of data generated relied on your contributions!

DEDICATIONS

This dissertation is dedicated to my parents, my spouse, my sister, her spouse, and all of our pets. You all supported my studies and have been my motivation, driving me further. I am grateful for your encouragement, and I love you all.

I present this work in memory, enthusiasm, and dedication to my family and my cherished friend.

TABLE OF CONTENT

LIST OF FIGURES

LIST OF TABLES

LIST OF ABBREVIATIONS

APCs	Antigen-presenting cells
BALF	Bronchoalveolar lavage fluid
BATF	Basic Leucine Zipper ATF-Like Transcription Factor
BCR	B cell receptor
BSA	Bovine serum albumin
CCR7	Chemokine receptor 7
CD	Crohn's disease
CD11c	Cluster Differentiation eleven c
CD123	Cluster Differentiation one hundred and twenty-three
CD28	Cluster Differentiation twenty-eight
CD3	Cluster Differentiation three
CD4	Cluster Differentiation four
CD45	Cluster Differentiation forty-five
CD45RA	Cluster Differentiation forty-five RA
CD45RO	Cluster Differentiation forty-five RO
CD56	Cluster Differentiation fifty-six
CD62L	Cluster Differentiation sixty-two Ligand
CD69	Cluster Differentiation sixty-nine
CD71	Cluster Differentiation seventy-one
cDNA	Complementary DNA
CFSE	Carboxyfluorescein succinimidyl ester
CM	Central memory
CRAC	Calcium release-activated calcium
CTLA-4	Cytotoxic T-lymphocyte-associated protein 4
CXCR5	Chemokine, CXC Motif, Receptor 5
DAG	Diacylglycerol
DAMPs	Damage-associated molecular patterns
DAPI	4′,6-diamidino-2-phenylindole
DCs	Dendritic cells
DNA	Deoxyribonucleic Acid

EDTA	Ethylenediaminetetraacetic acid
ELISA	Enzyme-linked immunosorbent assay
EM	Effector memory
ERK	Extracellular signal-regulated kinase
FBS	Fetal bovine serum
FDR	False discovery rate
FMO	Fluorescence-minus one
FSC	Forward scatter
GATA-3	GATA Binding Protein 3
GSEA	Gene Set Enrichment Analysis
HBV	Hepatitis B virus
HD	Healthy donor
HEPES	4-(2-hydroxyethyl)-1-piperazineethanesulfonic acid
HIV	Human Immunodeficiency Virus
HLA	Human leukocyte antigen
HRP	Horseradish peroxidase
IBD	Inflammatory bowel disease
ICOS	Inducible costimulator
IFI44	IFI44 interferon induced protein 44
IFIT1	Interferon-induced protein with tetratricopeptide repeats 1
IFN	Interferon
IFN-γ	Interferon-gamma
IFN-λ	Interferon-lambda
IFN-λR1	IFN-lambda receptor 1 (protein)
IFNLR1	IFN-lambda receptor subunit 1 (mRNA)
Ig	Immunoglobulin
IKK	Inhibitor of nuclear factor-κB (IκB) kinase
IL	Interleukin
IL-10RB	IL-10 receptor β subunit
IL-12p40	Interleukin twelve p40 subunit
IL-13	Interleukin thirteen

IL-1β	Interleukin-one β
IL-4	Interleukin four
ILC2	Type 2 innate lymphoid cells
IP3	Inositol triphosphate
IRFs	Interferon regulatory factors
ISGs	Interferon-stimulated genes
ISRE	Interferon-stimulated response element
ITAMs	Immunoreceptor tyrosine-based activation motifs
ITK	IL-2-inducible T-cell kinase
JAK	Janus kinase
JNK	c-Jun N-terminal kinase
LAT	Linker for activation of T cells
Lck	Lymphocyte-specific protein tyrosine kinase
LFA-1	Leukocyte function-associated antigen 1
MAPK	Mitogen-activated protein kinase
MFI	Median fluorescent intensity
MHC I	Major Histocompatibility Complex I
MHC II	Major Histocompatibility Complex II
MKKs	Mitogen-activated protein kinase kinases
mL	Millilitre
mM	Millimolar
mRNA	Messenger Ribonucleic Acid
mTORC	mammalian target of rapamycin complex
NA	Not applicable
NFAT	Nuclear factor of activated T cells
NF-κB	Nuclear factor kappa-light-chain-enhancer of activated B cells
ng	Nanogram
NK	Natural Killer
^{o}C	Celcius
PAMPs	Pathogen-associated molecular patterns
PBMCs	Human peripheral blood mononuclear cells

PBS	Phosphate Buffered Saline
PCR	Polymerase Chain Reaction
PD-L1	Programmed death-ligand 1
pDCs	Plasmacytoid DCs
PDK1	phosphoinositide-dependent kinase 1
PFA	Paraformaldehyde
PHA-L	Phytohaemagglutinin-L
PI3K	Phosphoinositide-3 kinase
PIP3	Phosphatidylinositol (3,4,5)-trisphosphate
PKB	Protein kinase B
PLCγ	Phospholipase C gamma
PRRs	Pattern recognition receptors
PTK	Protein tyrosine kinases
PTP	Protein tyrosine phosphatase
RORγt	Retineic-acid receptor-related orphan nuclear receptor gamma
RPMI 1640	Roswell Park Memorial Institute 1640 media
RT	Reverse Transcriptase
SSC	Side scatter
STAT	Signal transducer and activator of transcription
T reg	Regulatory T Cells
T-bet	T-box expressed in T cells
T_{CM}	Central memory T cell
TCR	T cell receptor
T_{EM}	Effector memory T cell
T_{EMRA}	Terminally differentiated effector memory cells re-expressing CD45RA
TGF-β	Transforming growth factor beta
Th	T helper cell
Th1	T Helper one
Th17	T Helper seventeen
Th2	T Helper two
TLR	Toll-like receptor

TNF	Tumor necrosis factor
TNF-α	Tumour necrosis factor alpha
UC	Ulcerative colitis
ZAP-70	Zeta chain of TCR-associated protein 70
μg	Microgram
μL	Microliter

CHAPTER 1. INTRODUCTION

1. T Cell Introduction

1.1 General Immunology Overview

1.1.1 General Immunology Overview

The immune system refers to the collections of cells, tissues, and molecules that mediate reactions that provide resistance to infectious pathogens, non-infectious environmental molecules, and tumours.[1] There are two groups of immunity, each with features allowing them to cope with different scenarios: innate immunity and adaptive immunity (also known as acquired immunity). Innate immunity serves as the initial defence and contains elements with little memory components, including but not limited to chemical barriers (i.e. low pH in stomach acid) physical barriers (i.e. skin and mucosa), immune cells capable of killing microbes through phagocytosis or restricting the microbe spread via NETosis, complement proteins and cationic host defence peptides (i.e. cathelicidin and defensin) that can form channels or pores in microbe membrane and cause leakage in cell content. The majority of innate immune responses remain relatively constant throughout an individual's life, with a lack of specificity for each immunogen. Adaptive immunity, however, develops over time, where the memory components are gradually established throughout life with high levels of specificity to a given antigen. Innate and adaptive immune systems work together, maintaining a homeostasis state in our body.[1]

There are two types of adaptive immunities: humoral immunity and cell-mediated immunity. In a classic humoral immunity scenario, B cells produce and secrete specific antibodies. The binding of these antibodies to their epitope on an antigen can restrict the spread of infections and opsonize the antigen, triggering a more efficient antigen clearance via the effector functions of other cells, such as phagocytosis by macrophages or degranulation by eosinophils. Meanwhile, cell-mediated immunity occurs in one example when helper T cells (CD4+ T cells) get activated by antigen and release cytokines (i.e. IFN-γ) to promote phagocytosis capacity in macrophages. Another key player in cell-mediated immunity is cytotoxic T cells (CD8+ T cells); CD8+ T cells are known for their function in releasing perforins and granzymes to kill altered cells upon activation. CD4+ T cells also play important roles in humoral immunity. Two signals are required to trigger the antibody production in B cells. The "first signal" is generated when the B cell receptor (BCR) binds the antigen with specificity, and the second signal comes from T helper cells. Upon

encountering an antigen, B cells can internalize the antigen, process it, and eventually present it on major histocompatibility complex II (MHC II) molecule to T cells. T cells then recognize the antigen through TCR and upregulate CD40L on its surface, which serves as the ligand for CD40 on B cells. The binding of CD40 to CD40L provides the "second signal"; together with the "first signal," B cells are activated and can initiate antibody production. In addition, the key element of cell-mediated immunity, CD4+ T cells, are required for releasing cytokines such as IL-4 to aid in specific types of B cell antibody production and, therefore, contribute to optimal humoral immune responses.[1] Recruited from the bone marrow and delivered through blood, common lymphoid progenitor cells give rise to T cells, natural killer (NK) cells and other innate lymphoid cells, B cells and some forms of dendritic cells.[2,3,4] B cells and T cells obtain their names after their respective maturation locations (primary lymphoid organs); "B" for bone marrow and "T" for thymus. However, it takes many stages for B and T cells to maturate. In the bone marrow, common lymphoid progenitors that successfully express antigen receptors become immature B and T cells; these immature B and T lymphocytes, in primary lymphoid organs, go through positive selection, where B and T cells with receptors that have a weak affinity to antigen get survival signals, followed by the negative selection where apoptosis signal is provided when that affinity is strong. Specific to T cells, derived from pro-T cells, which are double negative for CD4 and CD8, they then become CD4+CD8+ T cells. After the negative and positive selections, depending on their weak-affinity TCR tropism for antigen presented on MHC I or MHC II, they get signals to become CD8+ or CD4+ single positive T cells, respectively. The mature B and T cells then enter the blood circulation and eventually arrive in peripheral lymphoid organs such as the spleen, where they can interact with each other and other immune cells.[1,5] Antigen-presenting cells (APCs) refer to immune cells that act as professional APCs (B cells, macrophages, and dendritic cells (DCs)), and other non-professional APCs (e.g. endothelial cells, fibroblasts and lymph node stromal cells) capable of processing and presenting exogenous and endogenous antigens on their MHC I and MHC II on the cell surface.[1,6]

Unlike T cells and B cells, innate immune cells like DCs and macrophages do not express specific antigen receptors.[7] Instead, they express pattern recognition receptors (PRRs), which allow them to recognize common molecular patterns shared by pathogens, apoptotic and damaged cells, also known as pathogen-associated molecular patterns (PAMPs), or molecules released by damaged cells (the damage-associated molecular patterns (DAMPs).[7]

T cell activation occurs when a conventional CD4+T cell recognizes a specific peptide presented on the MHC II molecule of an APC. The CD4 coreceptors on their surface help stabilize the TCR-antigen-MHC II interactions. The molecule presenting antigen to CD8+ T cells is MHC I, and the CD8 coreceptor stabilizes this interaction. This MHC-antigen-TCR recognition event triggers the activation of T cells, which later induces the proliferation and differentiation of that clone of T cells with specificity to the antigen.[1] T cell activation has been intensively studied as a crucial event in T cell functioning; the following sections will discuss more details about how optimal activation occurs and the downstream molecular events.

1.1.2 TCR Signaling, Signal 1, 2 and 3 in T cell Activation.

T cells integrate extracellular and intracellular signals. As the core element of T cell activation, TCR signalling involves cascades of many biochemical intermediates, active enzymes, and transcription factors. The interaction of those players fine-tunes the fate of the cell after activation. The downstream effect on the T cells depends on the strength of TCR stimulation, engagement of co-stimulatory ligands, and the cytokine milieu, known as **signal 1**, **signal 2**, and **signal 3**, respectively.[8,9]

A T cell response initiates when the TCR binds a specific antigenic peptide presented on APC (**Signal 1**), triggering the formation of a supramolecular cell-to-cell junction to stabilize the TCR-antigen-APC complex called the immunological synapse, where TCR and coreceptor CD4 or CD8 are surrounded by leukocyte function-associated antigen 1 (LFA-1).[10] T cells are extremely sensitive to **Signal 1**. A study showed that even a single peptide presented on an MHC molecule can induce detectable intracellular Ca^{2+} flux in T cells.[11]

Signal 2 is essential for optimal T cell activation, which is also known as a co-stimulatory signal. Co-stimulatory signals regulate T cell activities, including proliferation, trafficking, survival, cytokine production, and degranulation in CD8+ T cells. One of the most well-studied **Signal 2** receptors on T cells is CD28.[12] In 1984, Gmünder *et al*. found that CD28 synergistically promotes T cell proliferation with phytohemagglutinin (PHA), and PHA is known for activating T cells via TCR cross-linking.[13] CD28 is essential as it keeps T cells from entering an anergy state and maintains their responsiveness to antigens, CD80 and CD86 are two B7 family proteins identified as ligands for CD28, and they are upregulated on the cell surface when DCs are activated with DAMPs or PAMPs. Besides binding CD28 in promoting TCR activation, CD86 and CD80 can also bind cytotoxic T lymphocyte-associated antigen-4 (CTLA-4) on T cells with a higher

affinity leading to an inhibition of T cell activation. Besides CD80/CD86-CD28 and CD80/CD86-CTLA-4, there are other co-stimulatory receptor-ligand combinations. Inducible costimulator-ligand (ICOS-L) on other cells can bind inducible costimulator (ICOS) on T cells, which is essential for follicular helper T cell generation;[14] programmed death-ligand 1 (PD-L1) and PD-L2 exert inhibitory effects on T cell activation when bound to PD-1 on T cells. A combination of **Signal 1** and **Signal 2** is required to release the activation and clonal expansion potential of T cells.[15]

Signal 3 often refers to cytokines that are important to T cell activation and cell functions. These cytokines utilize their own specific receptors and can promote T cell activation in different ways. IL-12 has been identified as one of the most important cytokines for CD8+ T cells. *In vivo*, when antigen-induced naïve CD8+ T cell activation is in combination with a CD28 co-stimulatory signal, IL-12 significantly promotes cell proliferation; this upregulation effect of IL-12 is not seen in memory T cells, indicating that memory T cells have a lower threshold of being activated.[16] Another study showed that for naïve CD8+ T cells, IL-12 produced by activated dendritic cells is capable of inducing a large increase in clonal expansion, especially when antigens are provided in low concentration.[17] It was also shown that IL-12 is required for the cytotoxic function development of CD8+ T cells, as CD8+ T cells not treated with IL-12 showed ablated capacity in lysing target cells.[17,18] IFN-α is also considered a **Signal 3** cytokine for CD8+ T cells. During peptide-vaccine-induced CD8+ T cell activation, IFN-α promotes IFN-γ production, proliferation, and persistence of tumor-specific CD8+ T cells.[16] In general, **Signal 3** facilitates robust CD8+ T cell cytotoxicity and plays an important role in CD8+ T cell persistence and proliferation; however, this effect is dependent on the presence of **Signal 1** and **Signal 2**.

Signal 3 for CD4+ T cells is less well defined, but IL-1 and tumour necrosis factor alpha (TNF-α) promote migration to the paracortex of draining lymph nodes and clonal expansion of antigen-specific CD4+ T cells in a mouse model.[19] IL-1-primed CD4+ T cells have enhanced persistence in that they are detected in lymph nodes till 16 months later.[20] Besides activation-promoting functions, researchers have identified certain **Signal 3** cytokines that can inhibit T-cell activation. IL-2-pretreated naïve murine and human CD4+, not CD8+ T cells, have significantly reduced Con-A-induced activation and proliferation via inhibition of STAT5.[21]

Signal 3- type cytokines are also crucial for naïve CD4+ T cell polarization. DCs provide **Signal 1** and **Signal 2** directly through interacting with T cells, while **Signal 3** cytokines from DCs

or other cell types (e.g. NK cells, NK T cells) can polarize naïve T helper cells into different effector subtypes such as Th1 and Th2.[22] The diversified T helper cells polarized upon different cytokine environments enable the generation of proper immune responses against different antigens, and the specific functions of these effector CD4+ T cell subtypes will be discussed later in this dissertation.

1.1.2.1 TCR Structure and Signalling Initiation

The TCR allows T cells to recognize specific antigenic peptides presented on MHC molecules, and it serves as the core of T cell signalling. Two groups of T cells are distinguished by TCR structure: the conventional αβ T cell and γδ T cells. These two types of T cells have different migration tropisms: the αβ T cell migrates towards lymphoid organs, while the γδ T cells tend to migrate to peripheral tissues. γδ T cells also function in an MHC-independent manner.[23] For both αβ and γδ T cells, the TCR consists of six different polypeptides, which include the core-heterodimer functioning in antigen recognition (αβ or γδ) and the conventional CD3ε, CD3γ, two of the CD3δ, and two of the TCRζ chains. The cytoplasmic compartment of these chains contains ten immunoreceptor tyrosine-based activation motifs (ITAMs); each TCRζ chain is associated with three ITAMs and one ITAM with each CD3 chain (**Figure 1**).[24,25] Upon activation, the number of ITAMs that get phosphorylated is related to the intensity of T cell signalling.[26] The proteins with SH3 domains can then bind to phosphorylated ITAMs and recruit other downstream signalling proteins.[25]

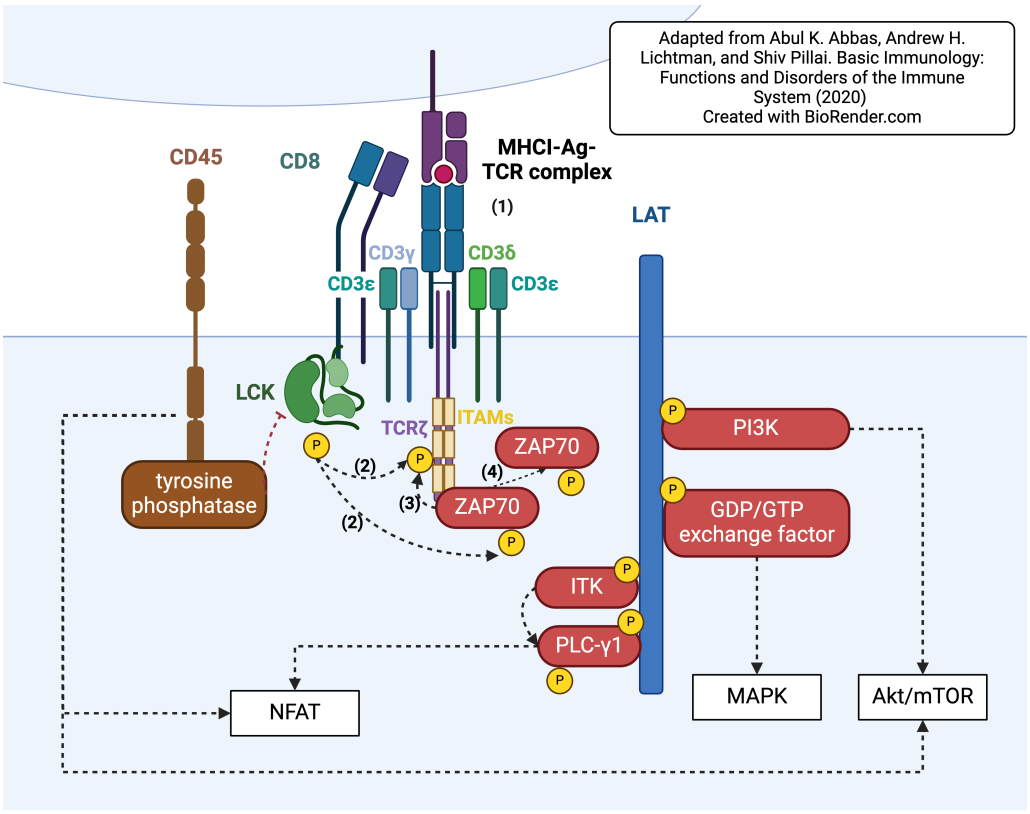

Figure 1. Simplified TCR structure and TCR signalling initiation.

(1) Upon specific peptide antigen recognition by the T-cell receptor (TCR), lymphocyte cell-specific protein-tyrosine kinase (Lck) (2) phosphorylates the TCR at ITAM and zeta chain of TCR-associated protein 70 (ZAP-70). (3) Phosphorylated ZAP-70 can also phosphorylate TCR at ITAM. (4) Phosphorylated ZAP-70 can also activate linker for activation of T cells (LAT), which is a crucial adaptor protein with docking sites for protein mediators such as IL-2-inducible T-cell kinase (ITK), phospholipase C gamma 1 (PLC-γ1), phosphoinositide-3 kinase (PI3K), and GDP/GTP exchange factor upon being phosphorylated at different sites. ITK phosphorylates PLC. The binding of these protein mediators can initiate the signalling of different downstream pathways, as indicated in the figure. A CD8+ T cell was used as an example representing T cells. CD45, as a regulatory mechanism, dephosphorylates Lck to deactivate it, preventing excessive T cell activation. ITAM, immunoreceptor tyrosine-based activation motif; LAT, the linker for activation of T cells. Created with BioRender.com.

Two protein tyrosine kinase (PTK) families are crucial for TCR signalling: Src and Syk families. The Src and Syk kinases regulate various cell activities, including replication, survival, differentiation, cytoskeleton rearrangement, and migration (**Figure 1**).[27,28] As a kind of Src PTK, Lck remains constitutively active at a low magnitude even in resting T cells; upon TCR-antigen-MHC interaction, it gets activated to a higher level, which permits instant activation and is in

charge of propagating TCR signalling.[29] The zeta-chain of TCR-associated protein 70 (ZAP-70) is another essential PTK, a member of the Syk family.[30]

TCR signalling initiates when the TCR interacts with a specific antigen presented on the MHC molecule on APCs. As mentioned above, CD4 and CD8 are known as co-receptors in this signalling cascade, and they help stabilize the TCR-antigen-MHC complex. Right after antigenic peptide recognition, Lck phosphorylates the intracellular domain of TCR at ITAMs and also concurrently phosphorylates to activate ZAP-70;[31] activated ZAP-70 gains enhanced catalytic activity and further phosphorylates T cell receptors at ITAMs, which is required for downstream IL-2 production.[9,32] Interestingly, Horkova *et al.* showed that CD4-bound Lck is required for functional T helper cell development, while CD8-bound Lck is dispensable for anti-viral and anti-tumor activities in cytotoxic T cells.[33] The linker for activation T cells (LAT), a transmembrane adaptor, opens up its docking sites for various adaptor proteins after its activation by ZAP-70 via phosphorylation.[34] LAT is considered the master switch of TCR signalling, as LAT-deficient variants of Jurkat cells (an immortalized human T cell line) showed a dramatic decrease in key T cell activation events, such as calcium flux and nuclear factor of activated T cells (NFAT) transcription, and in the expression of T cell activation marker CD69.[34] When other adaptor proteins (Grb2 family adaptor protein and SLP-76) are recruited and docked onto the LAT, it triggers the assembly of a higher-order signalosome, and then mitogen-activated protein kinases (MAPKs) are activated.[34] PLC-γ is also a binding partner for LAT, which will be discussed in detail below.

1.1.2.2 JNK Signalling

CD4+ T cells can produce high levels of IL-2, one of the essential cytokines that contribute to T cell proliferation and survival.[35,36] As shown in **Figure 2**, to transcribe *IL2*, several transcription factors need to cooperate, including activator protein 1 (AP-1), nuclear factor kappa B (NF-κB), NFAT, and NF-IL-2.[37] The MAPK pathway plays a central role in activating these transcription factors. MAPKs include three distinct types: p38, the extracellular signal-regulated kinases (ERKs), and c-Jun NH_2-terminal kinases (JNKs).[15] MAP kinase kinases (MKKs), on the other hand, phosphorylate MAPKs at threonine and tyrosine residues to activate them. MKK4 and MKK7 can phosphorylate JNK, and phosphorylated JNK can phosphorylate c-Jun.[38,39] AP-1, as a transcription factor activator protein, is one of the targets of JNK and plays an essential role in regulating cell activation, proliferation, and polarization. AP-1 is also involved in forming NFAT

and NF-IL-2.[40,41] Upon phosphorylation, c-Jun binds the Fos protein to form AP-1.[15] To achieve an optimal level of JNK activation, synergic activation through both TCR and co-stimulatory receptors is required (i.e. through CD28).[42]

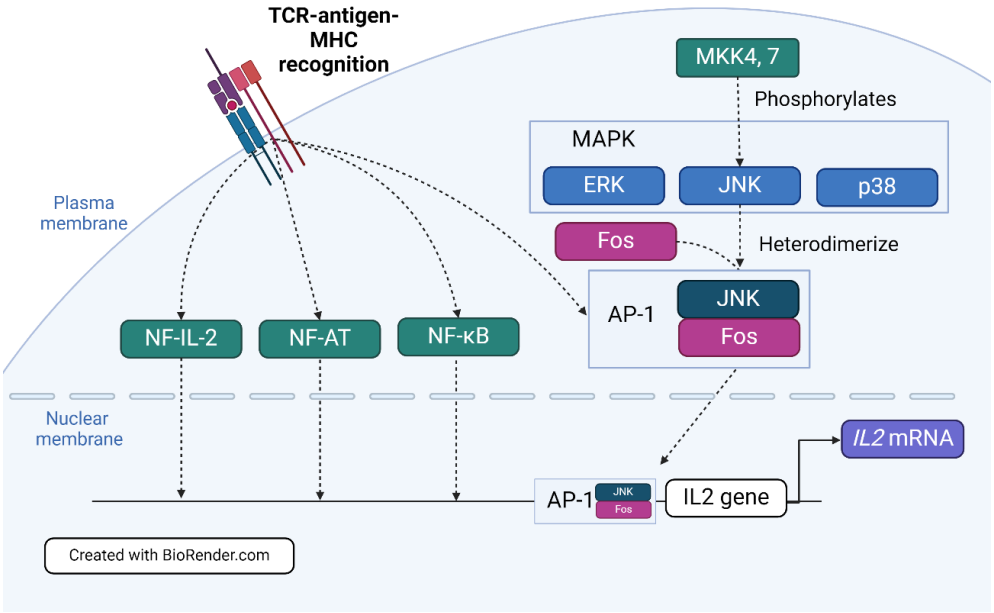

Figure 2. JNK heterodimerizes with Fos to form AP-1 and assist *IL2* gene transcription.

JNK, as a kind of MAPK, when phosphorylated by MKK4 or MKK7, can heterodimerize with Fos protein and form the AP-1 complex. AP-1 can translocate to the cell nucleus; together with other nuclear transcription factors (such as NF-IL-2, NFAT, and NF-κB listed in the figure), AP-1 promotes the transcription of IL2 gene ERK, extracellular-signal-regulated kinase; JNK, c-Jun N-terminal kinase; NF, Nuclear factor; NFAT, Nuclear factor of activated T-cells; NF-κB, Nuclear factor kappa-light-chain-enhancer of activated B cells; AP-1, Activator protein-1; MKK, Mitogen-activated protein kinase kinases; MAPK, mitogen-activated protein kinase. Created with BioRender.com.

1.1.2.3 PI3K, NFAT, and NF-κB Signalling

As an indispensable kinase, PI3K controls the trafficking, proliferation, activation, and polarization of T cells.[43] Involved in cell-to-cell and cell-extracellular matrix interactions, integrins are a group of proteins expressed on the cell surface, regulating cell migration and retention from inflamed tissues; a necessary integrin that governs T cell migration is LFA-1.[44] CD62L, also known as L-selectin, permits T cells to start rolling and slow down on high endothelial venules (HEVs) when interacting with peripheral node addressins; CCR7 on T cell surface, on the other hand, induces LFA-1 on T cells to help them leave endothelial system upon binding its ligand CCL21.[45]

Both lymphoid organ-homing chemokine receptors CCR7 and CD62L are downregulated upon PI3K activation.[43] As shown in **Figure 3**, in a classic PI3K-Akt pathway, class I PI3K phosphorylates PtdIns (4,5) P2 (PIP2) to generate phosphatidylinositol (3,4,5)-trisphosphate (PIP3).[43] PIP3 enables the recruitment of Akt to the plasma membrane and phosphorylation of Akt by phosphoinositide-dependent kinase 1 (PDK1) and mTOR complex 2 (mTORC2). Phosphorylated (activated) Akt then phosphorylates its substrates, regulating cell growth and survival through the mTORC1 complex.[46]

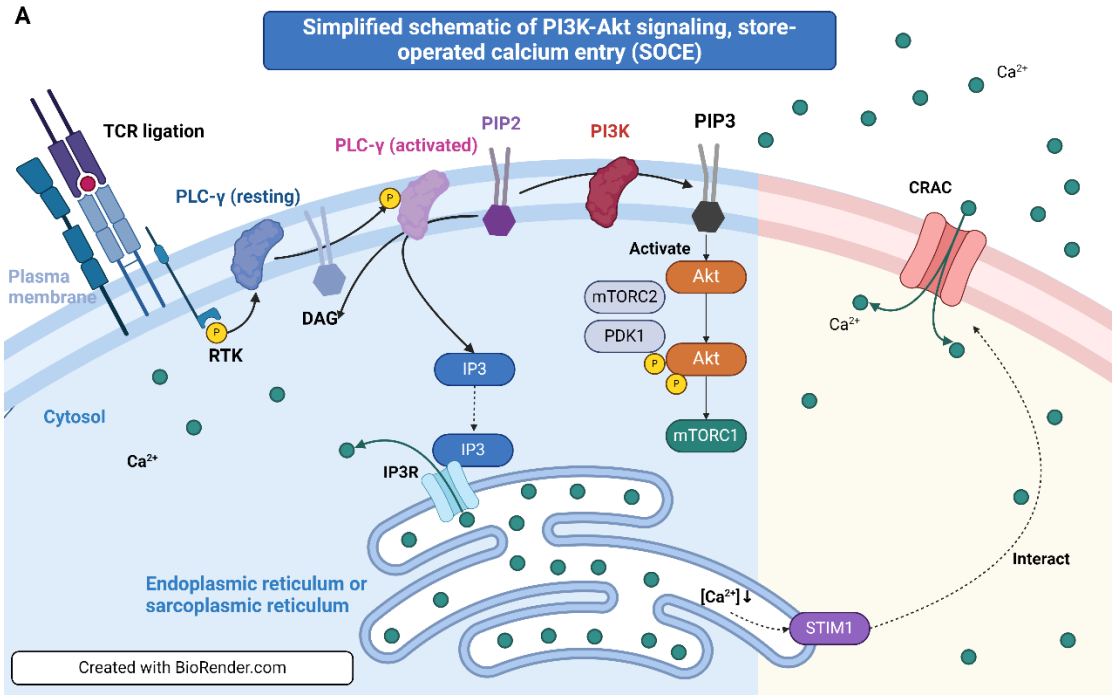

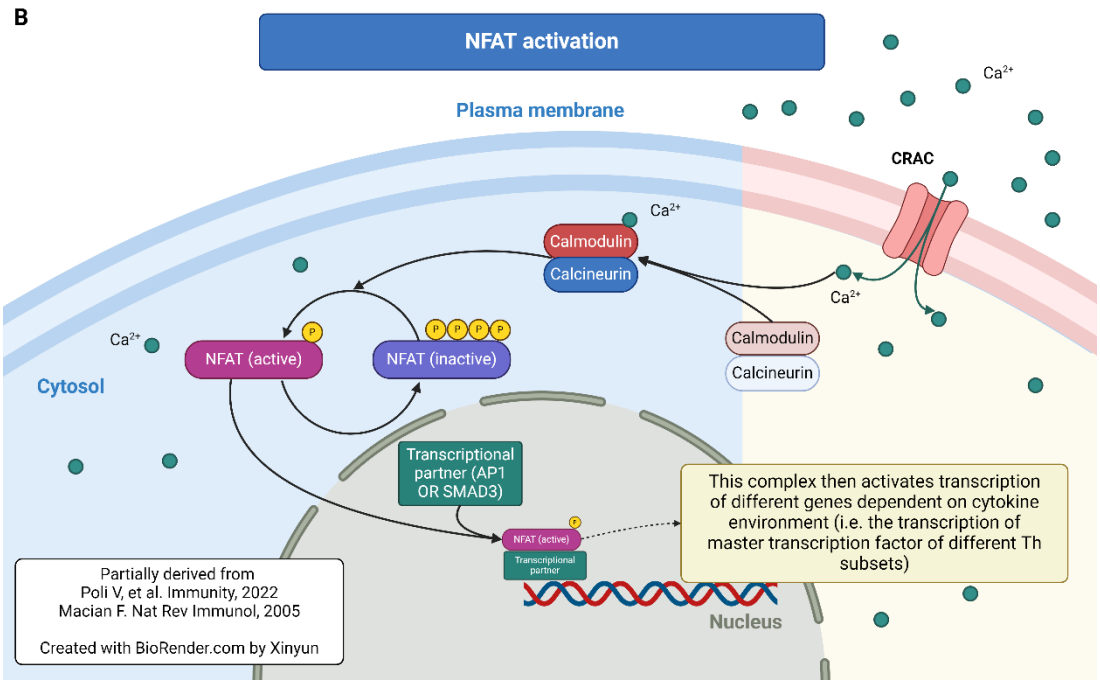

Figure 3. Simplified schematics of PI3K-Akt signalling, store-operated calcium entry and NFAT activation.

(A) Starting from PIP2, activated PI3K generates PIP3 by phosphorylating PIP2, and PIP3 allows the recruitment and the phosphorylation of Akt by PDK1 and mTORC2. Akt then regulates various cell activities through mTORC1. Upon TCR stimulation, RTK phosphorylates and activates PLC-γ, which, in turn, hydrolyzes PIP2 into diacylglycerol (DAG) and inositol triphosphate (IP3). IP3 can bind its receptor on either endoplasmic or sarcoplasmic reticulum, which serves as a calcium channel, allowing calcium release to cytosol following gradient difference. Decreased calcium concentration in the endoplasmic/sarcoplasmic reticulum triggers the activation of STIM1 proteins, which translocate and bind calcium release-activated channels on the plasma membrane, which permits more calcium entry into the cytosol. (B) Calcium binds calmodulin, then interacts with calcineurin, and the complex acts as an NFAT activator via dephosphorylation. The active form of NFAT enters the nucleus and interacts with AP-1, serving as a function transcription factor to induce the transcription of various genes dependent on the extracellular cytokine environment. RTK, Receptor tyrosine kinase; PLC, Phospholipase C; DAG, Diacylglycerol; STIM1, Stromal interaction molecule 1; calcium-release activated calcium (CRAC), Calcium release-activated channels; PIP2, Phosphatidylinositol 4,5-bisphosphate; IP3, Inositol trisphosphate; IP3R, IP3 (inositol 1,4,5-trisphosphate) receptor; mTORC, mammalian target of rapamycin complex; AP-1, Activator protein 1. Created with BioRender.com.

NFAT is essential in many immune functions in almost all cell types studied, but it is best studied in immune cells.[47] The phosphorylation at a specific site of LATs allows the recruitment and the activation of PLC-γ1; it also localizes PLC-γ1 to its substrate, phosphatidylinositol-4,5

bisphosphate (PIP2), therefore vital for NFAT and Ca^{2+} signalling.[48] The activated form of PLC-γ1 produces inositol-1,4,5-trisphosphate (IP3) and diacylglycerol (DAG) through the hydrolysis of plasma membrane-tethered PIP2.[47] IP3 then binds to its receptor IP3R, and IP3R serves as a calcium channel in the sarcoplasmic or endoplasmic reticulum membrane; upon binding IP3, IP3R allows Ca^{2+} to be released following its gradient to the cytosol.[47,49] Then, STIM1 on the endoplasmic or sarcoplasmic reticulum is activated, and it translocates to the plasma membrane, opening up CRAC channels on the plasma membrane, allowing more extracellular calcium to enter the cell.[47] Following the increase in calcium concentration in cytosol, calmodulin binds calcium and activates calcineurin, which functions in dephosphorylates NFAT; notice counter-intuitively, the dephosphorylated form of NFAT is the active form. NFAT can then interact with transcription factors such as AP-1 and SMAD-1 to promote the transcription of various genes, involving cell polarization, proliferation, and other cell activities, such as *IL4*, *IL2*, *TNFA, CXCR5,* and *CCR9*.[50,51]

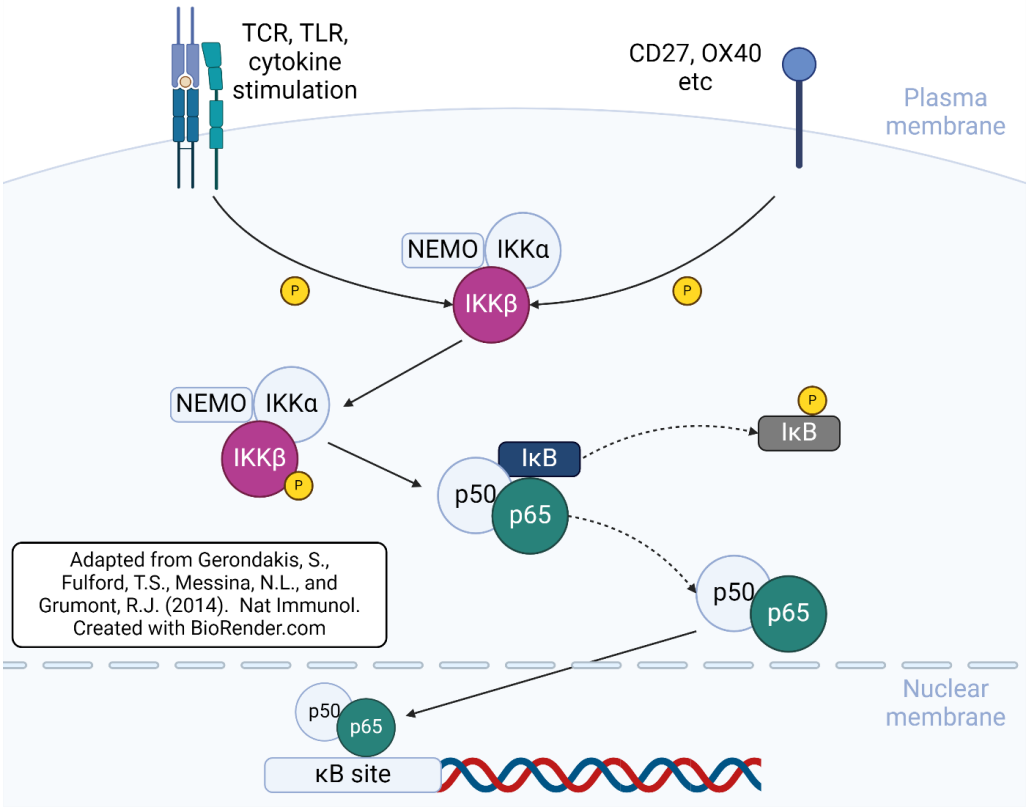

Figure 4. Simplified NF-κB signalling.

At steady state, NF-κB dimers (p50-p65 in the figure as an example; p65 is also known as RELA) in cytosol remain inactive. Upon receiving stimuli through various cell receptors (i.e. TCR, toll-like receptors (TLRs), OX40, CD27 and other cytokine receptors, etc.), the inhibitor of nuclear factor-κB (IκB) kinase (IKK) complex gets activated and phosphorylated at the IKKβ subunit, which, in turn, phosphorylates the protein associated with NF-κB dimer, IκB. At the steady state, IκB acts as an inhibitor, restricting NF-κB dimers from entering the cell nucleus and binding the κB site. IκB gets ubiquitinated after being phosphorylated by IKKβ. Therefore, its inhibitory effect on NF-κB dimers is removed, promoting the transcription of downstream genes related to inflammation, cell survival, proliferation, etc., to occur. NF-κB, Nuclear factor kappa-light-chain-enhancer of activated B cells; NEMO, NF-kB essential modulator.

Other than the PI3K, JNK, and NFAT pathways discussed, another signalling pathway essential in T cells is the nuclear factor kappa-light-chain-enhancer of activated B Cells (NF-κB) pathway (**Figure 4**). The NF-κB protein family consists of two subfamilies: NF-κB proteins and the "Rel" proteins, and they share a conserved Rel homology domain (as the DNA binding domain; they are crucial in cell signalling and have been extensively studied.[52] NF-κB proteins form hetero or homodimers, such as p65-p50, and interact with inhibitory protein IκB. At the steady state, NF-κB remains inactive and latent due to the suppression effect of IκB. IKK complex consists of three

subunits, IκB kinase α (IKKα), IκB kinase β (IKKβ), and NF-kB essential modulator (NEMO); in terms of function, IKK complex is capable of activating NF-κB dimers.[53] Upon stimulation signalling (i.e. TCR, TLR, and cytokines), IKKβ in the IKK complex is phosphorylated and activated, and that triggers the phosphorylation, ubiquitination, and degradation of inhibitory IκB associated with NF-κB dimers.[53] The removal of inhibitory IκB allows the translocation of NF-κB to the nucleus and binds to the κB sequence on DNA, which induces the transcription of a series of genes involved in inflammation, cytokine production, cell survival, development, and proliferation.[53]

1.1.2.4 CD28 Co-stimulatory Signalling

One of the most prominent effects of CD28 co-stimulation on T cells is the increase in IL-2 production. IL-2 is crucial in various immune cell activities, such as differentiation of Th2 cells and proliferation of CD4+ and CD8+ T cells.[36] Studies have shown that CD28 signalling promotes the transcription of *IL2* genes and stabilizes cytokine mRNA, such as *IL2*, *TNFA*, and *IFNG*.[54,55] When CD28 on T cells binds to its ligand (i.e. CD80 or CD86), Src phosphorylates the YMNM motif on the intracellular tail of CD28.[56] That phosphorylation event recruits PI3K, and PI3K can later phosphorylate PIP2 to produce PIP3. PIP3 is capable of recruiting PDK1 and Protein kinase B (PKB)/Akt, and PDKI can phosphorylate and activate PKB/Akt.[56] Upon phosphorylation, PKB/Akt can inactivate Glycogen synthase kinase-3 beta (GSK3β), and GSK3β in its inactive form can no longer phosphorylate and inactivate NFAT.[56] Therefore, PKB/Akt promotes NFAT signalling; it triggers PKB/Akt to release functional NF-κB protein by promoting IκB phosphorylation and ubiquitination and enhances mTORC, both propagating NF-κB signalling and effects (**Figure 5**).[56]

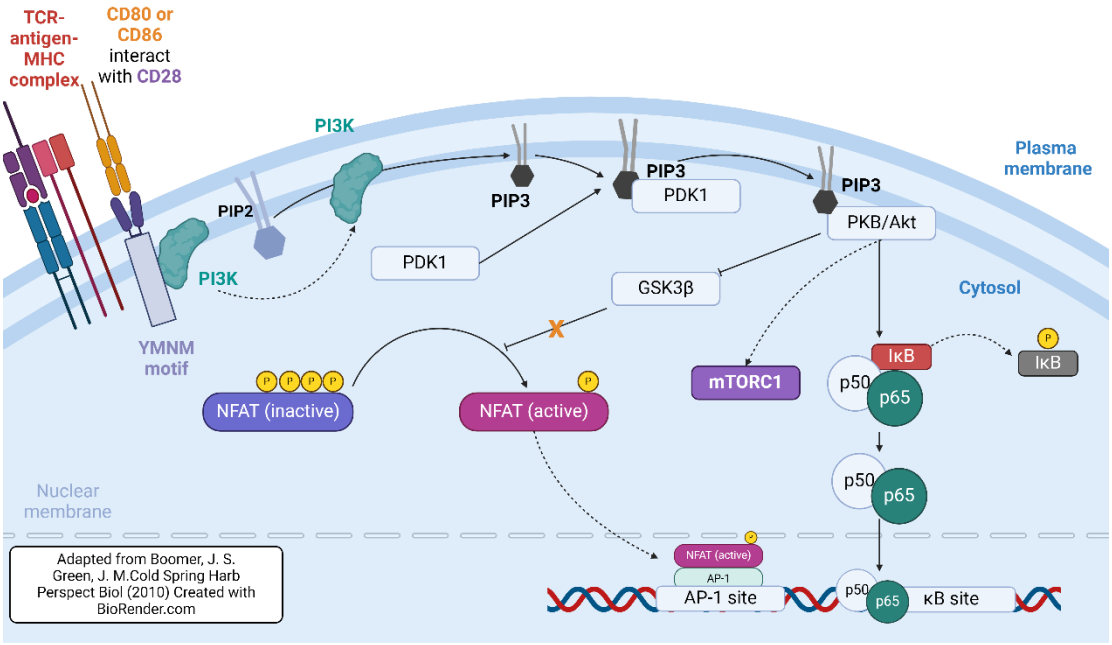

Figure 5. CD28 interaction with its ligand promotes NFAT and NF-κB signalling in T cells.

Upon binding to its ligand, the phosphorylation of the YMNM motif by Src on the intracellular tail of CD28 triggers the recruitment of PI3K, and PI3K can produce PIP3 from PIP2. PIP3 can recruit PDK1 and PKB/Akt, and PDKI can phosphorylate and activate PKB/Akt. Upon being phosphorylated, PKB/Akt can inactivate the NFAT repressor, Glycogen synthase kinase-3 beta (GSK3β). Besides, PKB/Akt promotes IκB phosphorylation and ubiquitin-dependent degradation, which releases functional NF-κB protein and enhances mTORC.

1.1.3 T Cell Subsets

The memory function of adaptive immunity allows a rapid and efficient response against previously encountered antigens, which serves as the basis for vaccination. During a primary encounter with an antigen, naïve T cells, referring to those mature T cells that went through negative and positive selections, are activated. Only a proportion of activated naïve T cells will differentiate into long-lived memory T cells; most of them polarize into antigen-specific effector T cells, producing cytokines and undergoing apoptosis after antigen clearance.[57,58] Using CD62L and CD45RA, T cells can be categorized into central memory T cells (T_{CM}) (CCR7+CD45RA-), effector memory cells (T_{EM}) (CCR7-CD45RA-), effector memory T cells re-expressing CD45RA (T_{EMRA}) (CCR7-CD45RA+), and naïve T cells (CCR7+CD45RA+).[59,60]

The relationship between memory and effector T cells is still in debate, and several models have been proposed. The first model that explains T cell differentiation and heterogeneity is the

Linear Differentiation Model, where effector T cells are generated from naïve T cells upon TCR stimulation, followed by the generation of long-lived memory cells from these effector cells, or the senescent T cell, which undergo apoptosis soon after antigen clearance.[61] The second model, the Bifurcative Differentiation Model, proposed that naïve T cells go through asymmetric division and produce two distinct daughter cells upon TCR stimulation.[61] T_{CM} is generated from the distal daughter cell, and the proximal daughter cell can have another round of asymmetric division, generating T_{EM} and effector T cells.[61] Just like in the Linear Differentiation Model, effector T cells in the Bifurcative Differentiation Model also undergo apoptosis soon after the removal of antigens.[61] The third model is the Self-renewing effector model, which states that TCR stimulation enables the naïve T cells to develop into self-renewable effector T cells and T_{CM}.[61] The effector T cells and T_{CM} can both give rise to T_{EM}, which can eventually become effector T cells.[61] All these T cell subsets differ from each other by their surface receptor profile, which is related to their function, distributions, and trafficking properties.[61,62]

High proliferative potential and IL-2-producing ability differ T_{CM} from effector cytokine-producing T_{EM}.[63] T_{CM}-expressed lymphoid homing receptors CCR7 and CD62L restrict them to secondary lymphoid tissues, but studies have also shown that they can perform tissue surveillance in inflamed and non-inflamed tissue in humans.[64] As antigen-experienced cells, T_{CM} can respond to antigens and produce cytokines, but this feature is dependent on the cytokine signals they receive. Pakpour *et al*. showed that the production of IFN-γ in effector T cells does not rely on exogenous IL-12, but T_{CM} requires IL-12 to develop into Th1 cells and produce effector cytokines in mouse models.[65] Although not committed to producing any effector cytokines, the rapid increase in the number of T_{CM} allows T cell-dependent B cell activation; some T_{CM} may also migrate to tissues aiding infection clearance.[66] A population of T_{CM} can give rise to follicular T helper cells, which are crucial in aiding B cell antibody production in the germinal center, generating persisting humoral responses.[67] T_{EM} secrete much less IL-2 compared to T_{CM}, but they can produce IFN-γ, TNF, IL-4, and IL-17. Distinguished by their cytokine production profile, T_{CM} are further grouped into subtypes, such as Th1, Th2, and Th17 cells; details about these subtypes will be introduced later. These T_{EM} subtypes have distinct and transient chemokine receptor profiles expressed on the cell surface, allowing them to migrate to various tissues dependent on the microenvironment.[68]

The important role of CD45 in T cell proliferation has been identified, where a possible mechanism is that CD45 dephosphorylates and activates the Lck molecule.[69] Two splicing variants

of CD45, known as CD45RO and CD45RA, have been considered the basis for distinguishing memory and naive T cell lineages.[70] The CD45 gene consists of 3 variable exons, A, B, and C, generating up to eight distinct isoforms.[70] The high molecular weight isoform CD45RA is expressed by naïve T cells, and upon activation, T cells express less exon A and more low molecular weight isoform CD45RO that lack all 3 variable exons.[70] CD45RA is normally considered a naïve T cell marker; its positive correlation with mitosis has been shown, while CD45RO-expressing cells are considered "memory."[71] CD45RO and CD45RA are both expressed on T_{EMRA} cells. T_{EMRA} are related to immuno-senescence and the proportion of T_{EMRA} increases with aging. During HIV progression, the number of naïve T cells and T_{CM} reduces over time, while CD8+ T_{EMRA} are maintained at a high level with a longer life span.[60,72] In human peripheral blood mononuclear cells (PBMCs), T_{EMRA} have the lowest proliferation potential compared to T_{CM} and T_{EM}.[73]

1.1.4 T Cell Activation Markers and Their Regulation and Functions

CD71

Also known as the transferrin receptor, CD71 functions in uptaking transferrin-iron complexes.[74] In 1989, Schuurmam *et al.* found that CD71 levels are low in resting immune cells and levels increase upon stimulation.[75] It has also been shown that at 12 hours post-stimulation, CD71 and Ki67 are positively correlated in both mouse and human T cells, and Ki67 is considered a cell proliferation marker.[76]

CD62L

As described in the previous section, CD62L is a crucial integrin regulating T-cell trafficking; a study also showed it is essential for activated CD8+ T cells to reach infected organs to clear viral infections.[77] TCR signalling reduces the level of CD62L on the T cell surface, therefore, CD62L had been considered an activation marker of T cells, with a higher level of CD62L representing a "less" activated T cell.[78] Chao *et al*. showed that the CD62L level on mouse T cells post-stimulation with anti-CD3 follows a triphasic pattern: It falls drastically within the first 4 hours and quickly goes back up; the level of CD62L reaches its peak on Day 2, about two times higher than the Day 0 baseline, and then decreases overtime again to reach about the same level as the Day 0 baseline level on Day 3.[79] CD62L functions in initiating the T cell adherence to HEVs via binding to its ligand, vascular addressin on HEV.[80]

CD69

Upon T cell activation, CD69 expression is detected within an hour and decreases after 4-6 hours.[81] A conserved cis-element in the promoter region regulates the expression of CD69.[82] In both airway and contact hypersensitivity mouse models, a higher level of Th2 and Th17 cytokines was detected in bronchoalveolar space and lung tissues and more eosinophilic infiltration at pulmonary sites for CD69-knock-out (KO) mice.[83] There are two putative ligands for CD69: Gal-1 and S100A8/S100A9 complex; the former *ligand* relates to a higher chance of auto-immune neuroinflammation,[84] and the latter is required for the differentiation of regulatory T (Treg) cells, which is a crucial CD4+ T cell subtype functioning in restricting inflammation and maintaining immune tolerance.[85,86] CD69+ Treg cells have been shown to express more inhibitory markers on the cell surface (e.g. ICOS and CTLA-4) and secrete elevated levels of anti-inflammation IL-10 compared to CD69- T reg cells.[87] The egress of lymphocytes, including T cells, from secondary lymph organs to peripheral tissues can be enhanced by the sphingosine-1-phosphate receptor (S1P1) on T cells.[88] It has been shown that CD69 expression downregulates T cell egress from the thymus via inducing the internalization and degradation of S1P1.[89,90] The absence of T cell egress from lymph nodes to peripheral tissues in CD69 KO mice confirms the function of CD69 in T cell egress modulation.[91] Upon activation, the expression of CD69 on the T cell surface is transient, and its levels decrease after rounds of T cell proliferation.[92] SIP1 is then re-expressed on the T cell surface, and the egress of T cells from secondary lymph organs to peripheral tissue is restored.[90,93,94]

1.1.5 CD4+ T Cell Polarization Requirement, Th Subtypes, and Their Functions

In order to respond to different immunological challenges, TCR-stimulated naïve CD4+ T helper (Th) cells have the potential to polarize into different Th effector cell subsets depending on the stimulation and cytokine environment. In 1986, Mosmann *et al*. identified Th1 and Th2 cells from effector CD4+ T cells, distinguished by their cytokine production profile.[95] In a classic paradigm, IL-12 and IFN-γ induce the polarization of Th1 cells, which produce IFN-γ, IL-2 and TNF-α as their signature.[96] Th2 cells are known to produce IL-13, IL-4, and IL-5. Later, researchers identified another Th subset, named Th17 cells, after their unique ability to produce IL-17, IL-21 and IL-22.[96] (**Figure 6**) Interestingly, Th17 cells have high flexibility, allowing them to be converted to the Th1 phenotype; the originally discovered Th1 and the Th17-derived Th1 cells are named the classic and non-classic Th1 cells, respectively.[97] There are other Th cell types,

such as Th9, Th22, and follicular T helper cells. Only the classic Th1 cells and Th2 cells will be introduced for this dissertation.

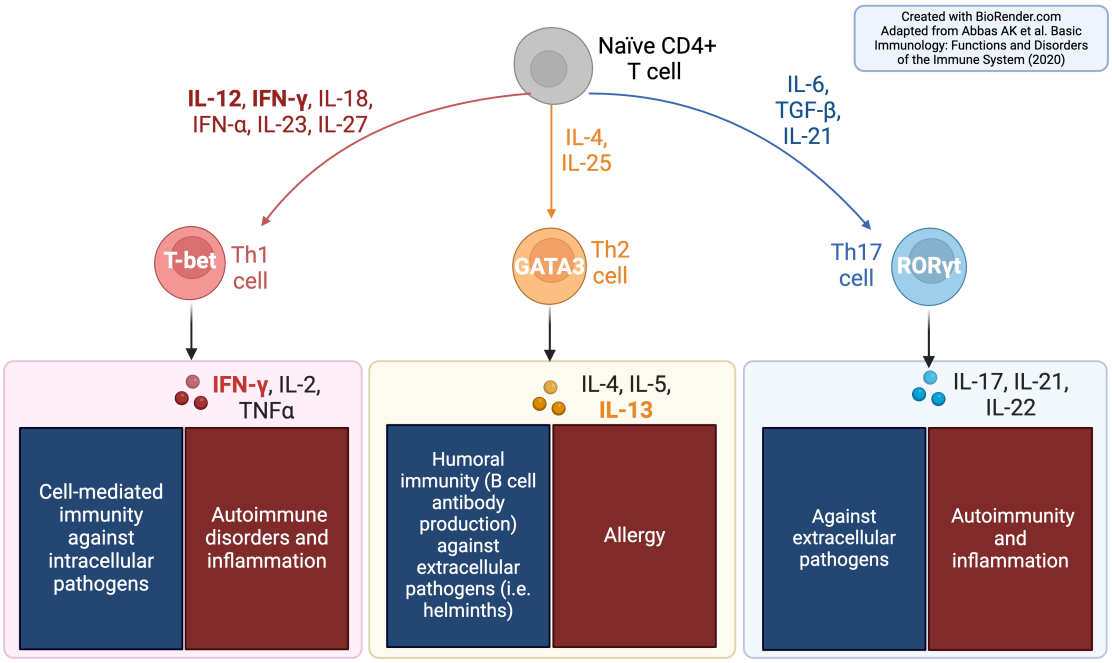

Figure 6. General overview of Th1, Th2, and Th17 subsets.

Upon receiving different extracellular cytokine stimuli, naïve CD4+ T cells have the potential to polarize into different Th subsets, such as Th1, Th2, and Th17 cells. IL-12, IFN-γ, IL-18, IFN-α, IL-23, and IL-27 have been shown to induce or promote Th1 polarization, which leads to IFN-γ, IL-2, and TNF-α production. T-bet is the master transcription factor of Th1 cells. Th1 cells are known to function in targeting intracellular pathogens through the production of IFN-γ, which activates immune effector cells such as macrophages. IL-4 and IL-25 favour the polarization of Th2 cells, with GATA Binding Protein 3 (GATA-3) being the master transcription factor governing the production of IL-13, IL-4, and IL-5 by Th2 cells. Th2 cell cytokines, especially IL-4, are important in targeting helminth infections by activating eosinophils. Th2 cytokines also contribute to antibody production in B cells and allergies such as Th2-high endotype asthma. Th17 cells are induced by IL-6, transforming growth factor beta (TGF-β), and IL-21, with ROR-γt being their master transcription factor, allowing the production of IL-17A, IL-17F, IL-21, and IL-22. Th17 cytokines, especially IL-17, provide host protection against several pulmonary infections (i.e. *Klebsiella pneumoniae*). The pathogenic role of IL-17 in psoriasis, inflammatory bowel diseases, and rheumatoid arthritis had also been identified.[98]. Created with BioRender.com.

1.1.5.1 The Role of Th1 Cells in Health and Diseases

Th1 or type I immunity is well-known for its role in targeting intracellular pathogens. Upon PRR recognition, DCs can migrate to secondary lymph organs and present the antigen on MHCII

molecules to CD4+ T cells. DCs are also a source of IL-12, one of the essential cytokines in inducing Th1 polarization by activating STAT4.[96] However, IL-12 receptor (IL-12R) is not expressed on naive CD4+ T cells at the steady state; cell surface IL-12R level can be upregulated by either TCR stimulation or IL-2.[99] Besides IL-12, other cytokines can contribute to Th1 polarization, including IL-18, IFN-γ, IFN-α, IL-23, and IL-27.[100,101,102] A stronger stimulation favours Th1 polarization, whereas a weaker TCR stimulation favours Th2 polarization.[103,104] IL-12Rβ2 is essential in heterodimerizing with IL-12Rβ1 to form a high-affinity IL-12R structure.[105] When polarizing mouse naïve CD4+ T cells using artificial APCs as stimulation sources, APC pre-treated with a higher dose of activation-inducing agent induced a higher level of IL-12Rβ2 on the T cell surface.[106] That upregulation of IL-12R allows T cells to receive IL-12 signalling with increased sensitivity and polarize into Th1 cells.[107] Co-stimulatory signals also play an important role in Th1 polarization. It has been shown that anti-CD28 is required for IFN-γ release after antigen stimulation.[108] The master transcription factor driving Th1 differentiation is T-box transcription factor TBX21 (T-bet), which governs the production of Th1 cytokines, such as IFN-γ. IFN-γ is crucial in activating and enhancing immune cell functions. It is known macrophages' phagocytic and microbicidal functions, Th1 cell cytokine production functions, and B cell class-switching to IgG-production can all be enhanced by IFN-γ.[96] IFN-γ also promotes the NK cell-mediated killing of tumour cells.[109] The role of Th1 cells is not always protective; they can also contribute to pathogenesis, especially autoimmunity. Pro-inflammatory cytokines produced by Th1 cells, including TNF-α and IFN-γ, lead to cartilage destruction and bone erosion in rheumatoid arthritis.[110] A higher level of IL-18 and IL-12 was observed in patients with Crohn's disease (CD), and anti-IL-12 helped reduce IFN-γ production through reduction of the number of Th1 cells helping patient outcomes.[111]

1.1.5.2 The Role of Th2 Cells in Health and Diseases

Th2 cells are crucial for humoral immunity against pathogens but also promote asthma and other allergic diseases. DCs provide co-stimulatory signals, such as OX40L. The binding of OX40L with OX40 on T cells is important for optimal Th2 polarization.[112] However, DCs are unable to produce IL-4, and IL-4 is essential for Th2 priming. Studies have shown that activated basophils migrate to lymph nodes and produce IL-4, aiding Th2 polarization.[113] Epithelial cells can recognize DAMPs and PAMPs with their PRRs, and this recognition induces the production of alarmins such as thymic stromal lymphopoietin (TSLP), IL-33, and IL-25. Differentiated Th2

cells upregulate the receptors for these alarmins, and the binding of these alarmins to their receptors is required for developing full Th2 functions *in vivo*.[107,114] During helminth infections, IgE production and the activation of mast cells rely on IL-4; IL-13 contributes to worm expulsion and mucus production.[115] Chen *et al*. also showed that Th2-mediated IL-4R signalling is vital in reducing proinflammatory IL-17 responses and promoting anti-inflammatory IL-10 production, allowing wound healing during helminth infections.[116] The master transcription factor for Th2 cells is GATA-3.[117] GATA-3 promotes Th2 responses through three routes simultaneously, including induction of Th2 feature cytokine production, selectively enhancing the growth of Th2 cells, and down-regulation of Th1-inducing factors.[118] IL-2 has been known as one of the essential cytokines required for Th2 responses. It has been shown *in vivo* in mouse models that the neutralization of IL-2 inhibits the production of IL-4.[119] During a Th2 response, IL-2 binds to its receptor, IL-2R, inducing the recruitment, phosphorylation, and homodimerization of STAT5, and STAT5 contributes to Th2 cytokine production.[107] T-cell receptor activation and other co-stimulatory stimuli (e.g. OX40 and CD28), contribute to Th2 responses by recruiting interferon regulatory factors 4 (IRF4) and Basic Leucine Zipper ATF-Like Transcription Factor (BATF).[107] IRF4 and BATF promote GATA3 transcription.[107] GATA-3 helps stabilize Th2 chromosome conformation; NLRP3, BATF, IRF5, and dimerized STAT5 permit optimal Th2 cytokine production.[107] Often beginning in childhood, type 2-high asthma is associated with Th2 responses. Th2 cytokines, such as IL-4, IL-5, and IL-13, lead to abundant infiltration of eosinophils in airways, mucus overproduction, and allergen-specific IgE production.[120] Blocking IL-13 and IL-4 simultaneously by addressing neutralizing antibodies protected the mice from airway hypersensitivity responses.[121]

In a form of IBD called ulcerative colitis (UC), increased *IL5, IL13, and IL33* mRNA transcripts are found in inflamed colonic biopsies compared to healthy control biopsies.[122] IL-5 can promote eosinophil infiltration to inflamed sites in the intestine in UC patients.[123] Another study showed significantly higher IL-13 levels produced by lamina propria mononuclear cells in UC patients compared to CD patients and healthy controls.[124] Therefore, overactive Th2 responses can have detrimental effects in both the lung and gut.

1.1.6 The Role of CD8+ T cells in Health and Diseases

At steady state, naïve CD8+ T cells have a minimal cytotoxic effect against altered cells. During infection or abnormal cell growth (e.g. cancer), antigenic peptides are synthesized in the cell cytosol, and they can be presented on MHC I molecules on the cell surface.[1] Alternatively, antigens (i.e. cancer cells, pathogens) can be ingested, processed and presented by APCs such as DCs and macrophages to be presented through cross-presentation pathways on MHC I molecules.[1] The coreceptor CD8 is also required for the activation of CD8+ T cells. The activation of CD8+ T cells triggers the degranulation of effector enzymes, including perforin and granzymes.[125] Perforin functions in forming pores in the plasma membrane of the target cells, and granzymes can enter the target cells either through those pores or through the mannose-6-phosphate receptor.[126] The most abundant and well-studied granzyme is granzyme B. Granzyme B cleaves after aspartic residues, and it induces cell death via cleavage of caspase 3 and triggers caspase-induced cell death; an alternative way of granzyme B killing is through mitochondria permeabilization.[125] Activated CD8+ T cells can also kill target cells via Fas ligand/Fas ligand receptor interactions. This recognition triggers an increased level of Fas ligand-receptor to be expressed on the cell surface and also caspase 8 activation, eventually inducing cell death in target cells.[127] Aside from being killer T cells, activated CD8+ T cells can also produce cytokines such as IFN-γ, which can activate various immune cells and promote the clearance of infections or tumours.

1.2 IFN General Introduction

1.2.1 Discovery, History and Classification of IFNs

As a group of immune proteins, interferons (IFNs) play an essential role in host defence against viruses and other pathogens. Like other cytokines, IFNs act as signalling messengers and are vital in maintaining homeostasis and clearing infections. Distinguished by the distinct receptor they use, the current classification of human interferons includes three families: Type I interferons (IFN-α, IFN-β, IFN-ε, IFN-κ and IFN-ω), type II interferons (IFN-γ), and type III interferons (IFN-λ1-4).[128] 46 years later after the discovery of type I IFNs, type III IFNs (also known as IFN-lambdas (λs)) were first identified as redundant IFNs produced to supplement the function of type I IFNs at epithelial tissues and mucosal sites.[129,130] All humans express IFN-λ1-3, and mice only express IFN-λ2 and IFN-λ3.[131,132,133] Human *IFNL4* was considered a non-functional pseudogene, while later researchers found that a significant proportion of humans have a certain frameshift

mutation in their gene due to a single nucleotide polymorphism (SNP), which allows their *IFNL4* gene to function.[134,135,136]

1.2.2 The Source and Antiviral Functions of Type III IFNs in Different Tissues

The major sources of type III IFNs are epithelial cells and dendritic cells, which are induced after PRRs and recognition of PAMPs and DAMPs.[137] In one of the pathways that induce type III IFN production, PRRs, which include TLRs and retinoic acid-inducible gene I-like receptors, recognize PAMPs, which leads to the activation of PRRs. This is followed by the recruitment and activation of adaptor proteins (e.g. MyD88), allowing the activation of a number of proteins, such as interferon regulatory factor (IRF) 3/7 and NF-κB.[138] Eventually, IRF3/7 enters the nucleus and activates IFN-λ expression upon binding the enhancer or promoter region of IFN genes.[138]

IFN-λs exhibit potent antiviral activities. In human cornea explants and mouse corneas, IFN-λ treatment enhanced interferon-stimulated genes (ISGs) and inhibited Zika virus and herpes simplex virus-1 dissemination.[139] IFN-λs reduced the blood-brain-barrier permeability and inhibited West Nile virus infections of the brain.[140] Published data from our group showed that IFN-λ3 pretreatment significantly reduced the percentage of HIV-infected CD4+ T cells compared to media alone.[141] During gastrointestinal viral infections with rotavirus and norovirus, IFN-λs are the main type of IFN produced in epithelial cells.[142,137] IFN-λs also protect mice from respiratory infections such as influenza A virus.[137] Our group showed that IFN-λ accelerates SARS-CoV-2 viral clearance, especially in those individuals with high viral load if given within 7 days of symptom onset.[143] Phillips *et al*. showed that pegylated (peg)-IFN-λ enhanced NK cell functions, IFN-γ production by hepatitis B virus (HBV)-specific CD4+ T cells, and the cytotoxic functions of HBV-specific CD8+ T cells in livers.[144] Last but not least, HIV-induced syncytium formation in macrophages and the spread of HIV-1 infection were also inhibited by IFN-λs.[145,141]

1.2.3 The Effects of Type III IFNs on Other Microbial Infections

Besides their well-known function in antiviral immunity, IFN-λs also play a role in controlling bacterial and fungal infections. The induction of IFN-λs had been shown during *Listeria monocytogenes* and *Salmonella typhimurium* infections in the gastrointestinal tract, *Staphylococcus aureus* and *Pseudomonas aeruginosa infections* in the lung, and *Borrelia burgdorferi* infections. [146-149] IFN-λ-pretreated T84 cells (a colon carcinoma cell line) also have greatly reduced epithelial barrier disruption, measured by trans-epithelial electrical resistance *in*

vitro, post-*Salmonella* inoculation compared to non-IFN-λs-pretreated cells.[150] While IFN-λs act against multiple types of infections, there are cases where IFN-λs can contribute to pathogenesis. *Ifnlr1* KO mice had less severe *Staphylococcus aureus* infections in the airway and lung when treated with IL-1β compared to wild-type mice. They also had reduced neutrophil elastase and caspase-1.[151] In addition, for *Klebsiella pneumoniae* infections, IFN-λ promoted respiratory tract epithelial permeability and bacterial transmigration, leading to worsened bacteremia; meanwhile, *Ifnlr1 KO* mice were protected from those exacerbations.[152] In the context of fungal infections, IFN-λs are crucial in inducing TNF production, reactive oxygen species, and extracellular traps in neutrophils upon *Aspergillus fumigatus* infections leading to invasive aspergillosis.[153]

1.2.4 The Detrimental Effects of Type III IFNs In Autoimmunity

Although not as well studied, IFN-λs can also contribute to autoimmunity. In a specific type of rheumatoid disease, systematic lupus erythematosus (SLE), IFN-λs have been associated with autoimmune CD11c+T-bet+CD21- B cell subsets; IFN-λs also speed up the process of plasma cell differentiation, rendering the disease more severe.[154] One of the key hallmarks of SLE is autoantibodies against cell nucleus materials; a positive correlation has been shown between IFN-λ1 levels and nucleosome-specific autoantibodies levels in the serum of SLE patients.[155] In addition, Goel *et al*. showed that IFN-λs promote immune cell recruitment by keratinocytes, and knocking out *Ifnlr1* decreased renal IgG level and lupus severity in a murine model.[156]

1.2.5 IFN-λ Receptor Components

IFN-λR1 and IL-10RB are the two components that make up the type III IFN receptor. IFN-λs bind to IFN-λR1 with a higher affinity than to the very low-affinity subunit IL-10RB.[131,157] Unlike ubiquitously expressed type I IFN receptor components IFN-αR1/IFN-αR2 and IL-10RB, IFN-λR1 was previously only demonstrated to be expressed on specific cell types, such as epithelial cells, including keratinocytes and gastrointestinal tract epithelial cells but not on the majority of immune cells.[158,159] The highest levels of IFN-λR1 were observed in the gastrointestinal tract and lungs, with the lowest levels seen in the brain.[160] A potential mechanism proposed back then to explain the disparity between IFN-λ receptor levels and responsiveness is the release of soluble IFN-λR1 (sIFN-λR1) by immune cells; Witte et al. showed that this short-splicing variant of IFN-λR1 has a moderate affinity for IFN-λ1 ligands, can compete for binding of IFN-λ1 to membrane-bound IFN-λR1, and, therefore, inhibits IFN-λR signalling.[161] Santer *et*

al. confirmed this mechanism by showing that sIFN-λR1 significantly inhibited ISG induction by at least 54%. Intriguingly, sIFN-λR1 achieved this inhibitory effect while promoting IFN-λ ligand binding to monocytes.[141]

IL-10 family cytokines, which includes structurally similar IL-10, IL-19, IL-20, IL-22, IL-24, IL-26, IL-29 (IFN-λ1), IL-28A (IFN-λ2), and IL-28B (IFN-λ3), play essential roles in protecting epithelial tissues from infections and inflammation.[162] Among these, IL-10, IL-19, IL-22, IL-26, IFN-λ1, IFN-λ2, and IFN-λ3 all use the IL-10RB component as their low-affinity second receptor subunit.[162] It has been shown that IL-10 can reduce the signalling of IFN-λ1 and downstream IL-6 induction in human PBMCs, with a proposed mechanism that IL-10 can compete for IL-10RB receptor component binding with IFN-λ1.[163] Meanwhile, IL-22 promoted IFN-λ signalling and rotavirus clearance in mice by up-regulating STAT1 phosphorylation.[164,136] This indicates that the interaction between IL-10 family cytokines is more complicated than the sharing of receptor components.

The majority of IFN-λR studies have used mice models due to the availability of *ifnlr1* KO mice that concretely show that IFN-λ signalling is essential for mucosal antiviral immune responses.[165-167] Our group and others have now shown that while most epithelial cells in both mice and humans express IFN-λR1, we now know that immune cells between the species vary dramatically in their responsiveness to type III IFNs.[141,168-171] (summarized in **Figure 7)**. In the mouse immune system, only specific DCs and CD11b+ neutrophils directly respond to IFN-λs or express the high-affinity IFN-λR component *Ifnlr1*;[131,137,172,173] In humans, plasmacytoid dendritic cells (pDCs) express the highest levels of *IFNLR1*, followed by myeloid DCs and B cells, with lower levels in macrophages and CD8+ T cells and undetectable levels in monocytes, NK cells, and surprisingly neutrophils (**Figure 7**).[141,174,175] The IFN-λR distribution disparity between humans and mice may lead to missing key immunoregulation mechanisms in mouse models. Therefore, it is essential to broaden our knowledge of IFN-λR1 signalling and expression regulation in humans. Also of note is that all studies to date have based their findings on mRNA levels due to the lack of good antibodies to IFN-λR1.

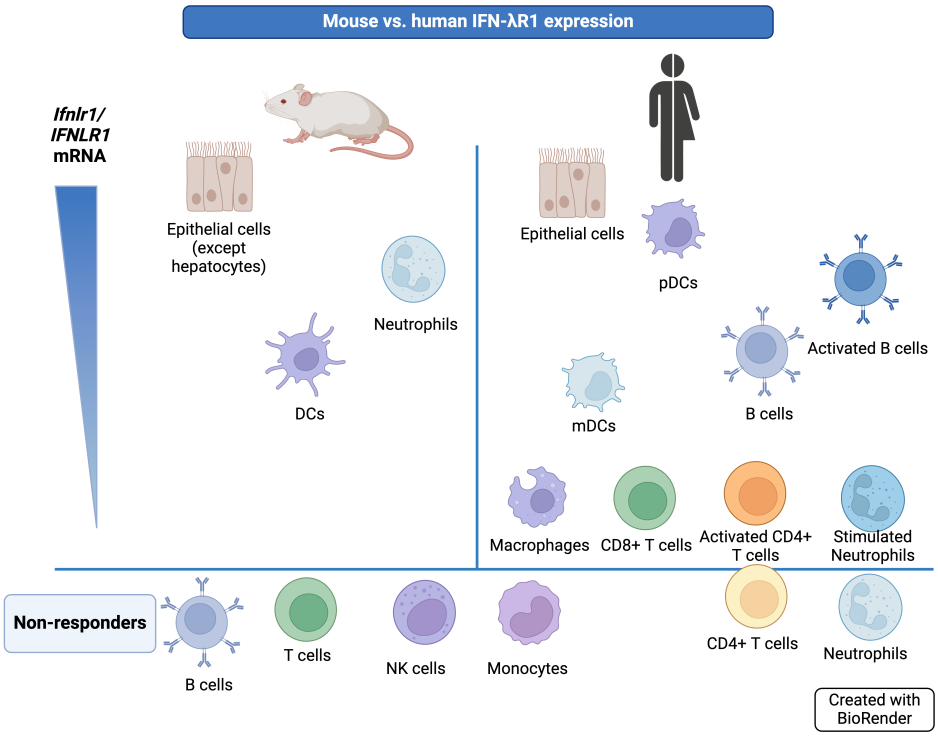

Figure 7. The differential expression of *IFNLR1* in mice and humans.

The differential expression of *IFNLR1* mRNA in mice (left) and humans (right). The up-and-down position of a given cell type in the figure indicates the *IFNLR1* levels on that cell type relative to other cell types shown. Dendritic cells (DCs); mDCs (myeloid DCs); pDCs (plasmacytoid DCs). Activation of B cells refers to B cell receptor stimulation, activation of CD4+ T cells refers to T cell receptor stimulation and stimulated neutrophils refers to toll-like receptor stimulation, all *in vitro*.

1.2.6 Type III IFN Receptor Direct Signaling Through JAK-STAT

Type III IFN signalling initiates upon IFN-λs binding their receptor (**Figure 8**). When IFN-λ binds IFN-λR1, it leads to the conformation change of the extracellular receptor component, followed by the recruitment of IL-10RB. The dimerization of IFN-λR permits the activation of kinases, including tyrosine kinase 2 (TYK2), associated with IL-10RB, and Janus kinase 1 (JAK1), associated with IFN-λR1. [138,157] Activated TYK2 and JAK2 phosphorylates the intracellular IFN-λR, followed by the recruitment and phosphorylation of signal transducer and activator of transcription 1 (STAT1) and STAT2.[138,176] A previous study showed that the TYK2 deficient cell line had a minimal impairment of IFN-λ-induced viral control, indicating TYK2 is not required for functional IFN-λ signalling in certain cell types.[177] Phosphorylated STAT1 and STAT2 then

heterodimerize and bind IRF9 as the IFN-stimulated gene factor 3 (ISGF3) complex. ISGF3 then enters the cell nucleus and binds IFN sensitive response element (ISRE) in the promoter region of ISGs, activating the transcription of many ISGs.[176]

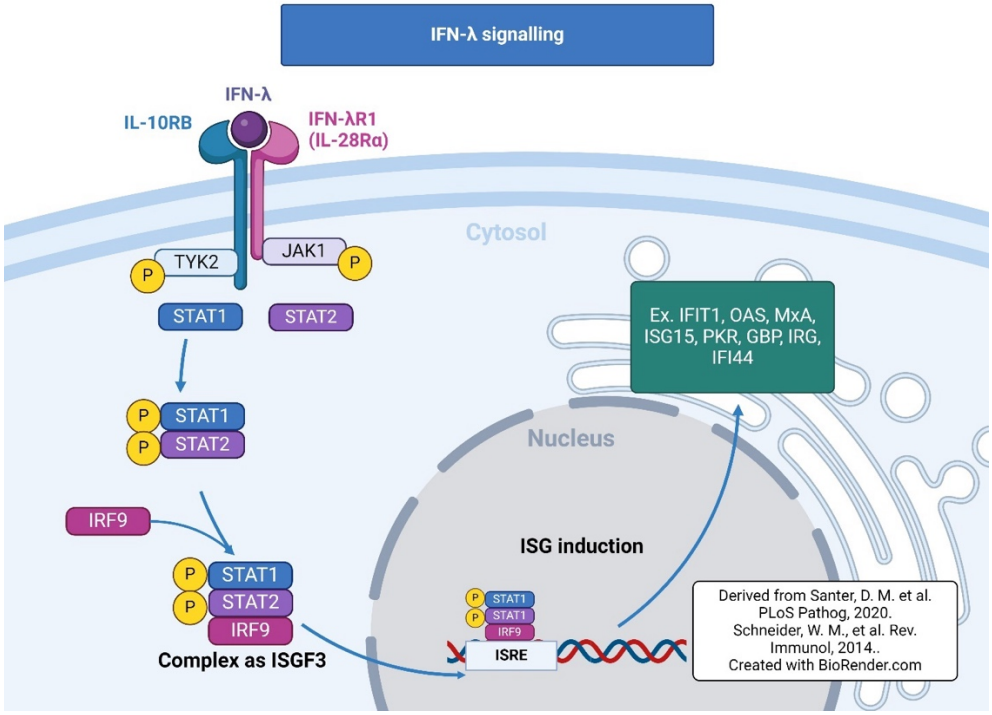

Figure 8. IFN-λ JAK-STAT signalling.

Upon binding IFN-λR1, IFN-λ induces the recruitment of IL-10RB and the dimerization of IFN-λR. TYK2 and JAK1, associated with IL-10RB and IFN-λR1, respectively, get phosphorylated and activated, allowing the autophosphorylation of TYK2 and JAK1. STAT1 and STAT2 are then recruited and phosphorylated, which leads to the heterodimerization and the binding of IRF9, forming the ISGF3 complex. The ISGF3 complex then translocate into the cell nucleus and binds to a specific DNA sequence (ISRE) in the ISG promoter, leading to the induction of hundreds of ISGs. Interferon regulatory factors (IRF), interferon-stimulated gene (ISG), signal transducer and activator of transcription (STAT), Janus kinase (JAK), tyrosine kinase 2 (TYK2). Created with BioRender.com.

1.2.6.2 Type III IFN Signalling Through MAPK

A combination of IFN-λ1, 2 and 3 induced the phosphorylation of p38 and ERK, but not JNK in a colonic cell line, but other signaling pathways downstream of IFN-λR1 are not as well studied.[137] The essential role of MAPK in IFN-λ-induced antiviral functions against respiratory syncytial virus has been shown by inhibition of p38 and JNK.[178] Meanwhile, in Raji cells (a Burkitt

lymphoma cell line), IFN-λ stimulated p38 and JNK, not ERK phosphorylation.[179] JNK and ERK phosphorylation upon IFN-λ1 and IFN-λ2 stimulation were also confirmed using HT-29 (a colorectal adenocarcinoma cell line) and primary intestinal epithelial cells.[180] Lastly, IFN-λs do not trigger canonical STAT phosphorylation in fibroblasts.[181] Instead, IFN-λ1 induces MxA production in an ERK-dependent manner.[176,181] These observations indicate that there is a disparity between IFN-λ signalling pathways among IFN-λ-responsive subsets of cells.

1.3 The Immune-Regulation Functions of Type III IFNs

1.3.1 The Immune-regulation Functions of Type III IFNs on T cells

Although less studied thus far, we are learning there are unique immune-modulation functions of type III IFNs on T cells. One of the contexts in which IFN-λ is being studied as an immune regulator is in Th2-high airway hypersensitivities. Airway hypersensitivity murine models are used to study hypersensitivities in the respiratory tract, such as asthma. A series of allergens, such as dust mites, air pollutants, and other chemicals, can be recognized by PRRs and induce cytokine production in airway epithelial cells. Some epithelial cell-derived cytokines, such as TSLP, IL-25, and IL-33, can induce Th2 cytokine production by basophils, type 2 innate lymphoid cells (ILC2s), and Th2 cells.[182] Jordan *et al*. showed that IFN-λ dampened IL-13 secretion during (1) mitogen stimulation, (2) mixed lymphocyte reaction, and (3) the activation of naïve T cells through IFN-λ-pretreated myeloid DCs (mDCs).[183] Koltsida *et al*. showed that IFN-λ2 overexpression by an adenovirus reduced the infiltration counts of eosinophils, neutrophils, and lymphocytes in bronchoalveolar lavage fluid (BALF) in the ovalbumin (OVA)-induced airway hypersensitivity mice model; Th2 and Th17 cytokine production, such as IL-13, IL-5, IL-10, and IL-17 were down-regulated in mesenteric lymph nodes of mice that had IFN-λ2 overexpression. Interestingly, IFN-γ levels in this model were upregulated, indicating that IFN-λ2 may be able to modulate the balance between Th1 and Th2 responses in mice. This was achieved through an indirect CD11c+ DCs- and IFN-γ-dependent mechanism, partially due to mouse T cells not expressing IFN-λR1 on their surfaces.[184] Li *et al*. showed a similar inhibitory effect of IFN-λ1 on Th2 cytokines in the OVA-induced airway hypersensitivity model, and they found that this inhibition and the reduction in disease severity is associated with an increasing number of Treg cells and declined levels of serum IgE.[185] Lastly, Won *et al*. showed that IFN-λ2/3 downregulated Th2-inducing cytokines from airway epithelial cells in a house dust mite-induced mice hypersensitivity model, such as TSLP and IL-33 in the BALF.[186,187] Other studies showed that

IFN-λ3 protects mice from OVA-induced hypersensitivity through an NK cell-dependent manner, indicated by the abolition of protection when NK cells were depleted.[188] A similar inhibition effect of IFN-λ3 on Th2 cytokines was seen in papain (a plant-derived protease)-induced hypersensitivity mice model.[189] Taken together, IFN-λs clearly regulate Th2 responses in the mouse lung, no matter the allergic asthma model attempted to date.

The functions of IFN-λs to regulate Th2 responses have been more intensively studied in mice; however, due to the differential IFN-λR1 distribution between mice and humans, it is necessary to investigate the immune-modulation functions in the human system. In humans, DCs treated with IFN-λ significantly promote the proliferation of CD25+Foxp3+ CD4+ Treg cells.[190] Our group has previously shown that IFN-λ3-pretreated PBMCs from healthy donors had significantly lower levels of Th2 cytokines production (IL-4, IL-5, IL-9, and IL-13) during 5-day H1N1 antigen stimulation compared to non-IFN-λ3-pretreated PBMCs. [191] More studies are needed to determine how IFN-λs directly regulate human T cell subsets instead of the potentially indirect actions mentioned above.

1.3.2 The Immune-regulation Functions of Type III IFNs on Other Immune Cells

Besides T cells, IFN-λs can regulate other immune cells. IFN-λ1 increases the number of T-bet+ B cells upon BCR and TLR7/8 stimulation; it also promotes human plasmablast differential and IgM production via enhancing the mTORC pathway in naïve B cells.[154,192] IFN-λ3-treated memory B cells have significantly decreased proliferation capacity upon H1N1 antigen stimulation compared to non-IFN-λ3-treated memory B cells.[191] TLR and BCR-induced B cell proliferation, IL-10 and IL-6 production, and TLR7/8-induced IgG and IgM production are also augmented by IFN-λs.[193] The production of IL-12B, IL-23A, and IL-27A is increased in macrophages by IFN-λ treatment.[194] At the early onset of collagen-induced arthritis in a murine model, IFN-λ2 dampened the neutrophil infiltration into the joint.[195] Lastly, IFN-λs greatly restrict intestinal inflammation in a murine colitis model by inhibiting the production of reactive oxygen species in TNF and lipopolysaccharide-stimulated neutrophils.[169] Altogether, type III IFNs have multiple mechanisms to dampen or promote specific types of immune responses, but the limiting factor is the expression of the IFN-λR1 subunit for which cells are directly affected.

1.4 Overall Dissertation Overview: Rationale, Hypothesis and Objectives

1.4.1 Rationale

The protein level of the IFN-λ receptor on the surface of different immune cell types had never been directly studied; in addition, data from us and others have shown that the distribution of the IFN-λ receptor is different between mice and humans. Therefore, it is important to investigate the regulation of IFN-λR1 on the human T cell surface. IFN-λs dampen Th2 cytokine production, especially in mouse models. However, this regulation depends on the type of stimulation the T cell receives and is not fully understood. For some Th2-high hypersensitivities, there is an urgent need to identify potential therapeutic intervention supplementing currently available treatment, and IFN-λ can, therefore, be a good candidate. Before we fully go into evaluating the therapeutic potential of IFN-λs, we need to have a further understanding of how the regulation of IFN-λ occurs in finer detail. Furthermore, it is still unclear how IFN-λ influences CD8+ T cell activation and functions.

1.4.2 Hypothesis

TCR stimulation specifically upregulates the unique, high-affinity IFN-λ receptor component (IFN-λR1) level on the human CD4+ and CD8+ T cell surface via a CD3-dependent manner, which promotes IFN-λ3 downregulation of Th2 polarization and enhancement of CD8+ T cell functions.

1.4.3 Research Aims

This dissertation has three main aims:

1. To quantify IFN-λR at the protein level on human T cells at baseline and after activation/polarization.
2. To investigate the regulatory effect of IFN-λ3 on polarization and cytokine production of CD4+ T cell lineages (Th1, Th2).
3. To profile the effect of IFN-λ3 on the transcriptome of CD8+ T cells at baseline and during TCR stimulation.

1.5 Significance

This is the first study to examine IFN-λR1 at the protein level on human T cell subsets and how the receptor is regulated by TCR activation on the T cell surface. We also are learning about

the regulatory effects of IFN-λ3 on Th2 immune responses and the universal impact of IFN-λ3's effect on human CD8+ T cells (genes/pathways). This fundamental knowledge can help us further understand IFN-λ biology and establish a base for evaluating IFN-λ3 as a potential therapeutic candidate for Th2-high hypersensitivities or inflammation. The initial studies of IFN-λ effects on CD8+ T cells serve as a starting point to understand if IFN-λs could be used to, for example, boost specific CD8+ T cell activation pathways.

CHAPTER 2. MATERIALS AND METHODS

2.1 Whole PBMCs Processing from the Human Healthy Donor

2.1.1 Ethics Statement

Human ethics protocols for blood collection were approved by the University of Manitoba Biomedical Research Ethics Board (No. HS25252). All blood donors gave written informed consents in accordance with the Declaration of Helsinki. The demographic information (including the age and the sex of the blood donor) was collected with consent during the blood collection and handled according to expectations around the Personal Health Information Act at the University of Manitoba.

2.1.2 Blood Donor Recruitment

Healthy donors (HD) were recruited from people aged between 18 and 65 who claimed no major medical concerns. A detailed checklist was provided to donors before blood donation to evaluate the eligibility of participation in the study, which includes inquiries regarding whether the donor has chronic conditions (i.e. diabetes, cancer, inflammatory bowel diseases, celiac, rheumatoid arthritis), whether the donor has a fear of needles or is prone to fainting, whether the donor is taking any long-term medications, and whether the donor is having or had any type of infections, including SARS-CoV-2 in the last a couple of weeks. The donors are eligible for the study if they deny all the questions above.

2.1.3 Peripheral Blood Mononuclear Cells (PBMCs) Isolation

Fresh blood was drawn from healthy donors using a Safety-Lok Blood Collection Set (BD Vacutainer) and stored at room temperature in a sodium heparin tube blood collection tube (BD Vacutainer) until it was processed (within 1 hour). PBMCs were then isolated using Lymphoprep (Stemcell Technologies) gradient centrifugation (acceleration 5, deceleration 0, 800 g, 22 ^{o}C, 23 mins). Pasteur pipettes were then used to pool lymphocyte layers from different tubes, followed

by a wash with DPBS (Gibco) and centrifugation (acceleration 9, deceleration 9, 500 g, 22 ºC, 15 mins). Pellets were resuspended with DPBS and centrifuged (acceleration 9, deceleration 8, 180 g, 10 ºC, 11 mins). After aspiration, cells were resuspended in complete RPMI 1640 media and counted using a Hemacytometer and Trypan Blue Stain (0.4%) (Gibco). The cell suspension was kept at 4ºC and ready for downstream experiments.

2.2 Primary Cell Stimulation

2.2.1 T Cell Enrichment and Purity Check

2.2.1.1 T Cell Enrichment (negative selection)

For naïve CD4+ T cell enrichment, PBMCs from *2.2.3* were incubated with EasySep Human Naïve CD4+T Cell Isolation Kit (Stemcell Technologies) for negative selection, following the manufacturer's protocol. Briefly, PBMCs (maximum 100 million) in complete RPMI 1640 media were spun at 400 g, 7 mins, at 4ºC, then resuspended in Stemcell buffer [1 mM Ethylenediaminetetraacetic acid (EDTA) (Thermo Scientific) in 2% FBS (Corning) in DPBS (Gibco)] at 50 million cells/mL. Cells were then transferred to a 5-mL Polystyrene round-bottom tube (sterile) (Falcon) and incubated with Biotinylated anti-CD45RO antibody and Isolation cocktail (both provided in the kit) at 50 uL/ 1 mL of the sample at room temperature for 5 mins. After vortexing, RapidSpheres™ (Beads) (provided in the kit) was added to the cell suspension at 50 uL / 1 mL of sample and incubated at room temperature for 5 mins. Stemcell buffer was then added to top up the cell suspension final volume to 2.5 mL, and the 5-mL Polystyrene round-bottom tube with cell suspension was then placed into an EasySep™ Magnet (Stemcell technologies) and incubated at room temperature for 5 mins. The cell suspension was then poured in one motion without touching the tube to a new 5-mL Polystyrene round-bottom tube and incubated in EasySep™ Magnet at room temperature for a second 5 mins. The cell suspension was then poured in one motion without touching the tube into a sterile 15-ml Conical centrifuge tube (Thermo Fisher, cat# 339650), topped up with 3 mL of complete RPMI 1640 media and centrifuged at 400 g, 7 mins, at 4ºC. The pellet was resuspended in 1 mL of complete RPMI 1640 media and then counted using a Hemacytometer and Trypan Blue Stain (0.4%) (Gibco, cat # 15250-061). The cell suspension was kept at 4ºC until being cultured. The total number of naïve CD4+ T cells obtained ranged from 1.75 to 4.525 million.

For total CD4+ T cells and total CD8+ T cells enrichment, PBMCs from *2.2.3* were incubated with EasySep Human CD4+ T Cell Enrichment Kit (Stemcell Technologies) and EasySep Human CD8+ T Cell Enrichment Kit (Stemcell Technologies) for negative selection, following the manufacturer's protocol. The protocols are similar to EasySep Human Naïve CD4+T Cell Isolation Kit (Stemcell Technologies) protocol but with incubation using respective antibodies/cocktail type and the amount indicated in the manufacturer's instructions. The total number of CD4+ T cells and CD8+ T cells obtained ranged from 29.45 to 32 million, and from 11.1 to 16.55 million, respectively.

2.2.1.2 Enriched T Cell Purity Check

The purity of putative naïve CD4+ T cells was evaluated using flow cytometry, where after *Naïve CD4+ T cell isolation,* at least 0.2 million cells were distributed into each of three 1.2 mL microtiter tubes (Fisherbrand), designated to be "unstained control," "all stained," and "CD45RA FMO" tube. Cells were washed with DPBS (Gibco) and then resuspended in Flow buffer (for the "unstained control") or staining cocktails (for the "all stained" and the "CD45RA FMO" tube), followed by a 25-min incubation at 4ºC in tin foil in the fridge. The staining cocktail for the "CD45RA FMO" tube contains the following antibodies: PE-Cy7 anti-CD4 (Invitrogen), FITC anti-CD8 (BioLegend), APC-Cy7 anti-CD19 (BioLegend), and AF700 anti-CD3 (BioLegend). The staining cocktail for the "all stained" tube contains all antibodies used for the "CD45RA FMO" tube and BV421 anti-CD45RA (BioLegend). All antibodies were diluted in Flow buffer (recipe included in **Table 6**). After the incubation and washing, the Fixation buffer was added to fix cells for 15 minutes at room temperature in the dark. Cells were then topped up by 600 uL of Flow buffer and spun at 400 g. 7 mins at 4 ºC, and then resuspended in 350 uL Flow buffer. Flow cytometry data was obtained from CytoFLEX LX (Beckman Coulter) with configuration listed in **Table 1**. FlowJo software (v10, BD Biosciences) was used for data analysis and graph generation. Only putative naïve CD4+ T cells, with a purity ≥ 94% (the percentage of CD3-positive, CD8-negative, CD4-positive, and CD45RA-positive cells in single cell gate), were used for downstream experiments.

For the total CD8+ T cell purity check, similar protocols were conducted as above, but only the "unstained control" and "all stained" tubes were used. The staining cocktail for total CD8+ T cell purity checks for the "all stained" tube contains the following antibodies: PE-Cy7 anti-CD4

(Invitrogen), FITC anti-CD8 (BioLegend), APC-Cy7 anti-CD19 (BioLegend), and BV421 anti-CD3 (BioLegend).

Table 1. CytoFLEX LX configuration.

Laser	Mirror/filter	Detection range	Fluorochrome
Violet (405nm)	450/50 BP	425-475	Pacific blue, 4′,6-diamidino-2-phenylindole (DAPI), V450, BV421, eFluor450
	525/40 BP	505-565	AmCyan, V500, BV510
	610/20 BP	600-620	BV605
	660/20 BP	650-670	BV650
	763/42 BP	742-784	BV785 (*BV711 available by request)
Blue (488nm)	525/40 BP	505-545	FITC, Alexa488, CFSE, GFP
	610/20 BP	600-620	PE-Texas red, PE-CF594, propidium iodide
	690/50 BP	665-715	PerCP / PerCP-Cy5.5
Yellow/green (561nm)	585/42 BP	564-606	PE, dsRed, PI
	610/20 BP	600-620	mCherry, ECD, PE-Texas red, PI, PE-CF594
	675/30 BP	660-690	PE-Cy5, PerCP
	710/50 BP	685-735	PE-Cy5.5, PerCP-Cy5.5
	763/42 BP	742-784	PE-Cy7, PE-Alexa750
Red (638nm)	660/20 BP	650-670	APC, Alexa647, Cy5
	712/25 BP	700-724	Alexa700
	763/42 BP	742-784	APC-cy7, APC-H7, APC-eFluor780

This table was adapted from the "Equipment Additional Detail" section of the Flow Cytometry Core Facility Website at the Rady Faculty of Health Sciences, University of Manitoba. (https://umanitoba.ca/health-sciences/research/flow-cytometry/equipment#cytoflex-lx)

2.2.1.3 Th1, Th2 cell polarization with IFN-λ3 treatment

Anti-CD3 (BioLegend) was diluted in DPBS (Gibco) to 2 μg/mL and then added to wells in U-bottom non-treated 96-well tissue culture plate (Avantor (VWR)). The 96-well plate was then transferred to a cell incubator at 37ºC and let sit for 2 hours. After 2 hours and right before cell seeding, anti-CD3 (BioLegend) in DPBS was aspirated, washed with 1xDPBS once, and aspirated. Naïve CD4+ T cells from *Naïve CD4+ T cell isolation (negative selection)* were seeded to anti-CD3 (BioLegend) coated wells with Th0 [1.5 μg/mL anti-CD28 (BioLegend) only], Th1 [1.5 μg/mL anti-CD28 (BioLegend), 5 ng/mL IL-12 (BioLegend), and 5 μg/mL anti-IL-4 (BioLegend)], and Th2 [0.5 μg/mL anti-CD28, 20 ng/mL IL-4 (BioLegend), 5 μg/mL anti-IFN-γ (BioLegend), and 50 IU IL-2 (BioLegend)] polarization cocktails. IFN-λ3 was added to wells where applicable at 100 ng/mL. On day 3, the plate was centrifuged at 300 g, 20ºC for 7 mins, cell supernatants were collected and stored in the -80 freezer for future Enzyme-linked immunosorbent assay (ELISA) analyses; Th1, Th2, Th0 cytokines and IFN-λ3 were replenished by adding to the wells at 2x concentration in RPMI 1640 complete media for Th1, Th2, and Th0 with or without IFN-λ3 conditions; on Day 6, Th2 cytokines and IFN-λ3 were replenished again. The cells were transferred from a 96-well Tissue Culture Plate (Avantor (VWR)) to a 48-well Tissue Culture Plate (Avantor (VWR)). The cells treated with Th0 and Th1 polarization conditions were incubated at 37ºC with 5% CO_2 in a cell incubator and collected on Day 6 for flow staining and downstream analysis and on Day 9 for the Th2 polarization condition.

2.3.2 Cell Stimulation for IFN-λR Studies

For IFN-λR quantification of PBMC with stimulation, anti-CD3 (BioLegend) was diluted to 0.03 or 0.3 μg/mL using 1×DPBS (Gibco) and then added to a 24-well plate (Thermo Scientific). The 24-well plate was then transferred to a cell incubator at 37ºC and let sit for 2 hours. After 2 hours and right before cell seeding, anti-CD3 in DPBS was aspirated, washed by adding 600 uL 1×DPBS, and aspirated. Cells were seeded to the wells right after the aspiration so the anit-CD3 coating would not dry out. Anti-CD28 (BioLegend) and PHA-L (Invitrogen) were diluted using complete RPMI 1640 media (recipe listed in **Table 6**) and added to wells at a final concentration of 1.5 μg/mL and 1 μg/mL where applicable. Cells were cultured in complete RPMI 1640 media incubated at 37ºC and supplemented with 5% CO_2 in a cell incubator and collected after 24 and 72 hours.

For experiments with drug treatment of PBMCs, PBMCs from healthy donors were pre-incubated for 1.5 hours at 37 ºC in a cell incubator with different inhibitors, including PI3K inhibitor Duvelisib (Selleck chem/ Cedarlane), JNK inhibitor sp600125 (Stemcell Tech), ZAP70 inhibitor ZAP 180013 (Biotechne, Tocris Bioscience), and calcineurin inhibitor FK506 (Cedarlane) in a 24-well plate (Thermo Scientific). Then, PBMCs were transferred to wells pre-coated with 0.3 μg/mL anti-CD3 as introduced above and incubated at 37 ºC in a cell incubator supplemented with 5% CO_2 for 20 hours.

For CD4+ T cell IFN-λR quantification with stimulation, a protocol similar to the above was conducted, but anti-CD3 (BioLegend) was diluted to 1 or 3 μg/mL to coat the plate for stimulating enriched total CD4+ T cells. Cells were cultured in complete RPMI 1640 media incubated at 37ºC and supplemented with 5% CO_2 in a cell incubator and collected after 36 hours.

2.3.3 PBMCs Stimulation for the Effects of IFN-λ3 on Th1 and Th2 Cytokine Production Studies

To investigate the effects of IFN-λ3 on PBMC cytokine production, PBMCs were stimulated as stated in *2.3.2*, but the concentration for anti-CD3 well coating was 1.5 μg/mL and anti-CD28 was 4.47 μg/mL in media. UofA IFN-λ3 (provided by Dr. Wakarchuk, University of Alberta), which had been tested by others in the Santer lab and found to be as potent as commercially available IFN-λ3 (R&D Systems), was added to wells at 100 ng/mL where applicable. Cells were incubated at 37ºC and supplemented with 5% CO_2 in a cell incubator and collected after 48 hours.

2.3.4 Total CD8+ T cell Stimulation

To examine the impact of IFN-λ3 on CD8+ T cells with and without TCR stimulation cultured with IFN-λ3 (100 ng/mL) (from Dr. Wakarchuk, University of Alberta) in complete RPMI 1640 media (Gibco) (recipe included in **Table 6**). For the TCR stimulation condition, 24-well plates (Thermo Scientific) were precoated with anti-human CD3 (BioLegend) at 3 μg/mL for 2 hours at 37ºC, similar to *2.3.2*, then washed with 1×DPBS (Gibco) right before adding cells to the plate; anti-human CD28 (BioLegend) was added to cell suspension at 1.5 μg/mL. Cells were incubated at 37ºC and supplemented with 5% CO_2 in a cell incubator and collected after 20 hours.

2.3.5 Post-culture Cell and Supernatant Collection

When collecting cells, cell suspensions were thoroughly mixed by pipetting up and down and then were collected and centrifuged at 400 g, 4ºC for 7 minutes. The supernatant was collected and stored in a -80ºC freezer for downstream protein quantification using ELISA. Cell pellets were then resuspended in 1xDPBS (Gibco) and centrifuged at 400 g, 4ºC for 7 minutes again to reduce the RPMI 1640 media residues. TRIzol (Ambion by Life Technologies) was then used to resuspend the cell pellets, and the cell suspension was stored in a -80ºC freezer until used for the production of cDNA.

2.3 PBMCs and CD8+ T cell surface IFN-λR1 quantification

2.3.1 Extracellular IFN-λR Staining

1.5 million cells (PBMCs) or 1 million cells (enriched CD4+ T cells) isolated from healthy donor blood were distributed into a 1.2 mL microtiter tube (Fisherbrand) for Day 0 baseline staining. Stimulated cells collected on Day 1 and Day 3 (PBMCs), or Day 1.5 (enriched CD4+ T cells) were stained using a 96-well micro-test plate (Sarstedt AG&Co).

Cell viability was quantified using Zombie AQUA Dye (BioLegend) with 1 in 1000 dilution in 1xDPBS, stained for 20 mins, and covered with tin foil at 4ºC. Samples were then washed with Flow buffer (recipe indicated in **Table 6**) and blocked using TruStain FcX (BioLegend) diluted in Flow buffer (recipe listed in **Table 6**) for 10 mins at room temperature to reduce the antibody unspecific binding. Without washing off the block, 2 μg/mL biotinylated mAb08-hIFN-λR1 or flow buffer (for FMO samples) was added to the cells and incubated for 45 min at 4 ºC, 0.33 mg/mL Cells were then washed with Flow buffer twice. After that, streptavidin–PE (SA-PE) (eBioscience) was added to detect biotin-labelled IFN-λR1 antibody, together with other staining antibodies: BUV496 anti-CD19 (BD Horizon), BUV395 anti-CD4 (BD Horizon), AF700 anti-CD3 (BioLegend), BUV737 anti-CD8 (BD Biosciences), BUV496 anti-CD14 (eBioscience), Super Bright 780 anti-CD56 (eBioscience), PE anti-CD210b (IL-10RB) (BioLegend), APC anti-CD71 (eBioscience), Alexa Fluor 488 anti-CD62L (BioLegend), Brilliant Violet 421 anti-CD45RA (BioLegend) (all listed in **Table 5**) and Brilliant Stain Buffer Plus (BD Horizon) to identify different cell populations (listed in **Table 3**) and incubated for 40 mins after wash, covered with foil at 4 ºC. After 2-time washing with Flow buffer, Flow fixation buffer (2% paraformaldehyde (made from 8% paraformaldehyde (PFA), diluted in 1xDPBS, Electron

Microscopy Sciences)) (recipe included in **Table 6**) was added to fix cells for 15 mins at room temperature in the dark, followed by another washing step and resuspension of cells using 350 uL Flow buffer Samples were covered with foil and stored at 4 ^{o}C until being analyzed on LSRFortessa (BD Biosciences) with the configuration listed in **Table 2**. FlowJo software (v10, BD Biosciences) was used for data analysis and graph generation, and **Table 3** guides how each cell type and subset studied were identified.

2.3.2 Compensation Control for Flow Cytometry

For compensation control, briefly, 100 uL of Flow buffer was added to a 5 mL polystyrene round-bottom tube for each compensation control, followed by adding antibodies listed in **Table 5** when the respective colour is used in the panel. After careful vortex, one full drop of the BD Compensation Beads Negative Control (BD) and one full drop of the BD Compensation Beads Anti-Mouse Ig, k beads (BD) were added to each tube, followed by a spin at 160 g for 1 min at room temperature. Each compensation control tube was then vortexed for 5 seconds and incubated at room temperature for 25 minutes, covered by tin foil to avoid exposure to direct light. After the incubation, each compensation control tube was topped up using 3 mL of Flow buffer, followed by a spin at 250 g for 10 minutes at room temperature. After spin, the liquid phase in each compensation control was removed by decanting once in a single motion; then, the leftover was resuspended with 350 uL Flow buffer. The compensation control tubes were stored in a 4^{o}C fridge covered by tin foil until being analyzed and were discarded two weeks after being made.

Table 2. LSRFortessa configuration.

Laser	Mirror/filter	Detection range	Fluorochrome
Blue 50mW 488nm solid state	505LP, 530/30	515-545	FITC, GFP, Alexa488
	685LP, 710/50	685-735	PerCP-Cy5.5
Red 40mW 633nm solid state	670/14	663-667	APC, Alexa647, Cy5
	690LP, 730/45	708-752	Alexa700
	50LP, 780/60	750-810	APC-Cy7, APC-H7
Violet 50mW 405nm solid state	450/50	425-475	Pacific blue, DAPI, V450, BV421
	505LP, 525/50	505-550	AmCyan, CFP, V500, BV510
	600LP, 610/20	600-620,	BrilliantViolet605

	630LP, 670/30	655-685	BrilliantViolet650
	690LP, 710/50	685-735	BrilliantViolet711
	750LP, 780/60	750-810	BrilliantViolet786
Yellow Green50mW 561nm solid state	545LP, 586/16	578-594	PE
	600LP, 610/20	600-620	PE-Texas Red
	635LP, 670/30	655-685	PE-Cy5
	750LP, 780/60	750-810	PE-Cy7
UV 20mW 355nm solid state	379/28	365-393	BUV395
	450LP, 515/30	500-530	BUV496
	690LP, 740/35	723-757	BUV737

This table was adapted from the "Equipment Additional Detail" section of the Flow Cytometry Core Facility Website at the Rady Faculty of Health Sciences, University of Manitoba. (https://umanitoba.ca/health-sciences/research/flow-cytometry/equipment#fortessa)

Table 3. The list of markers used to identify various cell types in PBMCs.

Cell types/subtypes	Markers
CD56-high NK cells	CD14-CD19-CD56^{high}CD3-
CD56-mid NK cells	CD14-CD19-CD56^{mid}CD3-
NK T cells	CD14-CD19-CD56+CD3+
Total CD4+ T cells	CD14-CD19-CD56-CD3+CD8-CD4+
Central memory CD4+ T cells	CD14-CD19-CD56-CD3+CD8-CD4+CD62L+CD45RA-
Effector memory CD4+ T cells	CD14-CD19-CD56-CD3+CD8-CD4+CD62L-CD45RA-
Effector memory with CD45RA phenotype CD4+ T cells	CD14-CD19-CD56-CD3+CD8-CD4+CD62L-CD45RA+
Naïve CD4+ T cells	CD14-CD19-CD56-CD3+CD8-CD4+CD62L+CD45RA+
Total CD8+ T cells	CD14-CD19-CD56-CD3+CD8+CD4-
Central memory CD8+ T cells	CD14-CD19-CD56-CD3+CD8+CD4-CD62L+CD45RA-

Effector memory CD8+ T cells	CD14-CD19-CD56-CD3+CD8+CD4-CD62L-CD45RA-
Effector memory with CD45RA phenotype CD8+ T cells	CD14-CD19-CD56-CD3+CD8+CD4-CD62L-CD45RA+
Naïve CD8+ T cells	CD14-CD19-CD56-CD3+CD8+CD4-CD62L+CD45RA+

2.4 Examining the Effect of IFN-λ3 on PBMCs and CD8+ T cell Stimulation at the mRNA Level.

2.4.1 RNA Extraction

RNA extraction was performed using cell pellets collected and a Direct-zol RNA MicroPrep kit (Zymo Research), following the manufacturer's instructions. Briefly, an equal volume of Ethyl Alcohol Anhydrous (LES Alcools) was used to dilute cell lysate in TRIzol (Ambion by Life Technologies). The diluted lysate was then transferred to a Zymo-Spin™ IC Column (provided in the kit) in a Collection Tube (provided in the kit) and centrifuged. The samples were then treated with DNase I (provided in the kit) for 15 mins at room temperature, followed by prewash using Direct-zol™ RNA PreWash (provided in the kit) and wash using RNA Wash Buffer (provided in the kit) respectively. RNA was then eluted with UltraPure Distilled Water (Invitrogen) into 1.7 mL Microtubes (Axygen). RNase AWAY (Molecular BioProduct) was used to clean the countertop and equipment. RNA concentration and purity (A260/280 ratio) were measured on a NanoDrop Lite Spectrophotometer (Thermo Fisher Scientific).

2.4.2 cDNA Preparation

The extracted RNA was then used to prepare a cDNA mix using UltraPure Distilled Water (Invitrogen) and SuperScript IV VILO Master Mix (Invitrogen). cDNA was prepared using an S1000 Thermal Cycler (BIO-RAD), using the following program: Step 1: 25°C for 10 mins; Step 2: 50°C for 10 mins; Step 3: 85°C for 5 mins. The cDNA obtained was stored in a -20°C freezer until being used for downstream analyses.

2.4.3 Real-time Reverse Transcription Polymerase Chain Reaction (RT-qPCR)

All data was obtained using the QuantStudio™ 3 Real-Time PCR System (Applied Biosystems) or Roche LightCycler (Roche Diagnostics GmbH). For the QuantStudio 3 system, ROX passive reference dye was embedded in the program before or after data acquisition to

normalize differences within each run. Primers used in RT-qPCR including *IL13*, *TNF*, *IFNG*, *IL2*, *GZMB*, *IFIT1*, *IFI44*, *mIFNLR1*, *sIFNLR1*, and *IL4*. Primers (details included in **Table 5**), UltraPure distilled water (Invitrogen), and the PowerSYBR Green PCR Master Mix (Applied Biosystems) were used to make the master mix. The master mix for samples was loaded using a repeater pipette (E3, Eppendorf) into either a 0.1 mL 96-well plate (Applied Biosystems) if using QuantStudio 3 or LightCycler 480 Multiwell Plate 96 (Roche Diagnostics) if using Roche LightCycler System, under an AirClean 600 PCR Workstation (AirClean Systems). After loading all samples, a piece of MicroAmp Optical Adhesive Film (Applied Biosystems) was used to seal the plate, followed by centrifugation (1000 rpm, 1 min, 10 °C) using the program described in **Table 4**. A comparison of reference genes was conducted by calculating the standard deviation of Cq of each reference gene candidate using PRISM10 and GeNorm (https://genorm.cmgg.be/). The data was processed using QuantStudio™ Design & Analysis Software for the QuantStudio3 system or LightCycler® 96 SW 1.1 for the Roche LightCycler.

Table 4. RT-qPCR program used in transcription analysis of IFN-λ3-treated PBMCs.

Program	Cycle	Step	Acquisition mode
Preincubation	1	95°C for 600s	None
Power SYBR	40	95°C for 15s	None
		60°C for 60s	Single
Melting	1	95°C for 10s	None
		60°C for 60s	None
		97°C for 1s	Continuous

2.4.4 CD8+ T cell RNA Sequencing Sample Preparation, Validation, and Data Processing

RNA concentration was determined with the NanoDrop 1000 spectrophotometer (NanoDrop Technologies), and RNA quality was assessed with the Agilent Bioanalyzer 2100 (Agilent Technologies). All samples passed Novogene's quality control (QC) test for both RNA sample quality and sequencing quality. Bulk RNA sequencing data was analyzed using R (version 4.3.2). Gene set enrichment analysis (GSEA) was done on ranked differential gene expression data to identify overrepresented pathways using GSEA (version 4.3.2). Visualization of

overrepresented pathways was done using Cytoscape (version 3.10). Data cleaning and processing were done with the help of Dayhoff Technologies and Testimony Olumade in the Santer lab.

2.5 Cytokine secretion analyses using the enzyme-linked immunosorbent assay (ELISA)

2.5.1 ELISA

ELISA kits used to detect cytokine in cell supernatant following manufacturer's instructions, including ELISA MAX Deluxe Set Human IFN-γ kit (BioLegend), Human IFN Gamma Uncoated ELISA Kit (Invitrogen), Human IL-13 Uncoated ELISA Kit (Invitrogen), Human TNF alpha Uncoated ELISA Kit (Invitrogen), and DuoSet Human Granzyme B (R&D Systems). All shaking in this ELISA section used a Microplate Genie Digital Shaker (Scientific Industries) at 600 rpm. EIA/RIA No Lid 96 Well Easy Wash Plate (Costar) was coated with the coating antibody diluted in the coating buffer (provided in the kit) or 1x DPBS on a plate shaker at 4^{o}C overnight. After washing three times using ELISA wash buffer (recipe included in **Table 6**) and decanted, plates were loaded with a blocking agent, either ELISA diluent [1% BSA (Sigma) in DPBS (Gibco)] or 1x reagent diluent (provided in the kit), decanted and followed by another three times of washing. Samples were diluted on a non-treated, 96 wells-U, sterilized Tissue Culture Plate (Avantor (VWR)) using ELISA diluent (provided in ELISA kit or 1%BSA in DPBS depending on specific kit) and then loaded to the blocked 96-well plate with standards in duplicate, followed by 2-hour incubation with shaking at room temperature. After 2 hours of incubation and three times washing with ELISA wash buffer, Detection antibodies (provided in the kit) were loaded onto the plate and incubated for 1.5 hours at room temperature with shaking after decanting. Then, the plate was washed and decanted, loaded with Streptavidin-HRP (provided in each kit) and incubated for 30 mins covered by tin foil at room temperature with shaking. After three times washing, a substrate solution (provided by each kit) was loaded onto the plate after washing and aspirating the plate, followed by 30-min incubation covered by tin foil at room temperature with shaking. Stop solution (R&D Systems) systems were added to terminate the reaction. Optic reading was obtained from Spectra MAX 190 Spectrophotometer (Molecular Devices), with a wavelength correction done using the reading at 570 nm minus the reading at 450 nm. Data analysis was done using a standard curve and calculation by SoftMax Pro Software (Molecular devices).

2.5.2 Intracellular flow staining evaluating the impact of IFN-λ3 on naïve CD4+ T cell polarization.

Cells collected from Th1 and Th2 cell polarization with IFN-λ3 treatment were transferred to 1.2 mL microtiter tubes, then topped up by adding 700 uL DPBS and spin at 350 g, 4ºC, for 7 mins. They were then resuspended using 1x Intracellular staining stimulation master mix (recipe included in **Table 6**) and incubated for 5 hours at 37ºC in a cell incubator with 5% CO_2. Cell viability was evaluated using Zombie AQUA Dye (BioLegend), stained for 20 mins, and covered with tin foil at 4ºC. Samples were then washed with the Flow buffer (recipe included in **Table 6**) and blocked using ChromPure Human IgG (Jackson Immuno Research Laboratories INC) diluted in Flow buffer to 150 μg/mL for 30 mins at room temperature to reduce the antibody unspecific binding. After washing, the Flow fixation buffer (recipe included in **Table 6**) was added to fix cells for 15 mins at room temperature in the dark, followed by washing using the flow buffer. Perm wash buffer [Intracellular Staining Perm Wash Buffer (10x) (BioLegend) diluted in MilliQ water to make 1x] was then used to permeabilize the cells, followed by resuspending cells in either Th1 [AF488 anti-IFN-γ (BioLegend)] or Th2 [PE anti-IL-13 (BioLegend), APC anti-IL-4 (Invitrogen) and AF488 anti-IFN-γ (BioLegend)] cytokine staining cocktail diluted in the Perm wash buffer, incubate for 40 mins in tin foil at 4 ºC in the fridge. Samples were analyzed on LSRFortessa (BD Biosciences). FlowJo software (v10, BD Biosciences) was used for data analysis and graph generation.

2.6 Statistical Analyses

All analyses were performed using PRISM 10.2.2. For all comparisons, the normality of each group was first determined by the Shapiro-Wilk test, D'Agostino & Pearson test, Anderson-Darling test, and Kolmogorov-Smirnov test determined whether each data set follows (Gaussian) normality, and then one-way ANOVA was used to compare groups. If a group of data passes all four tests, it is considered normal, which follows the Gaussian distribution (parametric); if not, then it is considered not following the Gaussian distribution and is non-parametric. Then, if two groups are compared, a t-test is performed, and the normal results are used to select the "experiment design" section of the t-test (parametric or non-parametric). If more than two groups are compared in the same panel and if all data follows the Gaussian distribution, then one-way or two-way-ANOVA was used; non-parametric tests were used otherwise. For one-way and two-way analysis, if there is a significant difference observed between groups, the multiple comparisons

were made using Tukey's multiple comparisons test or Dunnett's multiple comparison test, respectively.

For correlation studies, data groups were first tested for normality using the Anderson-Darling, D' Agostino & Pearson, Shapiro-Wilk, and Kolmogorov-Smirnov tests. If the data set passes all four tests mentioned above, it is considered to follow a Gaussian distribution; otherwise, it is considered not to follow a Gaussian distribution. Then, all data set comparisons were computed using Pearson correlation coefficients (when following a Gaussian distribution) or non-parametric Spearman correlation (when not following a Gaussian distribution).

2.7 Figure generation

Wherever indicated, figures were generated using BioRender.com. The flow dot plots were generated through FlowJo™ v10.8 Software (BD Life Sciences). X-Y plots or bar graphs were generated using GraphPad Prism version 10.0.0 (GraphPad Software).

2.8 Reagents, equipment, and other materials used in the experiments included in this dissertation.

Table 5. Reagents, equipment, and other materials used in the experiments.

REAGENT or RESOURCE	SOURCE	IDENTIFIER
Blood drawing supply		
Safety-Lok Blood Collection Set	BD Vacutainer	cat# 367281
Sodium heparin tube blood collection tube	BD Vacutainer	cat# 367874
Reagents / other materials		
Lymphoprep™ Density gradient medium	Stemcell Technologies	cat# 07851/07861
DPBS(1X) (Dulbecco's Phosphate-Buffered Saline) without calcium & magnesium	Gibco	cat# 14190-144
Trypan Blue Stain (0.4%)	Gibco	cat # 15250-061
Ethylenediaminetetraacetic acid (EDTA), 0.5 M Solution, Molecular Biology Grade, Ultra-pure	thermo scientific	cat# J15694-AE
Dimethyl Sulfoxide (DMSO)	Sigma Life Science	D2650-100ML
Phytohemagglutinin-L (PHA-L) Solution	Invitrogen	cat# 00-4977-93

Dynabeads Human T-Activator CD3/CD28	Gibco	cat# 11161D
ImmunoCult Human CD3/CD28 T cell Activator	Stemcell Technologies	cat# 10971
Duvelisib (IPI-145)	Selleck chem/ Cedarlane	cat# S7028
sp600125	Stemcell Tech	cat# 72642
ZAP 180013, 10 mg, Tocris Bioscience	Biotechne, Tocris Bioscience	cat# 6821/10
FK506, 5x10 mg	Cedarlane	cat# INH-FK5-5
TRIzol Reagent	Ambion by life technologies	cat# 15596026
Ethyl Alcohol Anhydrous	LES Alcools	cat# P006EAAN (OR P016EA95)
RNase AWAY	Molecular BioProduct	cat# 7002
UltraPure Distilled Water	Invitrogen	cat# 10977
SuperScript IV VILO Master Mix	Invitrogen	cat# 11756050
PowerSYBR Green PCR Master Mix	Applied Biosystems	cat# 4367659
Paraformaldehyde 8% Aqueous solution, EM Grade	Electron Microscopy Sciences	cat# 157-8-100
Brilliant Stain Buffer Plus	BD Horizon	cat# 566385
Zombie AQUA Dye	BioLegend	cat# 77143
Zombie NIR Dye	BioLegend	cat# 77184
Human TruStain FcX	BioLegend	cat# 422302
ChromPure Human IgG, whole molecule	Jackson Immuno Research Laboratories INC	cat# 009-000-003
Cell Stimulation Cocktail (500X)	Invitrogen (eBioscience)	cat# 00-4970-93
Intracellular Staining Perm Wash Buffer (10x)	BioLegend	cat# 421002
Brefeldin A solution (1000X)	BioLegend	cat# 420601

BD CompBeads Negative Control	BD	cat# 51-90-9001291
BD CompBeads Anti-Mouse Ig, k	BD	cat# 51-90-9001229
Recombinant Human IFN-beta	R&D SYSTEMS	cat# 8499-IF-010/CF
UofA IFN-λ3 (2023)	provided by Dr. Wakarchuk, University of Alberta	NA
Recombinant Human IL-28B/IFN-lambda 3 Protein	Bio-Techne	5259-IL-025/CF
Ultra-LEAF Purified anti-human IL-4 (clone 8D4-8)	BioLegend	cat# 500838
Ultra-LEAF Purified anti-human IFN-γ (clone 4S.B3)	BioLegend	cat# 506532
Ultra-LEAF Purified anti-human CD28 (clone CD28.2)	BioLegend	cat# 302934
Ultra-LEAF Purified anti-human CD3 (clone HIT3a)	BioLegend	cat# 300331
Recombinant Human IL-2 carrier-free	BioLegend	cat# 589104
Recombinant human IL-12 (p70) carrier-free	BioLegend	cat# 573002
Recombinant human IL-4 carrier-free	BioLegend	cat# 574002
Recombinant Human IL-2 carrier-free	BioLegend	cat# 589104
EasySep™ Magnet	Stemcell technologies	cat# 18000
Substrate Reagent Pack	R&D Systems	DY999B
Stop Solution (15 x 6 mL)	R&D Systems	DY994
Kits		
EasySep Human CD4+ T Cell Enrichment Kit	Stemcell technologies	cat# 19052
EasySep Human CD8+ T Cell Enrichment Kit	Stemcell technologies	cat# 19013

EasySep Human Naïve CD4+T Cell Isolation Kit	Stemcell technologies	cat# 19555
Direct-zol RNA MicroPrep 50 preps	ZYMO Research	cat# R2060
ELISA MAX Deluxe Set Human IFN-γ	BioLegend	cat# 430104
Human IFN Gamma Uncoated ELISA Kit	Invitrogen	cat# 88-7316-88
Human IL-13 Uncoated ELISA Kit	Invitrogen	cat# 88-7439-88
Human TNF alpha Uncoated ELISA Kit	Invitrogen	cat# 88-7346-88
DuoSet Human Granzyme B (5 plate)	R&D Systems	cat# DY2906-05
Agilent RNA 6000 Nano Kit (kindly provided by Dr. Neeloffer Mookherjee)	Agilent Technologies	cat# 5067-1511
Primers		
Primer: HPRT Primer 1: 5'-CCCCAAAATGGTTAAGGTTGC-3' Primer 2: 5'-AACAAAGTCTGGCCTGTATCC-3'	IDT (Integrated DNA Technologies)	ref# 308728418
Primer: hRPL13A R Primer: 5'-TTG AGG ACC TCT GTG TAT TTG TCA A-3'	IDT (Integrated DNA Technologies)	ref# 304888491
Primer: hRPL13A F Primer: 5'-CCT GGA GGA GAA GAG GAA AGA GA-3'	IDT (Integrated DNA Technologies)	ref# 304888490
Primer: hIFI44 F Primer: 5'-CCA CCG AGA TGT CAG AAA GAG-3'	IDT (Integrated DNA Technologies)	ref# 304888496
Primer: hIFI44 R Primer: 5'-TGG TAC ATG TGG CTT TGC TC-3'	IDT (Integrated DNA Technologies)	ref# 304888497
Primer: hIFIT1 F	IDT (Integrated DNA Technologies)	ref# 304888492

Primer: 5’-AGA AGC AGG CAA TCA CAG AAA A-3’		
Primer: hIFIT1 R Primer: 5’-CTG AAA CCG ACC ATA GTG GAA AT-3’	IDT (Integrated DNA Technologies)	ref# 304888493
Primer: hSDHA (Geigges) R Primer: 5’-CTC CAT GTT CCC CAG AGC AG-3’	IDT (Integrated DNA Technologies)	ref# 304888512
Primer: hSDHA (Geigges) F Primer: 5’-CTC CAT GTT CCC CAG AGC AG-3’	IDT (Integrated DNA Technologies)	ref# 304888511
Primer: hHPRT1 F Primer: 5’-TGA CAC TGG CAA AAC AAT GCA-3’	IDT (Integrated DNA Technologies)	ref# 304888488
Primer: hHPRT1 R Primer: 5’-TGA CAC TGG CAA AAC AAT GCA-3’	IDT (Integrated DNA Technologies)	ref# 304888498
Primer: hGUSB F Primer: 5’-AAG TCC TTC ACC AGC AGC G-3’	IDT (Integrated DNA Technologies)	ref# 304888505
Primer: hGUSB R Primer: 5’-CCA CGG TGT CAA CAA GCA T-3’	IDT (Integrated DNA Technologies)	ref# 304888506
Hs_IL13_1_SG (IL13)	QIAGEN	cat# QT00000511
Hs_B2M_1_SG (B2M)	QIAGEN	cat# QT00088935
Hs_IL2_1_SG (IL2)	QIAGEN	cat# QT00015435
Hs_IFNG_1_SG (IFNG)	QIAGEN	cat# QT00000525
Hs_TNF_1_SG (TNF)	QIAGEN	cat# QT00029162
Primer: mIFNLR1 743 F CACGGGCCCTGGACTTTTCT	IDT (Integrated DNA Technologies)	ref# 304888498

Primer: m/s IFNLR1 R CTGCAAGGTCCTTCTTCCATCTT	IDT (Integrated DNA Technologies)	ref# 304888499
Flow cytometry antibodies used in actual staining		
BUV395 Mouse Anti-human CD4 antibody clone SK3	BD Horizon	cat# 563550
AF700 anti-human CD3 antibody clone UCHT1	BioLegend	cat# 300424
BUV737 anti-human CD8 antibody clone SK1	BD Biosciences	cat# 564629
BUV496 anti-human CD19 antibody clone SJ25C1	eBioscience (Invitrogen)	cat# 364-0198-41
BUV496 anti-human CD14 antibody clone 61D3	eBioscience (Invitrogen)	cat# 364-0149-41
Anti-Hu CD56 (NCAM) Super Bright 780 antibody clone TULY56	eBioscience (Invitrogen)	cat# 78-0566-41
PE anti-human CD210b (IL-10RB) Antibody clone S17009F	BioLegend	cat# 396803
Anti-human CD71 APC antibody clone OKT9	eBioscience (Invitrogen)	cat# 01-0719-42
Alexa Fluor 488 anti-human CD62L antibody clone dreg-56	BioLegend	cat# 304816
Brilliant Violet 421 anti-human CD45RA antibody clone HI100	BioLegend	cat# 304130
Brilliant Violet 421 anti-human CD69 antibody clone FN50	BioLegend	cat# 310929
Alexa Fluor 488 anti-human IFN-γ clone 4S.B3	BioLegend	cat# 502517
PE Anti-human IL-13 antibody clone JES10-5A2	BioLegend	cat# 501903
APC Anti-human IL-4 antibody clone 8D4-8	eBioscience (Invitrogen)	cat# 17-7049-41

APC/Cy7 anti-human CD19 antibody clone HIB19	BioLegend	cat# 302218
FITC anti-human CD8 antibody clone SK1	BioLegend	cat# 344704
Anti-human CD4-PE/Cy7 antibody clone RPA-T4	Invitrogen (eBioscience)	cat# 25-0049-41
PE-SA (Streptavidin) clone NA	eBioscience	cat# 12-4317-87
Flow cytometry antibodies/reagents used in compensation control		
BV510 anti-human CD4 clone SK3	BioLegend	cat# 344633
APC anti-human CD307e (FcRL5) clone 509Ff6	BioLegend	cat# 340305
BUV395 Mouse Anti-Human CD4 clone SK3	BD Horizon	cat# 563550
BUV496 Mouse Anti-Human CD19 clone SJ25C1	BD Horizon	cat# 612938
BV421 anti-human CD24 clone ML5	BioLegend	cat# 311100
PE anti-human CD45RB clone MEM-55	BioLegend	cat# 310204
AF488 anti-human CD11c clone Bu15	BioLegend	cat# 337236
BV786 Mouse anti-Human CD27 clone L128	BD Horizon	cat# 563327
BUV737 Mouse anti-Human CD38 clone HB7	BD Horizon	cat# 612824
PE/Cy7 anti-human CD21 clone Bu32	BioLegend	cat# 354912
AF700 anti-human CD45 clone 2D1	BioLegend	cat# 368514
APC/Cy7 anti-human CD3 clone UCHT1	BioLegend	cat# 300426
BD CompBeads Negative Control	BD	cat# 51-90-9001291
BD CompBeads Anti-Mouse Ig, k	BD	cat# 51-90-9001229
Machine and equipment		
AirClean 600 PCR Workstation	AirClean Systems	NA
Spectra MAX 190 Plate Reader (for ELISA)	Molecular Devices	NA
QuantStudio™ 3 Real-Time PCR System	Applied Biosystems	cat# A28567

LightCycler® 96 System	Roche Diagnostics GmbH	NA
NanoDrop Lite Spectrophotometer	Thermo Fisher Scientific	SN# 2983
S1000 Thermal Cycler	BIO-RAD	SN# SC007001
2100 Bioanalyzer Instrument	Agilent Technologies	NA
CytoFLEX LX Digital Flow Cytometry Analyzer	Beckman Coulter	NA
LSRFortessa Flow Cytometry Analyzer	BD	NA
Microplate Genie Digital Shaker	Scientific Industries	SN# M4A-1015
Consumables		
Nunc™ Cell-Culture Treated Multidishes, 24-well plate	Thermo Scientific	cat# 142475
5 mL Polystyrene Round-bottom tube (sterile)	Falcon (Fisher Scientific)	cat# 352054
5 mL polystyrene round-bottom tube (non-sterile)	Falcon (Fisher Scientific)	cat# 14-959-5
Tissue Culture Plate 96 wells, Round Bottom (treated)	Fisherbrand	cat# FB012932
Tissue Culture Plate, Non-treated, 48 well, sterilized	Avantor (VWR)	cat# 734-2780
Tissue Culture Plate, Non-treated, 96 wells U, sterilized	Avantor (VWR)	cat# 10861-564
Tissue Culture Plate, Nunclon Delta Surface, 24-well	Thermo Scientific	cat# 142475
Biosphere SafeSeal Tube 0.5 mL	Sarstedt AG&Co	cat# 72.704.200
Microtest plate 96-well, C (c = conical)	Sarstedt AG&Co	cat# 82.1583.001
15 ml Conical Centrifuge Tube, Bulk, Pack of 50	Thermo Fisher	cat# 339650
Microtiter tube	Fisherbrand	cat# 02-681-376

LightCycler 480 Multiwell Plate 96, white	Roche Diagnostics GmbH	cat# 4729692001
MicroAmp Fast 96-well Reaction Plate (0.1 mL)	Applied Biosystems	cat# 4346907
MicroAmp Optical Adhesive Film	Applied Biosystems	cat# 4311971
Software		
LightCycler® 96 SW 1.1	Roche Diagnostics GmbH	NA
QuantStudio™ Design & Analysis Software	Applied Biosystems	NA
GraphPad Prism version 10.0.0	GraphPad Software	NA
FlowJo™ v10.8 Software	BD Life Sciences	NA
SoftMax Pro Software (ELISA data acquisition and analysis)	Molecular Devices	SN# N02712

ref#, reference number; cat#, catalog number; NA, not applicable.

Table 6. Recipe for making buffer, media, or other reagents used in experiments.

Reagents	**Source**	**Cat#**
Complete RPMI 1640 media (supplemented with 10% FBS, 1% 2-4-(2-hydroxyethyl)-1-piperazineethanesulfonic acid (HEPES), 1%Penstrep, 1%Glutamax)		
RPMI Medium (1X) [-] L-Glutamine	Gibco	cat# 21870-076
Fetal Bovine Serum	Corning	cat# 35-077-CF
Pen Strep (Penicillin Streptomycin)	Gibco	cat# 15140-122
HEPES (1M) Buffer Solution	Gibco	cat# 15630-080
GlutaMAX (100X)	Gibco	cat# 35050-06
Complete OpTmizer CTS T-Cell Expansion media (supp1emented with % Pen Strep)		
OpTmizer CTS T-Cell Expansion Basal Medium	Gibco	cat# A10221-01
Pen Strep (Penicillin Streptomycin)	Gibco	cat# 15140-122
Complete ImmunoCult-XF T Cell Expansion Medium (supplemented with 1% Pen Strep and 1x Glutamax)		
Pen Strep (Penicillin Streptomycin)	Gibco	cat# 15140-122

GlutaMAX (100X)	Gibco	cat# 35050-06
ELISA blocking reagent/diluent (1%BSA in PBS)		
Bovine Serum Albumin	Sigma	cat# A9647-100G
DPBS(1X) (Dulbecco's Phosphate-Buffered Saline) without calcium & magnesium	Gibco	cat# 14190-144
ELISA wash buffer (0.05% Tween in 1% PBS)		
Sodium Phosphate Monobasic Monohydrate (500 g) $NaH_2PO_4 \cdot H_2O$	Fisher Scientific	cat# S369-500
Sodium Phosphate Dibasic Anhydrous (1kg) Na_2HPO_4	Fisher Scientific	cat# BP-332-1
Sodium Chloride (3 kg) NaCl	Fisher Chemical	cat# S271-3
Polysorbate 20 (Tween® 20)	Fisher BioReagents	cat# BP337-500
Flow buffer (2% FBS in 1x DPBS)		
Fetal Bovine Serum	Corning	cat# 35-077-CF
DPBS(1X) (Dulbecco's Phosphate-Buffered Saline) without calcium & magnesium	Gibco	cat# 14190-144
Flow fixation buffer (2%PFA diluted with 1xDPBS)		
DPBS(1X) (Dulbecco's Phosphate-Buffered Saline) without calcium & magnesium	Gibco	cat# 14190-144
Paraformaldehyde 8% Aqueous solution, EM Grade	Electron Microscopy Sciences	cat# 157-8-100
Intracellular staining stimulation cocktail (diluted with Complete RPMI 1640 media listed above to 1x)		
Cell Stimulation Cocktail (500X)	Invitrogen (eBioscience)	cat# 00-4970-93
Brefeldin A solution (1000X)	BioLegend	cat# 420601
Intracellular staining permeabilization wash buffer (Diluted in MilliQ water to 1x)		
Intracellular Staining Perm Wash Buffer (10x)	BioLegend	cat# 421002

Stemcell buffer (1 mM EDTA & 2%FBS in 1xDPBS)		
DPBS(1X) (Dulbecco's Phosphate-Buffered Saline) without calcium & magnesium	Gibco	cat# 14190-144
Fetal Bovine Serum	Corning	cat# 35-077-CF
Ethylenediaminetetraacetic acid (EDTA), 0.5 M Solution, Molecular Biology Grade, Ultra-pure	Thermo Scientific	cat# J15694-AE

CHAPTER 3. RESULTS

3.1 Aim 1. To quantify IFN-λR at the protein level on human T cells at baseline and after activation/polarization.

3.1.1 Investigate the Protein Levels of IFN-λR1 and IL-10RB at the Baseline on the Surface of CD4+ and CD8+ T cell Subsets.

Hypothesis: Human CD8+ T cells express a higher level of IFN-λR1 but a similar level of IL-10RB on the cell surface than CD4+ T cells at the steady state.

Previously, all IFN-λR1 studies relied on mRNA level detection or indirect quantification, such as histidine-tagged IFN-λ measurement.[196] To directly study IFN-λR1, we needed an antibody that can detect IFN-λR1 on the cell surface, which is the unique and high-affinity component of IFN-λR. Through collaboration with a company (PBL Assay Science) and two other labs, we recently identified and published two monoclonal antibodies specific for human IFN-λR1 derived from the same parental clone (HLR9 and HLR14) that our lab optimized for flow cytometry analyses. Both clones bound IFN-λR1 on various cell lines that are known to express IFN-λR1, including in Huh7.5 (hepatoma cell line), A549 (lung epithelial carcinoma cell line), Caco-2 (colon epithelial carcinoma), and Daudi cells (B cell lymphoblast, Burkitt's lymphoma cell line), with 40% to 80% positivity.[197] Using a biotinylated version of HLR14 for multi-colour flow cytometry, I performed the experiments with Olamide Ogungbola with Figure 4 in the publication, which shows for the first time the distribution of IFN-λR1 on total human CD4+ T cells, CD8+ T cells, B cells, and pDCs within PBMCs from 5 donors.[197] In the rest of my unpublished data, I used biotinylated HLR9 anti-IFN-λR1 to enable larger multi-colour flow cytometry panels to characterize IFN-λR1 levels on human T cell subsets at baseline and after activation.[197]

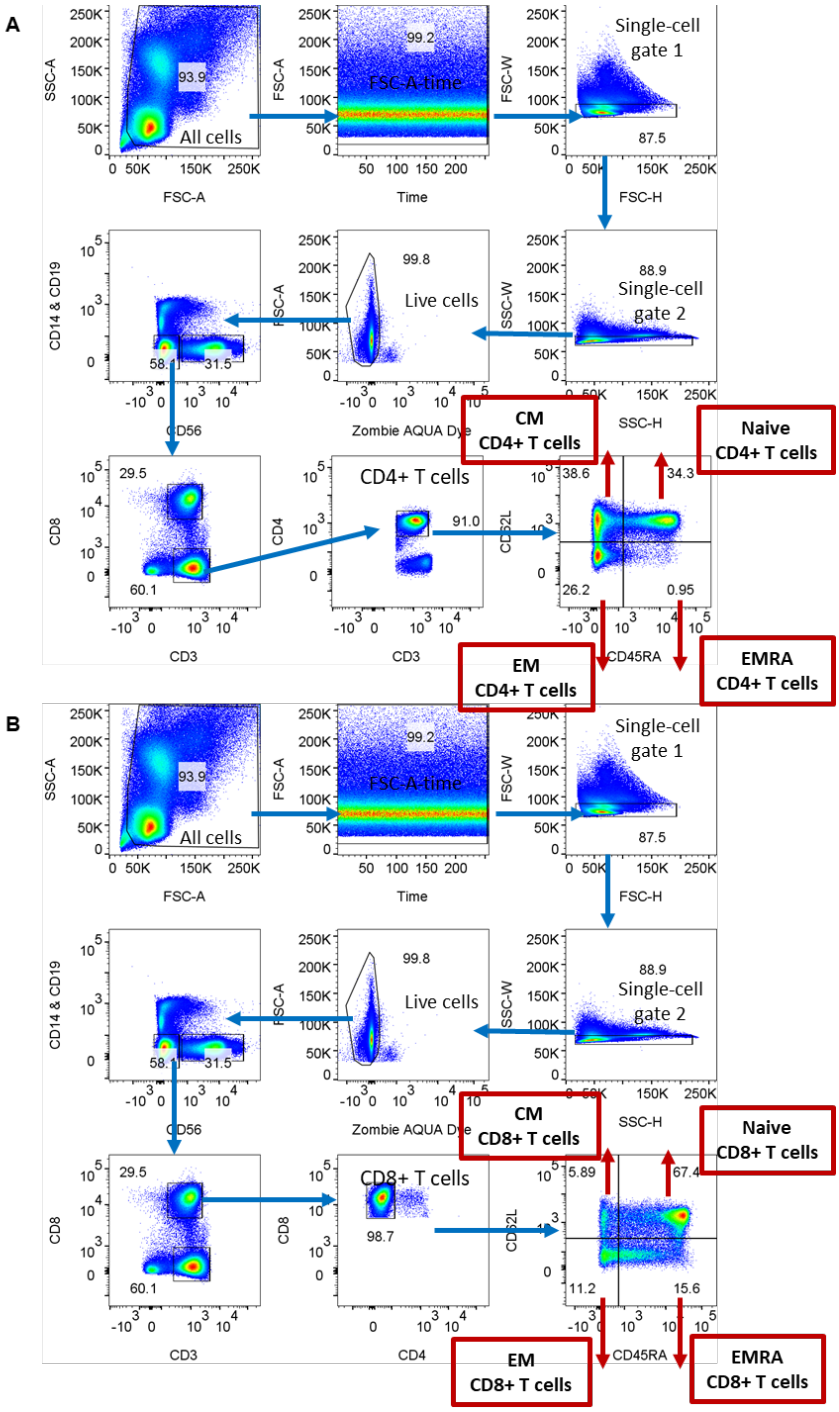

Figure 9. Gating strategy sample for CD4+ and CD8+ T cells in whole PBMCs.

Gating strategy for central memory (T_{CM}) (CM), effector memory (T_{EM}) (EM), effector memory with CD45 RA phenotype (T_{EMRA}) (EMRA), naïve (Naive), and total CD4+ T cells (A) and CD8+ T (B) cells are shown. Numbers in the flow dot plot represent the percentage of cells (events) of the respective gate of the parental population. The gating strategy is a representative of five experiments.

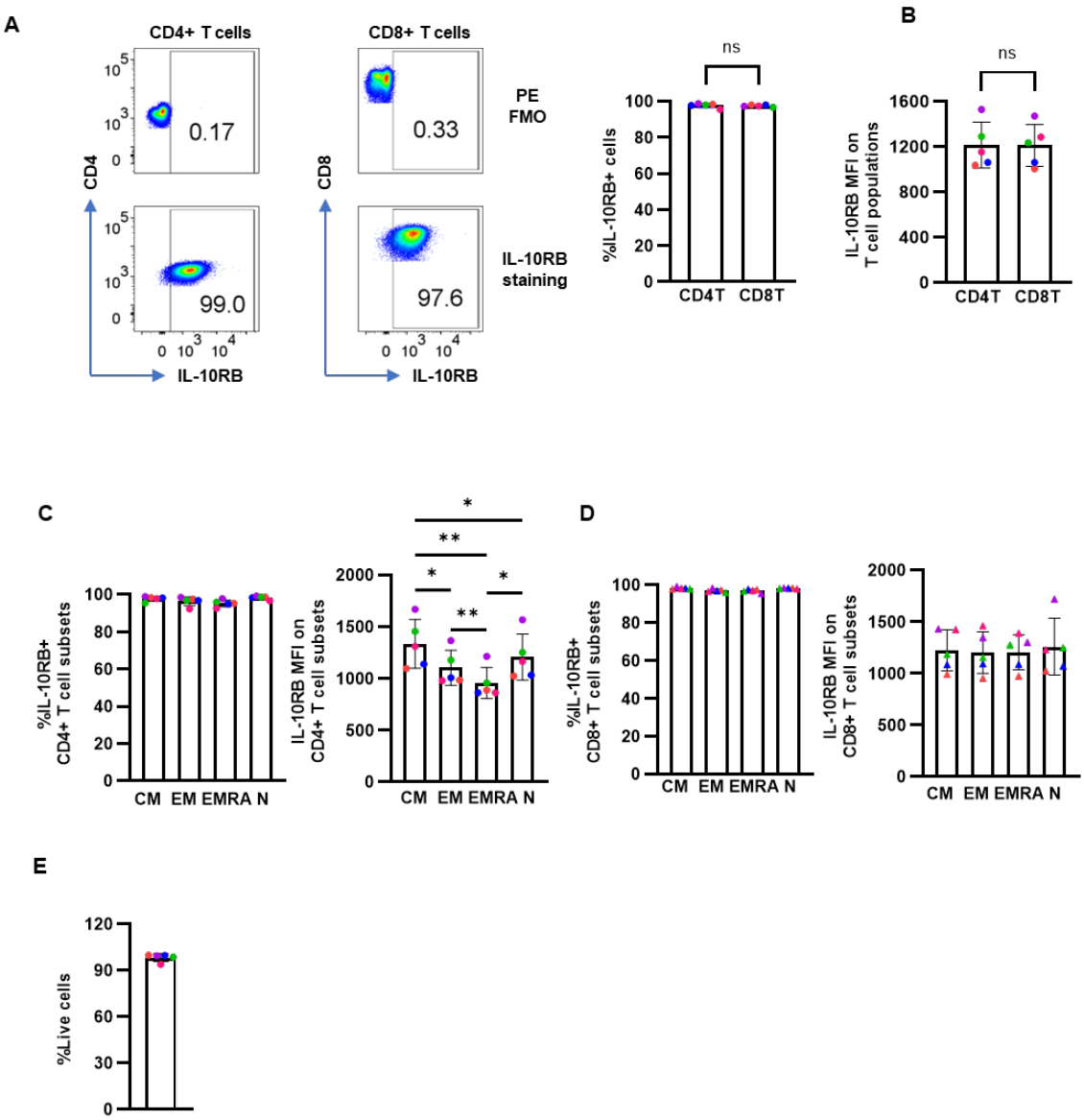

Figure 10. The baseline IL-10RB level is comparable on CD4+ and CD8+ T cells, similar on memory subsets and naïve T cells.

(A-E) Multi-colour flow cytometry of healthy donor whole PBMCs. (A) IL-10RB+% with sample PE FMO and IL-10RB PE sample staining dot plot and compiled bar graph; (B) IL-10RB median fluorescent intensity (MFI) on total CD4+ and CD8+ T cells. IL-10RB+% and IL-10RB MFI of FMO were subtracted to normalize IL-10RB+% and IL-10RB MFI. Paired t-test; IL-10RB+% and MFI of IL-10RB in (C) CD4+ T cell and CD8+ T cell (D) subsets. Comparisons in (C) and (D) via one-way ANOVA and Tukey's multiple comparison post-test to compare groups. ns, $p > 0.05$; *, $p < 0.05$. Central memory (T_{CM}) (CM), effector memory (T_{EM}) (EM), effector memory with CD45 RA phenotype (T_{EMRA}) (EMRA), naïve (Naive). CD4 T, CD4+ T cells; CD8 T, CD8+ T cells. Each dot colour in the column graphs represents cells from a different healthy donor. Data are mean ± SEM, n=5.

Now, with the ability to quantify IFN-λR1 surface levels, the first goal of my project was to fully characterize IFN-λR1 levels on CD4+ and CD8+ T cells, including multiple subsets, at steady state. Santer *et al*. showed that at the mRNA level, *IFNLR1* expression is higher on CD8+ T cells compared to CD4+ T cells and barely detected in NK cells, monocytes, and neutrophils; *IL10RB* mRNA was detected in all abovementioned immune cell types.[141] We isolated PBMCs from 5 healthy donors, stained the cells and analyzed IFN-λR levels on different cell types. Using gating strategies shown in **Figure 9**, we examined the level of IFN-λR on total CD4+ and CD8+ T cells and subsets of T cells, including T_{CM}, T_{EM}, T_{EMRA}, and naïve T cells. I chose to look at these subsets because they play a distinct role in generating immune responses and have different functions. IL-10RB was detected on almost 100% of CD4+ and CD8+ T cells. However, no difference in IL-10RB+% was observed between total CD4+ and CD8+ T cell populations (**Figure 10A and 10B**). For CD4+ T cells, the highest IL-10RB levels were seen on T_{CM} cells, followed by naïve cells ($p < 0.05$) and then T_{EM} cells ($p < 0.05$). T_{EMRA} expressed the lowest levels of IL-10RB ($p < 0.01$) compared to other cell types (**Figure 10C**). For CD8+ T cells, all four subsets had comparable IL-10RB levels (MFI and percentage). (**Figure 10D**). We also checked cell viability using Zombie AQUA dye, and we found that more than 94% of the cells were alive (**Figure 10E**).

Next, I quantified IFN-λR1 and found a significantly greater percentage of IFN-λR1+ CD8+ T cells in all healthy donors compared to matched CD4+ T cells ($p < 0.05$) (**Figure 11A**). This was consistent when also measuring IFN-λR1 MFI (**Figure 11B**). The lowest proportion of CD4+ T cells expressed the IFN-λR1 on the cell surface compared to all other subsets was seen in naïve CD4+ T cells (**Figure 11C**), with less than 2% of IFN-λR1+ and CD8+ T cells with less than 5% IFN-λR1+ (**Figure 11D**). While T_{EMRA} CD4+ T cells had the highest IFN-λR1+% detectable among CD4+ T cells (average around 4.5%), T_{EM} CD8+ T cells had the highest IFN-λR1+% detectable among CD8+ T cells (average 22%) (**Figure 11C and 11D**).

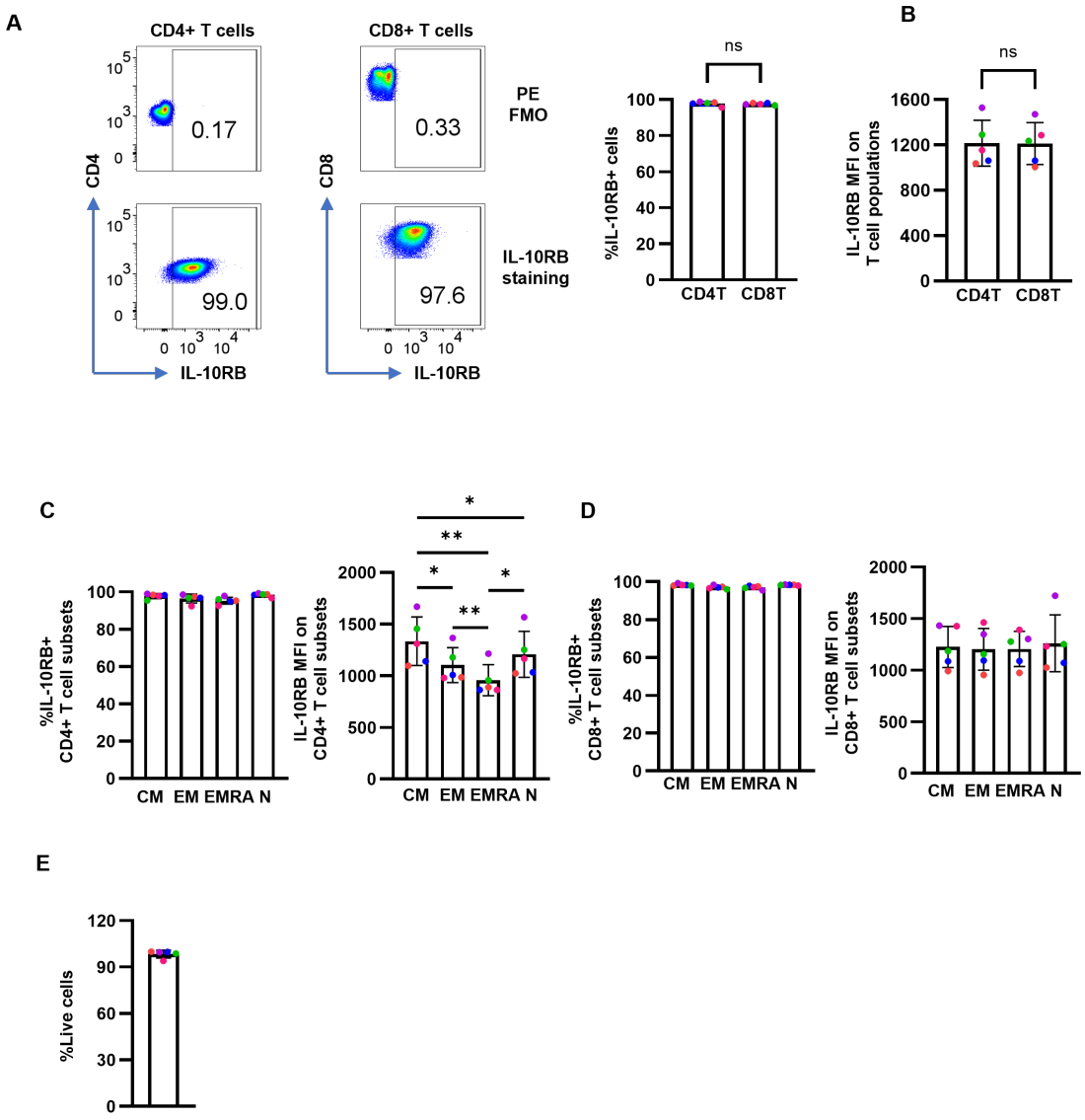

Figure 11. At steady state, more IFN-λR1 is expressed on CD8+ T cells than CD4+ T cells and more is also detected on memory than naïve T cell subsets.

(A) IFN-λR1+% with sample PE FMO and IFN-λR1 sample staining dot plot and compiled bar graph; (B) IFN-λR1 median fluorescent intensity (MFI) in total CD4+ and CD8+ T cells. IFN-λR1+% and IFN-λR1 MFI of FMO were subtracted from respective actual staining to calculate actual IFN-λR1+% and IFN-λR1 MFI. Paired t-test. IFN-λR1+% and MFI of IFN-λR1 in (C) CD4+ T cell and (D) CD8+ T cell subsets. Comparisons in (C and E) one-way ANOVA and Tukey's multiple comparison test. ns, $p > 0.05$; *, $p < 0.05$; **, $p < 0.01$. Central memory (T_{CM}) (CM), effector memory (T_{EM}) (EM), effector memory with CD45 RA phenotype (T_{EMRA}) (EMRA), naïve (Naive). CD4T, CD4+ T cells; CD8 T, CD8+ T cells. Each dot colour in the column graphs represents cells from a different healthy donor. Data are mean ± SEM, n=5.

3.1.2 Investigate if Various TCR Stimulation Conditions Alter IFN-λR Levels on the Surface of CD4+ and CD8+T Cell Subsets within PBMCs.

Hypothesis: TCR stimulation by anti-CD3 and anti-CD28 upregulates the level of IFN-λR1 but does not alter IL-10RB level on human CD4+ and CD8+ T cell surface within PBMCs.

Published data from our group previously showed that upon TCR stimulation, *IFNLR1* mRNA increased in human CD4+T cells sorted from PBMCs stimulated with anti-CD3 and anti-CD28.[141] CD8+ T cell data was not included in the publication. We wanted to investigate whether a similar change applies at the protein level and whether the magnitude of IFN-λR1 upregulation is related to the upregulation magnitude of an activation marker of TCR stimulation. To address that, we used different anti-CD3 and anti-CD28 concentration combinations. There was not a significant difference in IFN-λR1+% and IFN-λR1 MFI when PBMCs were stimulated with anti-CD3 at 0.3μg/mL and 1 μg/mL (data not shown), so we used a lower anti-CD3 concentration (0.03 μg/mL) to elucidate the relationship between the percentage of T cells expressing IFN-λR1 and IFN-λR1 levels. To mimic the stimulation that T cells are receiving, we used plate-bound anti-CD3 as it resembles the TCR stimulation by crosslinking the CD3 component of TCR. Meanwhile, we added anti-CD28 into cell culture media as *in vivo,* the co-stimulatory signal is not known as a stagnant interaction. Known as transferrin receptor, CD71 level is detectable on T cells as early as 6-8 hours post-stimulation; previous studies have shown its levels remain high till 72-hour post-stimulation.[76] We selected CD71 as a T cell activation marker for our studies to evaluate the magnitude of TCR stimulation.

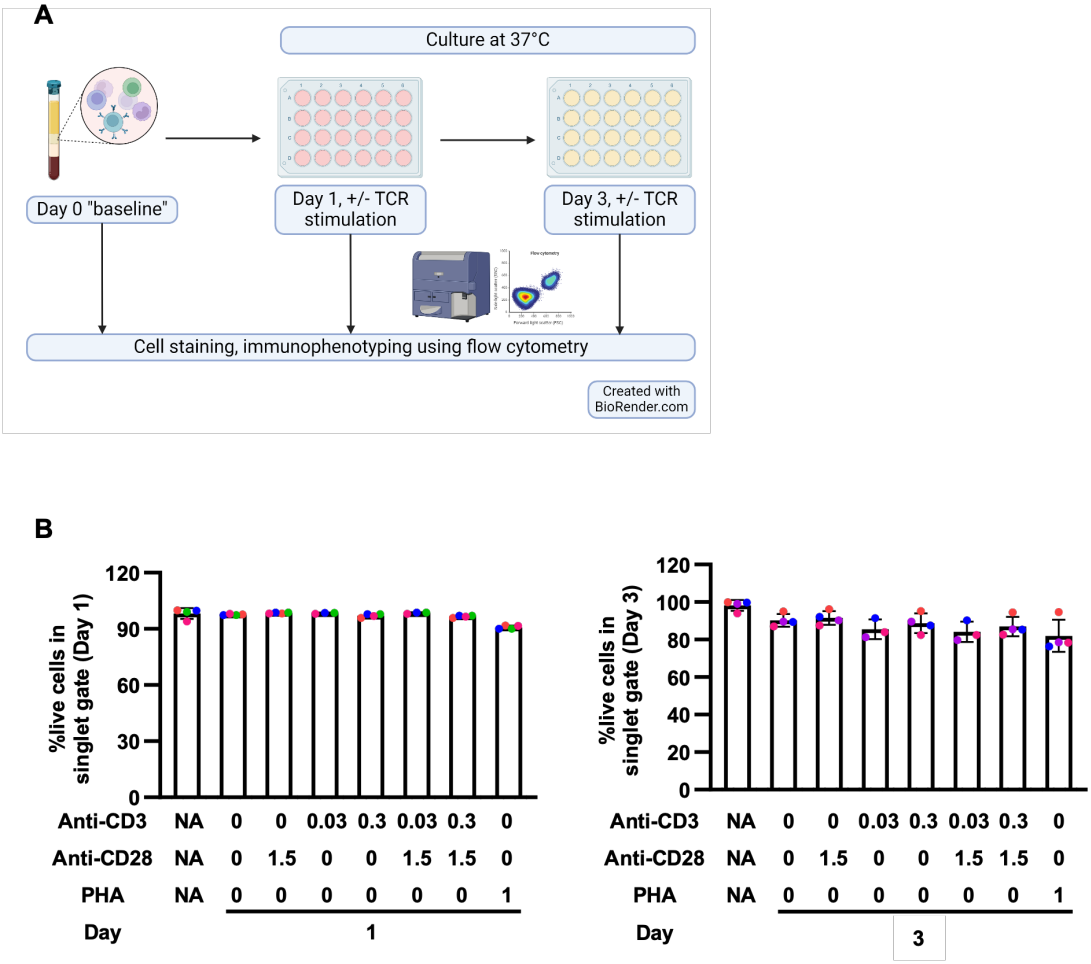

Figure 12. Cell viability of total PBMCs did not significantly decrease among different stimulation conditions on Day 1 and Day 3.

(A) Schematic design of the experimental setup. Briefly, whole PBMCs from healthy donors were cultured with or without anti-CD3 and anti-CD28 at different concentrations and were harvested after 24 and 72 hours for IFN-λR analyses. The levels of IFN-λR at the steady state were analyzed by flows staining on Day 0. (B) Percentage of live cells (cells negative for Zombie AQUA staining) in single-cell flow gate for whole PBMCs on Day 1 (left) and Day 3 (right) post-culturing. Each colour of dots in the column graph represents a different healthy donor. Numbers listed under the graph indicate the concentration of the respective antibody or PHA, unit μg/mL. Comparisons were made between the respective condition average and Day 1 control without anti-CD3, anti-CD28, and PHA (second column from the left in (B)). all comparisons not marked with a star(s) "*" indicate no significant differences via two-way ANOVA and Tukey's multiple comparison test. Data are mean ± SEM, n=4. Panel (A) was created with BioRender.com.

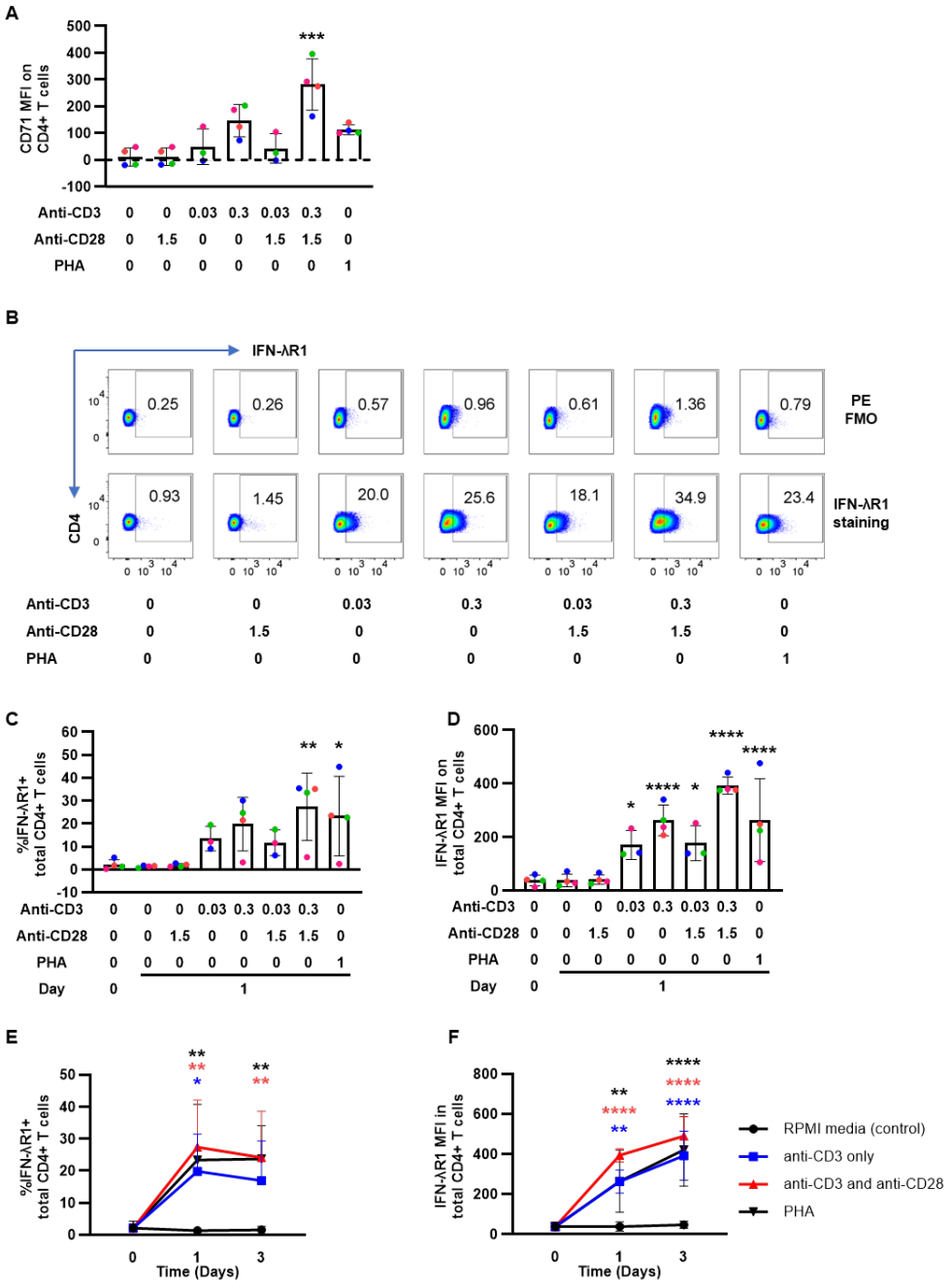

Figure 13. TCR stimulation increases IFN-λR1 levels on CD4+ T cells.

(A) CD71 MFI on CD4+ T cell population under TCR stimulation conditions with or without different concentrations of anti-CD3 (coated on the 24-well plate) and anti-CD28 (in cell culture media suspension) on Day 1. (B) Gating strategy example for IFN-λR1+ CD8+ T cell PE FMO and IFN-λR1 staining on Day 1 across different stimulation conditions. (C) IFN-λR1+% and (D) IFN-λR1 MFI on CD4+ T cells on Day 1. For panels (A-D), the numbers listed under the graph indicate the concentration of the respective antibody or PHA, unit µg/mL. All anti-CD3 were used to pre-coat the wells, anti-CD28 and PHA were added to cell suspensions. For (A), (C-D), comparisons were made between the respective condition average and Day 1 control

(without anti-CD3, anti-CD28, and PHA (second column from the left in (A-B, and D). (E) IFN-λR1+% and (F) IFN-λR1 MFI for selected TCR stimulation conditions on CD4+ T cells from Day 0 (baseline) to Day 3; in these two panels, all anti-CD3 used to coat wells was 0.3 μg/mL, anti-CD28 was 1.5 μg/mL in cell suspension, PHA was 1 μg/mL in cell suspension if applicable. All comparisons in (F-G) were made between the respective conditions and RPMI media control (no anti-CD3, anti-CD28, and PHA) at the given time point (Day). For (A-B, E-G), IFN-λR1+% and IFN-λR1 MFI of FMO were used to normalize IFN-λR1+% and IFN-λR1 MFI, respectively. Each colour of dots in the column graph represents a different healthy donor. Comparisons in panels (A), (C-F) all used two-way ANOVA and Dunnett's multiple comparison test. *, $p < 0.05$; **, $p < 0.01$; ***, $p < 0.005$; ****, $p < 0.001$; all comparisons not marked with a star(s) "*" indicate no significant differences. Data are mean ± SEM, n=4.

Using the experiment design shown in **Figure 12A**, we examined the cell viability using Zombie AQUA staining with flow cytometry. We confirmed that more than 90% of total PBMCs were viable under all stimulation conditions tested on Day 1 and Day 3 (anti-CD3 +/- anti-CD28 or PHA). On Day 1, the viability of PBMCs remained above 96% in all stimulated and unstimulated conditions, but in the PHA-stimulated condition, which is around 90.8% (**Figure 12B**). On Day 3, the viability across conditions slightly dropped, but cells in all conditions still had viability above 82%. (**Figure 12B**) Without any stimulation, CD71 levels (MFI) on CD4+ T cells on Day 0 and Day 1 were at about 12. I tested two concentrations of anti-CD3 coating of the plate, 0.03 and 0.3 μg/mL. Anti-CD3 alone did not significantly increase CD71 MFI, but anti-CD3 + anti-CD28 stimulation significantly increased the CD71 MFI on CD4+ T cells in whole PBMCs from, on average, 20 to about 280 on day 1 ($p < 0.005$), confirming the maximum stimulation condition within my experiments (**Figure 13A**). Anti-CD28 alone did not significantly upregulate CD71 and IFN-λR1 levels on CD4+ T cells, indicating that the T cell co-stimulatory signal itself is not sufficient. (**Figure 13A and 13B**). PHA increased CD71 MFI by 8.4-fold compared to the unstimulated condition (**Figure 13A**).

Next, I compared all the stimulation conditions for the specific upregulation of IFN-λR1. Compared to the unstimulated control (2% IFN-λR1+), anti-CD3 at both concentrations caused an upregulation of IFN-λR1 to 11.7 to 27.3%, and the max IFN-λR1 upregulation was seen with anti-CD3 and anti-CD28 at the highest concentration tested (27.35) ($p < 0.01$) (**Figure 13B-C**). That trend aligns with the CD71 expression pattern on the CD4+ T cell surface (**Figure 13A**). When quantifying MFI, anti-CD3 alone or with anti-CD28, or PHA significantly upregulated IFN-λR1 levels (**Figure 13D**). In terms of the time course, the percentage of CD4+ T cells that express IFN-

λR1 dramatically increased within the first 24-hour stimulation, reaching ~30% level, followed by another minor increase on day 3 when cells were treated with both anti-CD3 and anti-CD28. A similar trend was observed when only anti-CD3 was provided (**Figure 13E**). Anti-CD3 alone induced a stronger increase in CD71 MFI, IFN-λR1 MFI, and IFN-λR1% in the CD4+ T cell population compared to anti-CD28 alone, indicating CD3 signalling, in this context, plays a more crucial role in upregulating IFN-λR1 compared to CD28 signalling (**Figure 13A, 13B, and 13E**).

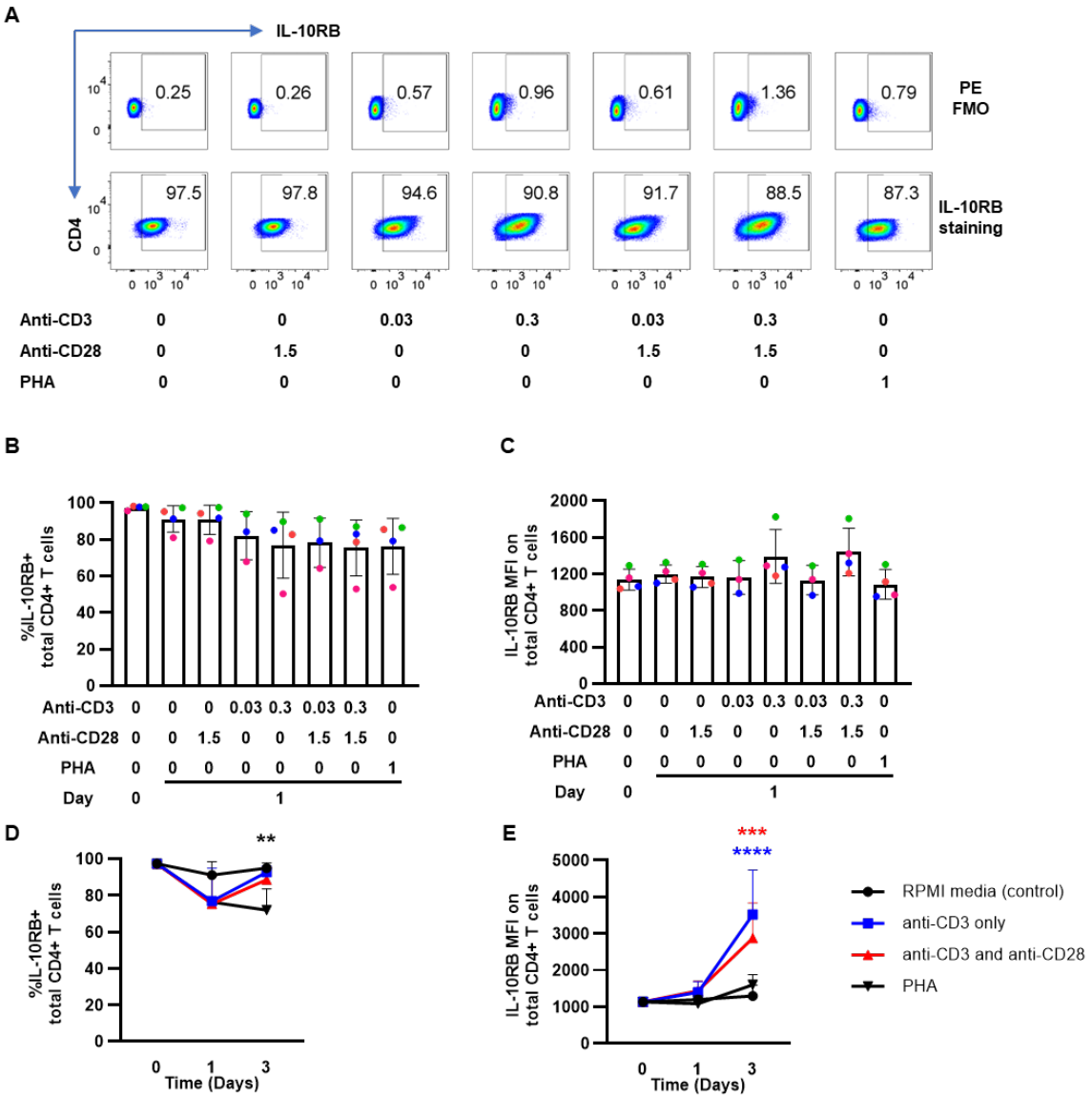

Figure 14. TCR stimulation increases IL-10RB levels on the CD4+ T cell surface on day 3.

(A) Gating strategy example for IL-10RB+ CD8+ T cell PE FMO and IL-10RB staining on Day 1 across different stimulation conditions. (B) IL-10RB+% and (C) IL-10RB MFI on CD4+ T cells on Day 1. For panels (A-C), the numbers listed under the graph indicate the concentration of the respective antibody or PHA, unit μg/mL. All anti-CD3 were used to pre-coat the wells, and anti-CD28 and PHA were added to cell suspensions. For (B-C), comparisons were made between the respective condition average and Day 1 control (without anti-CD3, anti-CD28, and PHA (second column from the left in (A-B, and D). (D) IL-10RB+% and (E) IL-10RB MFI for selected TCR stimulation conditions on CD4+ T cells from Day 0 (baseline) to Day 3; in these two panels, all anti-CD3 used to coat wells was 0.3 μg/mL, anti-CD28 was 1.5 μg/mL in cell suspension, PHA was 1 μg/mL in cell suspension if applicable. All comparisons in (D-E) were made between the respective conditions and RPMI media control (no anti-CD3, anti-CD28, and PHA) at the given time point (Day). For (B-E), IL-10RB+% and IL-10RB MFI of FMO were

used to normalize IL-10RB+% and IL-10RB MFI, respectively. Each colour of dots in the column graph represents a different healthy donor. Comparisons in panels (A, and C-F) all used two-way ANOVA and Dunnett's multiple comparison test. **, $p < 0.01$; ***, $p < 0.005$; ****, $p < 0.001$; all comparisons not marked with a star(s) "*" indicate no significant differences. Data are mean ± SEM, n=4.

The impact of TCR stimulation on IL-10RB on CD4+ T cells was less prominent than on IFN-λR1. With a sample flow cytometry gating dot plot shown (**Figure 14A**), IL-10RB+% on CD4+ T cells remained high and slightly decreased in one donor, with at least 80% of CD4+ T cells under all stimulation conditions expressing IL-10RB on the cell surface for all donors (**Figure 14B**). IL-10RB MFI also remained relatively stable across different TCR stimulation with different anti-CD3 concentrations, all of which stayed in the range of 1200 ± 200 on Day 1. (**Figure 14C**) IL-10RB+% on Day 1 decreased to below 80% when cells were treated with anti-CD3 alone, anti-CD3 with anti-CD28, and PHA, from over 98% on Day 0, but on Day 3 the IL-10RB+% increased back to over 95%, except PHA-treated cells, which remain below 80%. (**Figure 14D**) Interestingly, even though IL-10RB MFI on CD4+ T cells remained at a comparable level on Day 1, anti-CD3 alone or anti-CD3 together with anti-CD28 significantly increased the IL-10RB MFI on CD4+ T cells on Day 3 compared to the unstimulated or PHA-treated cells. (**Figure 14E**). Notice that PHA, which serves as a potent T cell stimulation agent, did not up-regulate IL-10RB MFI of CD4+ T cells or IL-10RB+% CD4+ T cells compared to unstimulated control on Day 1 and Day 3 like anti-CD3 and anti-CD28 did (**Figure 14D and 14E**); however, up-regulation was seen for IFN-λR1 (**Figure 13E and 13F**).

For CD8+ T cells within PBMCs, CD71 MFI in cells treated with anti-CD28 alone or unstimulated were around 33. (**Figure 15A**) When stimulated with 0.3 μg/mL anti-CD3 alone, CD71 MFI increased to 204, with an even higher CD71 MFI when anti-CD28 was provided at the same time (453) (**Figure 15A**) PHA increased CD71 MFI to 159. (**Figure 15A**) Anti-CD3 alone at 0.03 and 0.3 μg/mL increased IFN-λR1+% from ~4% to 18.8% and 33.3%, respectively. (**Figure 15B and 15C**) Compared to anti-CD3 (0.3 μg/mL) alone (33.3%), CD8+ T cells in PHA-treated PBMCs had a comparable IFN-λR1+% (31.2%). (**Figure 15B and 15C**) Although anti-CD28 alone did not alter IFN-λR1+% in CD8+ T cells, however, when added with 0.3 μg/mL anti-CD3, it promoted IFN-λR1+% CD8+ T cells from 33.3% to 38.3%. ($p < 0.005$) (**Figure 15B and 15C**). IFN-λR1 MFI showed a similar trend, that the combination of anti-CD3 with higher

concentration induced a higher increase in IFN-λR1 MFI (**Figure 15D**). Notice the donor shown in pink colour had a relatively lower magnitude up-regulation of CD71 MFI, IFN-λR1+% across different stimulation conditions (**Figure 15A and 15C**); meanwhile, this donor had a 300% higher IFN-λR1 MFI when stimulated with 0.3 μg/mL plate-bound anti-CD3 and 1.5 μg/mL anti-CD28 compared to the unstimulated control (**Figure 15D**). In CD8+ T cells from Day 1 to Day 3, IFN-λR1 MFI and IFN-λR1+% increase, with a more significant magnitude seen in MFI, indicating CD8+ T cells expressing more IFN-λR1 on the cell surface on average compared to baseline (**Figure 15E and 15F**). Adding anti-CD3 and anti-CD28 led to the highest IFN-λR1 level among all stimulation conditions on day 3 (**Figure 15F**). Notice in CD4+ and CD8+ T cells, anti-CD3 and anti-CD28 together upregulated CD71 and IFN-λR1 to a higher level than anti-CD3 only, confirming the role of co-stimulatory signal in regulating IFN-λR1 levels in both CD4+ and CD8+ T cells.

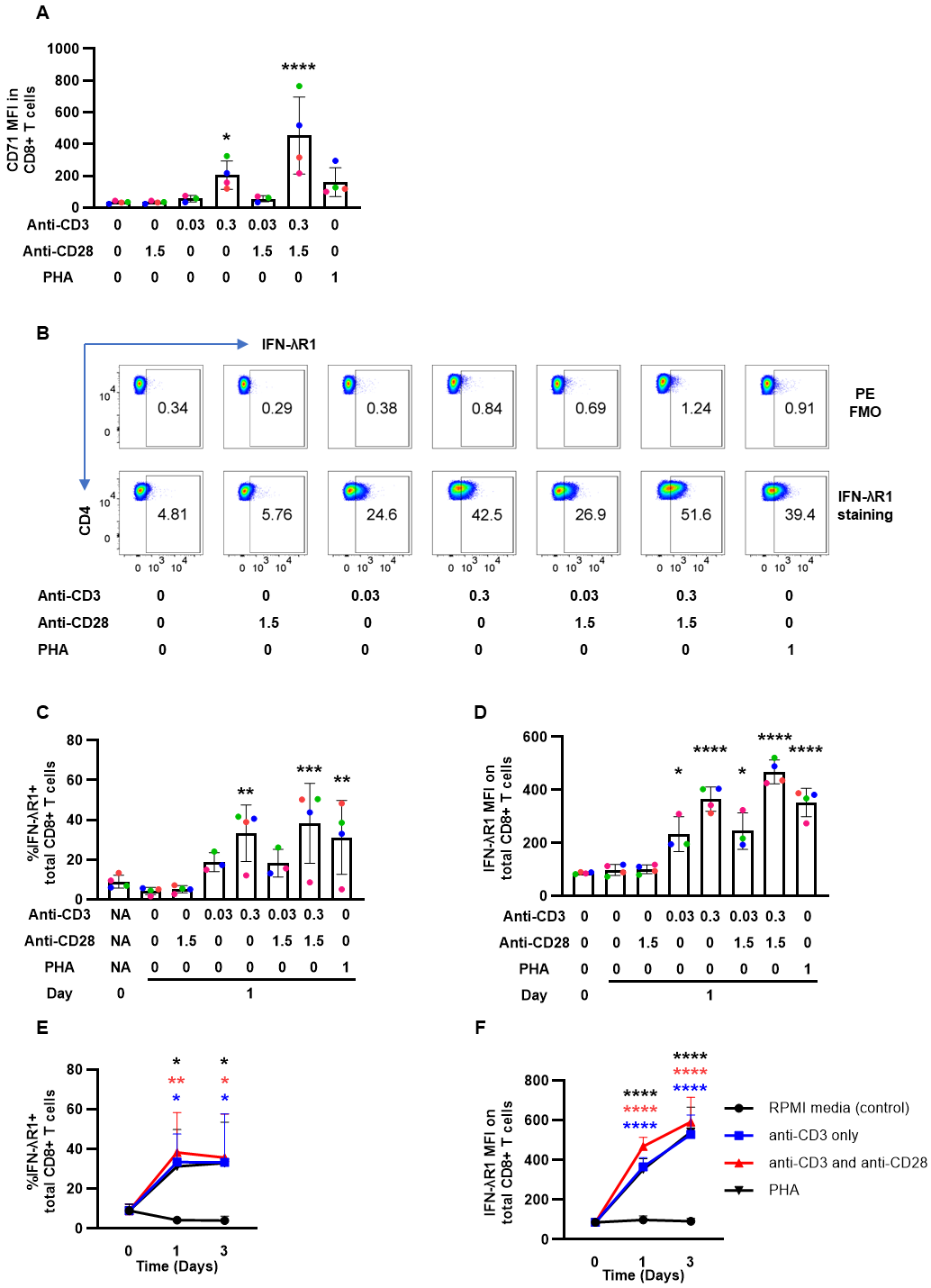

Figure 15. TCR stimulation promotes IFN-λR1 levels on CD8+ T cells.

(A) CD71 MFI on CD8+ T cell population under TCR stimulation conditions with or without different concentrations of anti-CD3 (coated on the 24-well plate) and anti-CD28 (in cell culture media suspension) on Day 1. (B) Gating strategy example for IFN-λR1+ CD8+ T cell PE FMO and IFN-λR1 staining on Day 1 across different stimulation conditions. (C) IFN-λR1+% and (D) IFN-λR1 MFI on CD8+ T cells on Day 1. For panels (A-D), the numbers listed under the graph

indicate the concentration of the respective antibody or PHA, unit μg/mL. All anti-CD3 were used to pre-coat the wells, anti-CD28 and PHA were added to cell suspensions. For (A, and C-D), comparisons were made between the respective condition average and Day 1 control (without anti-CD3, anti-CD28, and PHA (second column from the left in (A-B, and D). (E) IFN-λR1+% and (F) IFN-λR1 MFI for selected TCR stimulation conditions on CD8+ T cells from Day 0 (baseline) to Day 3; in these two panels, all anti-CD3 used to coat wells was 0.3 μg/mL, anti-CD28 was 1.5 μg/mL in cell suspension, PHA was 1 μg/mL in cell suspension if applicable. All comparisons in (F-G) were made between the respective conditions and RPMI media control (no anti-CD3, anti-CD28, and PHA) at the given time point (Day). For (A-B, E-F, and G), IFN-λR1+% and IFN-λR1 MFI of FMO were used to normalize IFN-λR1+% and IFN-λR1 MFI, respectively. Each colour of dots in the column graph represents a different healthy donor. Comparisons in panels (A, and C-F) all used two-way ANOVA and Dunnett's multiple comparison test. *, $p < 0.05$; **, $p < 0.01$; ***, $p < 0.005$; ****, < 0.001; all comparisons not marked with a star(s) "*" indicate no significant differences. Data are mean ± SEM, n=4.

Similar to CD4+ T cells, anti-CD3 and anti-CD28 treated CD8+ T cells in PBMCs had a slightly reduced IL-10RB+%, from around 97% to 75% (**Figure 16A and 16B**). However, the MFI of IL-10RB remains unaltered across different stimulation conditions (**Figure 16C**). IL-10RB+% remained relatively constant from Day 0 to Day 3 when cells were treated with anti-CD3 alone, anti-CD28 alone, both, or PHA (**Figure 16D**). Meanwhile, IL-10RB MFI increased from day 0 to day 3, with a more prominent increase post-one-day stimulation with anti-CD3-only treatment, indicating it is likely that TCR stimulation selectively enhanced the surface level of IL-10RB on a group of CD8+ T cells (**Figure 16E**).

To further elucidate the relevance between T cell activation and IFN-λR on the cell surface, we compared the IFN-λR1+% and IFN-λR1 MFI between cell populations distinguished by the activation marker expression on the cell surface. Known that the TCR signalling reduces the level of CD62L on the T cell surface, CD62L had been considered an activation marker of T cells, with a higher level of CD62L representing a "less" activated T cell.[78] We added CD62L as an activation marker and checked CD71+, CD71-, CD62+, and CD62L- separately. Across all stimulation conditions tested, there was no significant difference in IFN-λR1+%, IFN-λR1 MFI, IL-10RB+%, and IL-10RB MFI on CD4+ T cell populations between CD62L+ and CD62L- CD4+ T cells. (**Figure 17A and 17B**). When using CD71 as the activation marker and examining the CD71-positive and negative populations, the CD71-positive population CD4+ T cells had a higher IFN-λR1+% than their CD71- counterpart when stimulated with 0.03 μg/mL of anti-CD3 and 1.5 μg/mL anti-CD28 (**Figure 18A**). The same difference was seen in MFI when anti-CD3 (0.03

μg/mL) and anti-CD28 (1.5 μg/mL) were provided, where MFI was about 200 units higher, which is 100% higher than that in CD71- cells ($p < 0.05$) (**Figure 18A**). When stimulated with anti-CD3 alone (0.03 μg/mL) or anti-CD3 (0.3 μg/mL) and anti-CD28 (1.5 μg/mL), CD71-positive CD4+ T cells also had significantly higher IFN-λR1 MFI than CD71+ negative CD4+ T cells on Day 1 ($p < 0.05$) (**Figure 18A**). CD71+ CD4+ T cells did not differ from the CD71- population in terms of IL-10RB+% (**Figure 18B**). However, IL-10RB MFI was significantly higher in CD71+ CD4+ T cells within PBMCs when cells were treated with anti-CD28 alone, anti-CD3 (0.03 μg/mL) with anti-CD28, and untreated. ($p < 0.05$) (**Figure 18B**). We did not observe a disparity between the IFN-λR1 or IL-10RB level between CD62L+ and CD62L- populations or between CD71+ and CD71- populations in CD4+ T cells when treated with PHA (**Figure 18A and 18B**).

In CD8+ T cells, we observed higher levels of IFN-λR1 in CD62L- cells than in CD62L+ cells when cells were treated with anti-CD3 only (0.03 μg/mL) and when anti-CD3 (0.03 μg/mL) was added together with anti-CD28 (**Figure 19A**). There were no differences between the CD62L+ and CD62L- populations in terms of IFN-λR1+%, IL-10+%, and IL-10RB MFI (**Figure 19A and 19B**). Notice the levels of CD62L get downregulated on the cell surface during T cell activation. CD71+ CD8+ T cells expressed 1.8-fold higher IFN-λR+% than CD71- CD8+ T cells when cells were stimulated with anti-CD3 (0.03 μg/mL), with or without anti-CD28 (**Figure 20A**). When examining IFN-λR1 MFI, CD71+ also had a higher level compared to their counterpart in all stimulation conditions provided with anti-CD3 ($p < 0.005$), with the biggest absolute MFI difference of 300 observed post-TCR stimulation with anti-CD3 (0.03 μg/mL) and anti-CD28 (**Figure 20A**). No difference was seen in IL-10RB levels comparing positive and negative populations of CD71 or CD62L on Day 1 across different stimulations. **(Figure 20B**).

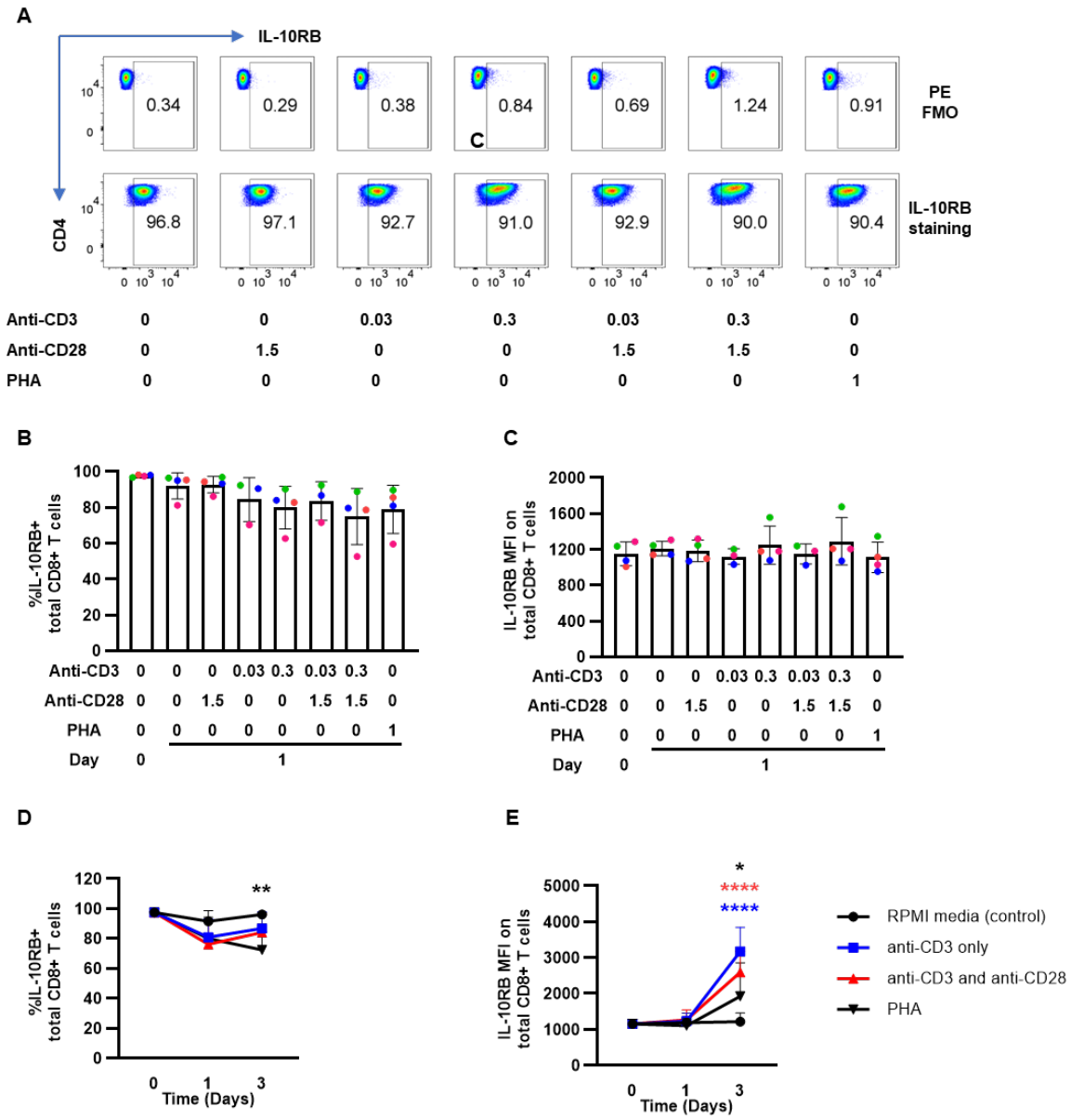

Figure 16. TCR stimulation enhances IL-10RB levels on CD8+ T cells on day 3, but not on day 1.

(A) Gating strategy example for IL-10RB+ CD8+ T cell PE FMO and IL-10RB staining on Day 1 across different stimulation conditions. (B) IL-10RB+% and (C) IL-10RB MFI on CD8+ T cells on Day 1. For panels (A-C), the numbers listed under the graph indicate the concentration of the respective antibody or PHA, unit μg/mL. All anti-CD3 were used to pre-coat the wells, anti-CD28 and PHA were added to cell suspensions. For (B-C), comparisons were made between the respective condition average and Day 1 control (without anti-CD3, anti-CD28, and PHA (second column from the left in (A-B, and D). (D) IL-10RB+% and (E) IL-10RB MFI for selected TCR stimulation conditions on CD8+ T cells from Day 0 (baseline) to Day 3; in these two panels, all anti-CD3 used to coat wells was 0.3 μg/mL, anti-CD28 was 1.5 μg/mL in cell suspension, PHA was 1 μg/mL in cell suspension if applicable. All comparisons in (D-E) were

made between the respective conditions and RPMI media control (no anti-CD3, anti-CD28, and PHA) at the given time point (Day). For (B-E), IL-10RB+% and IL-10RB MFI of FMO were used to normalize IL-10RB+% and IL-10RB MFI, respectively. Each colour of dots in the column graph represents a different healthy donor. Comparisons in (A, and C-F) all used two-way ANOVA and Dunnett's multiple comparison test. *, $p < 0.05$; **, $p < 0.01$; ****, $p < 0.001$; all comparisons not marked with a star(s) "*" indicate no significant differences. Data are mean ± SEM, n=4.

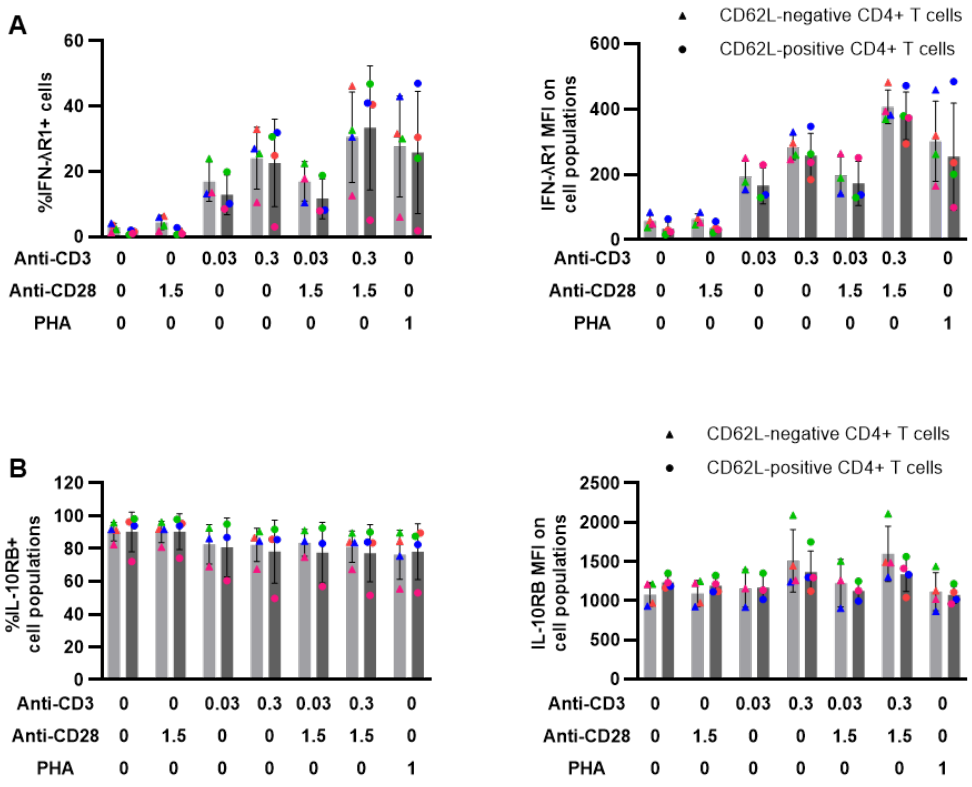

Figure 17. CD62L+ and CD62L- CD4+ T cells express comparable levels of IFN-λR1 and IL-10RB on the cell surface at baseline and post-TCR stimulation.

(A) IFN-λR1+% and IFN-λR1 MFI on CD62+ and CD62L- CD4+ T cells after 24-hour TCR stimulation. (B) IL-10RB+% and IL-10RB MFI on CD62L+ and CD62L- CD4+ T cells after 1-day TCR stimulation. Each colour of dots in the column graph represents a different healthy donor. The table below the x-axis indicates the concentration of anti-CD3, anti-CD28, or PHA, unit μg/mL. IFN-λR1+% and IFN-λR1 MFI of FMO were used to normalize IFN-λR1+% and IFN-λR1 MFI. Two-way ANOVA and Dunnett's multiple comparison tests were used to compare the indicated IFN-λR components between CD62L+ and CD62- CD4+ T cell populations at different stimulation contexts. *, $p < 0.05$; **, $p < 0.01$; ***, $p < 0.005$; ****, $p < 0.001$; all comparisons not marked with a star(s) "*" indicate no significant differences. Data are mean ± SEM, n=4.

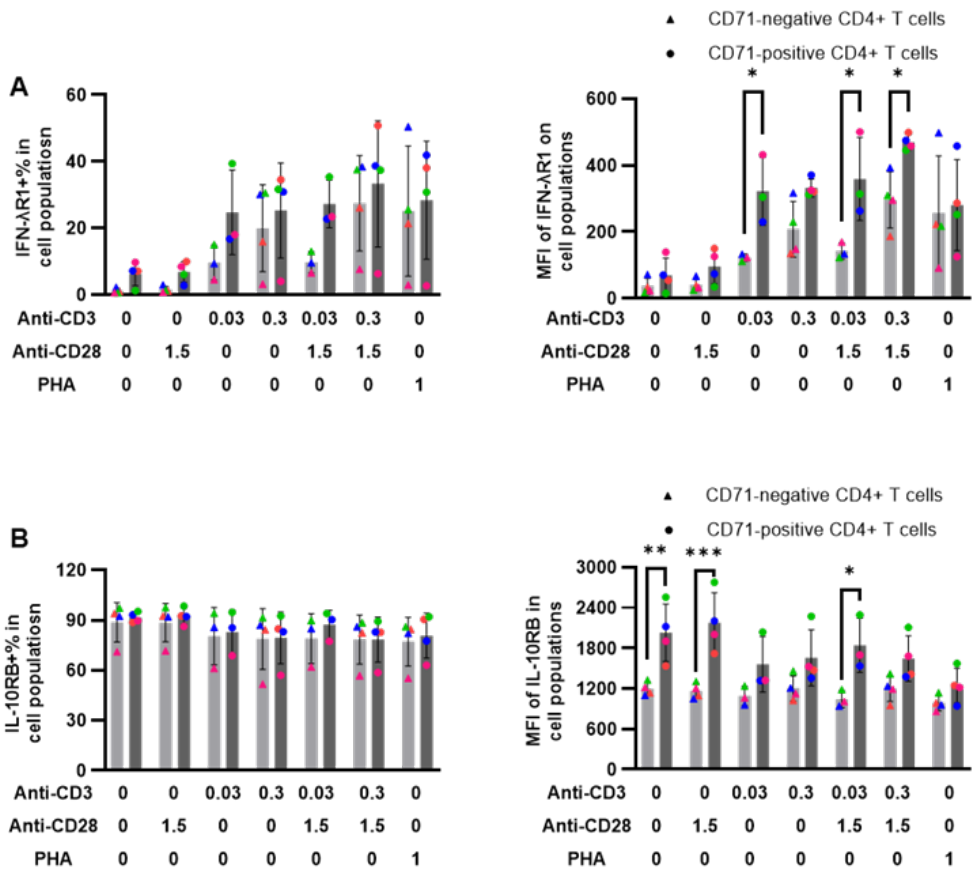

Figure 18. More activated CD4+ T cells express significantly higher levels of IFN-λR1 and IL-10RB in certain stimulation conditions.

(A) IFN-λR1+% and IFN-λR1 MFI on CD71+ and CD71- CD4+ T cells after 24-hour TCR stimulation. (B) IL-10RB+% and IL-10RB MFI on CD71+ and CD71- CD4+ T cells after 1-day TCR stimulation. Each colour of dots in the column graph represents a different healthy donor. The table below the x-axis indicates the concentration of anti-CD3, anti-CD28, or PHA, unit μg/mL. IFN-λR1+% and IFN-λR1 MFI of FMO were subtracted from respective actual staining to calculate actual IFN-λR1+% and IFN-λR1 MFI. Two-way ANOVA and Dunnett's multiple comparison test were used to compare the indicated IFN-λR components between CD71+ and CD71- CD4+ T cell populations at different stimulation contexts. *, $p < 0.05$; ***, $p < 0.005$; ****, $p < 0.001$; all comparisons not marked with a star(s) "*" indicate no significant differences. Data are mean ± SEM, n=4.

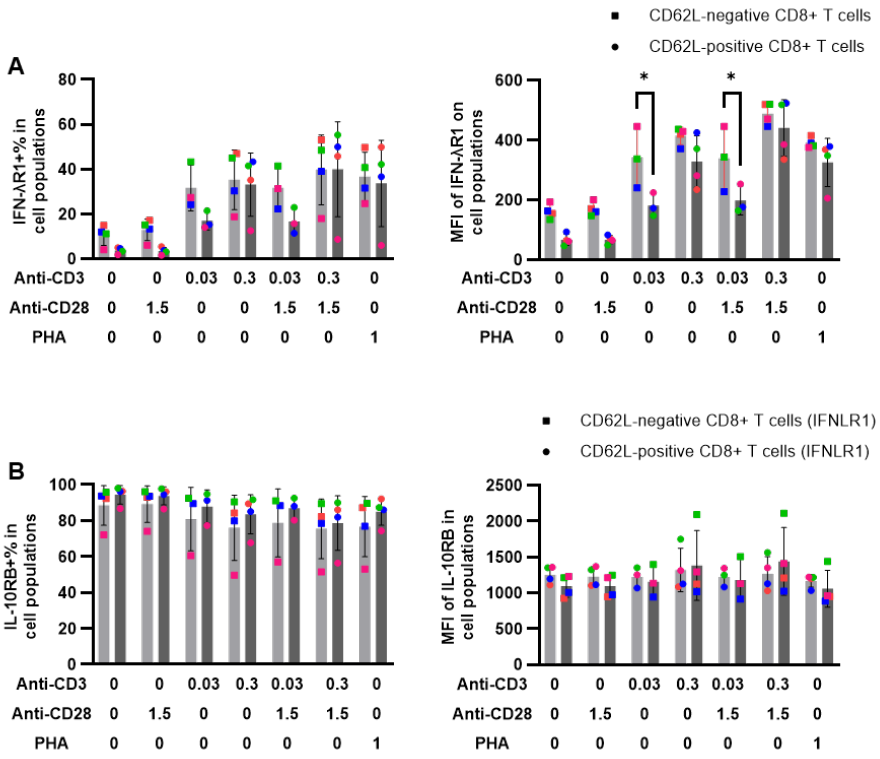

Figure 19. Similar IFN-λR1+, IL-10RB+%, and IFN-λR1 MFI, but a lower level of IFN-λR1+% on less activated CD8+ T cells post-TCR stimulation.

(A) IFN-λR1+% and IFN-λR1 MFI on CD62L+ and CD62L- CD8+ T cells after 24-hour TCR stimulation. (B) IL-10RB+% and IL-10RB MFI on CD62L+ and CD62L- CD8+ T cells after 1-day TCR stimulation. Each colour of dots in the column graph represents a different healthy donor. The table below the x-axis indicates the concentration of anti-CD3, anti-CD28, or PHA, unit μg/mL. IFN-λR1+% and IFN-λR1 MFI of FMO were subtracted from respective actual staining to calculate actual IFN-λR1+% and IFN-λR1 MFI. Two-way ANOVA was used to compare the indicated IFN-λR components between CD62L+ and CD62L- CD8+ T cell populations at different stimulation contexts. *, $p < 0.05$; all comparisons not marked with a star(s) "*" indicate no significant differences. Data are mean ± SEM, n=4.

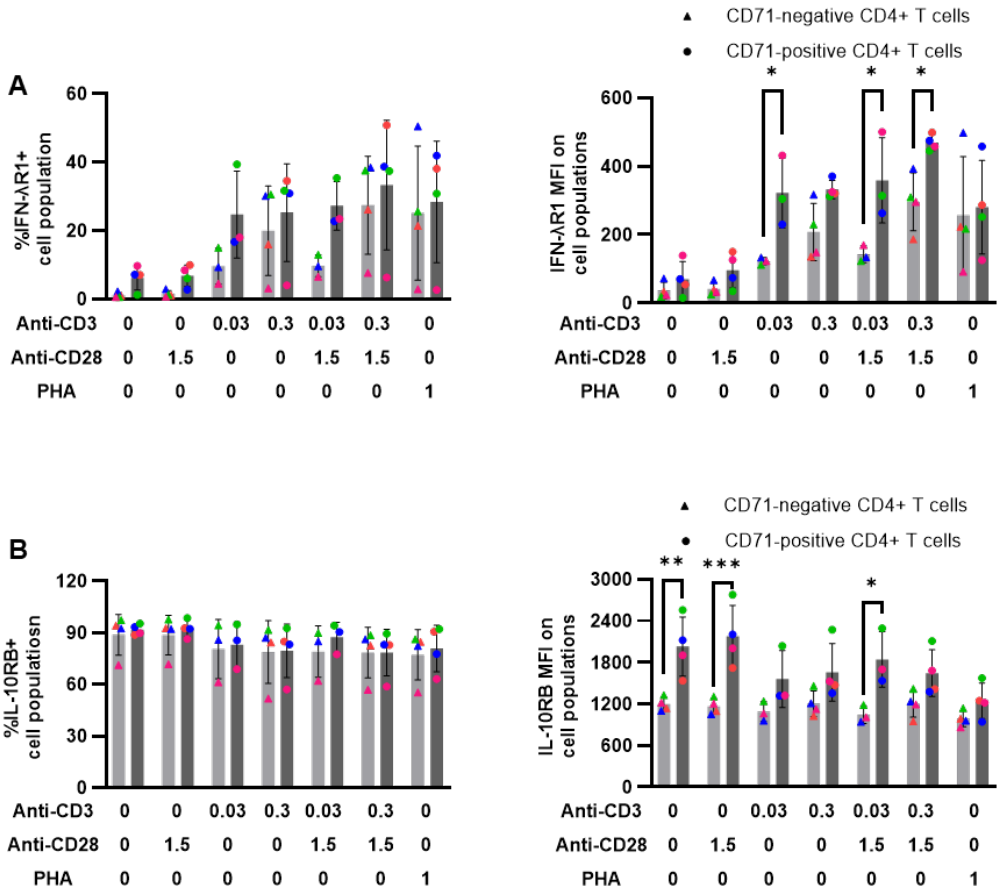

Figure 20. Upon TCR stimulation, more activated CD8+ T cells express more IFN-λR1 and IL-10RB than their counterpart, while IFN-λR1+% and IL-10RB+% remain comparable.

(A) IFN-λR1+% and IFN-λR1 MFI on CD71+ and CD71- CD4+ T cells after 24-hour TCR stimulation. (B) IL-10RB+% and IL-10RB MFI on CD71+ and CD71- CD4+ T cells after 1-day TCR stimulation. Each colour of dots in the column graph represents a different healthy donor. The table below the x-axis indicates the concentration of anti-CD3, anti-CD28, or PHA, unit μg/mL. IFN-λR1+% and IFN-λR1 MFI of FMO were subtracted from respective actual staining to calculate actual IFN-λR1+% and IFN-λR1 MFI. Two-way ANOVA and Dunnett's multiple comparison test were used to compare the indicated IFN-λR components between CD71+ and CD71- CD4+ T cell populations at different stimulation contexts. *, $p < 0.05$; **, $p < 0.01$; ***, $p < 0.005$; ****, $p < 0.001$; all comparisons not marked with a star(s) "*" indicate no significant differences. Data are mean ± SEM, n=4.

Table 7. IFN-λR1 MFI on total CD4+ and CD8+ T cells is positively correlated to CD71 MFI on both Day 1 and Day 3.

Data set from	Group A	Group B	Correlation *p*-value	Correlation Pearson r
Day 1	CD71 MFI in total CD4+ T cells	IFN-λR1 MFI in total CD4+ T cells	**** <0.0001	0.7440
	CD71 MFI in total CD8+ T cells	IFN-λR1 MFI in total CD8+ T cells	**** <0.0001	0.8741
Day 3	CD71 MFI in total CD4+ T cells	IFN-λR1 MFI in total CD4+ T cells	**** <0.0001	0.7436
	CD71 MFI in total CD8+ T cells	IFN-λR1 MFI in total CD8+ T cells	**** <0.0001	0.7160

All correlation statistical analysis was done between "Group A" and "Group B" in the table on PRISM 10. Data set comparison computation used either Pearson correlation coefficients (when following a Gaussian distribution) or non-parametric Spearman correlation (when not following a Gaussian distribution). ns, $p > 0.05$; ****, $p < 0.0001$.

We showed that in PBMCs, TCR stimulation upregulates the levels of IFN-λR1 on CD4+ and CD8+ T cells, and this upregulation is dependent on CD3. To show the correlation directly, we conducted correlation analysis, and it is observed that on both day 1 and day 3, CD71 MFI positively correlates with IFN-λR1 MFI levels on CD4+ and CD8+ T cells, with Pearson $r > 0.716$ and $p < 0.0001$ (**Table 7**) The strongest correlation was seen between CD71 MFI and IFN-λR1 MFI on CD8+ T cells, with Pearson $r = 0.8741$ and $p < 0.0001$ (**Table 7**).

When examining the correlation between CD71 MFI and IL-10RB MFI on T cells, we observed that there was not a strong correlation between those two subjects; however, there was a strong correlation between CD71 MFI and IL-10RB MFI on Day 3 for both CD4+ and CD8+ T cells ($p < 0.0001$, $r > 0.7082$) (**Table 8**). In general, the correlation analysis results support our hypothesis that the strength of TCR stimulation regulates IFN-λR1 levels on the T cell surface at both time points, but only the later time point for IL-10RB.

Table 8. IL-10RB MFI in total CD4+ and CD8+ T cells is positively correlated to CD71 MFI on Day 3.

Data set from	Group A	Group B	Correlation *p*-value	Correlation Pearson r
Day 1	CD71 MFI in total CD4+ T cells	IL-10RB MFI in total CD4+ T cells	ns 0.0909	0.3384
	CD71 MFI in total CD8+ T cells	IL-10RB MFI in total CD8+ T cells	ns 0.1034	0.3266
Day 3	CD71 MFI in total CD4+ T cells	IL-10RB MFI in total CD4+ T cells	**** <0.0001	0.7082
	CD71 MFI in total CD8+ T cells	IL-10RB MFI in total CD8+ T cells	**** <0.0001	0.7451

All correlation statistical analysis was done between "Group A" and "Group B" in the table on PRISM 10. Data set comparison computation used either Pearson correlation coefficients (when following a Gaussian distribution) or non-parametric Spearman correlation (when not following a Gaussian distribution). ns, $p > 0.05$; ****, $p < 0.0001$.

3.1.3 Investigate if Various TCR Stimulation Conditions Alter IFN-λR Levels on the Surface of Purified CD4+ T cells.

Hypothesis: TCR stimulation by anti-CD3 and anti-CD28 upregulates the level of IFN-λR1 but does not alter the level of IL-10RB on purified human CD4+ T cells.

As PBMCs contain many immune cell types, such as monocytes and B cells, even though the stimulant we used are relatively T-cell specific, we want to know if the stimulation directly upregulates the IFN-λR1 levels on T cells, without requiring intermediate cells. To rule out the impact of other cell types in this process, I first isolated CD4+ T cells by negative selection from PBMCs. Then, I stimulated them with various stimuli to quantify IFN-λR1 levels on the cell surface. To match the level of TCR stimulation, we increased the concentration of anti-CD3 used to precoat the cell culture plate compared to whole PBMC stimulation.

The Zombie AQUA staining showed that over 93% of cells were viable (**Figure 21A**), and the purity of CD4+ T cells cultured was 94.9%. We also added CD69 as a second activation marker besides CD71 to evaluate the magnitude of TCR stimulation. The highest level (MFI) of CD71 was observed when purified CD4+ T cells were treated with anti-CD3 (3 μg/mL) and anti-CD28 (1.5 μg/mL) (**Figure 21B and 21C**) We noticed the CD71 MFI and CD69 MFI levels across

different stimulation conditions vary, and CD71 and CD69 MFI does not share a same pattern (**Figure 21B and 21C**). Similar to CD4+ and CD8+ T cells within PBMCs, IFN-λR1+% and IFN-λR1 MFI on purified CD4+ T cells increased when stimulated with anti-CD3 and anti-CD28, and a bigger increase was observed in cells treated with a higher concentration of anti-CD3 (3 μg/mL) compared to cells treated with less concentrated anti-CD3 (1 μg/mL) **(Figure 21D** and **21E**). Anti-CD28 alone did not alter the IFN-λR1+% or IFN-λR1 MFI on CD4+ T cells, but it contributes to an increase of IFN-λR1 levels on cells when added together with anti-CD3(**Figure 21D and 21E**). It confirmed that the T cell co-stimulatory signal alone was not sufficient in inducing the upregulation of IFN-λR1 on the cell surface. IL-10RB+% across stimulation conditions was not altered by anti-CD3 and anti-CD28 stimulation (**Figure 21F**), but IL-10RB MFI increased in TCR-stimulated CD4+ T cells, which has a pattern similar to IFN-λR1+%, where the highest IL-10RB MFI also seen in cells treated with more concentrated anti-CD3 (**Figure 21G**).

Similar to PBMCs, we observed that CD71+ and CD69+ CD4+ T cells express more IFN-λR1 on the cell surface (both IFN-λR1+% and IFN-λR1 MFI) compared to their respective activation marker-negative counterparts (**Figure 22A and 22B**). Besides, IL-10RB+% CD4+ T cells were not altered on Day 1.5 upon TCR stimulation, but the MFI of IL-10RB got upregulated, with a magnitude associated with the extent that CD71 or CD69 got upregulated (**Figure 22C and 22D**). Admitting lack of repeat as a limitation, the preliminary data showed that TCR stimulation using anti-CD3 and anti-CD28 directly upregulates IFN-λR1+%, IFN-λR1 MFI, and IL-10RB MFI in purified human CD4+ T cells.

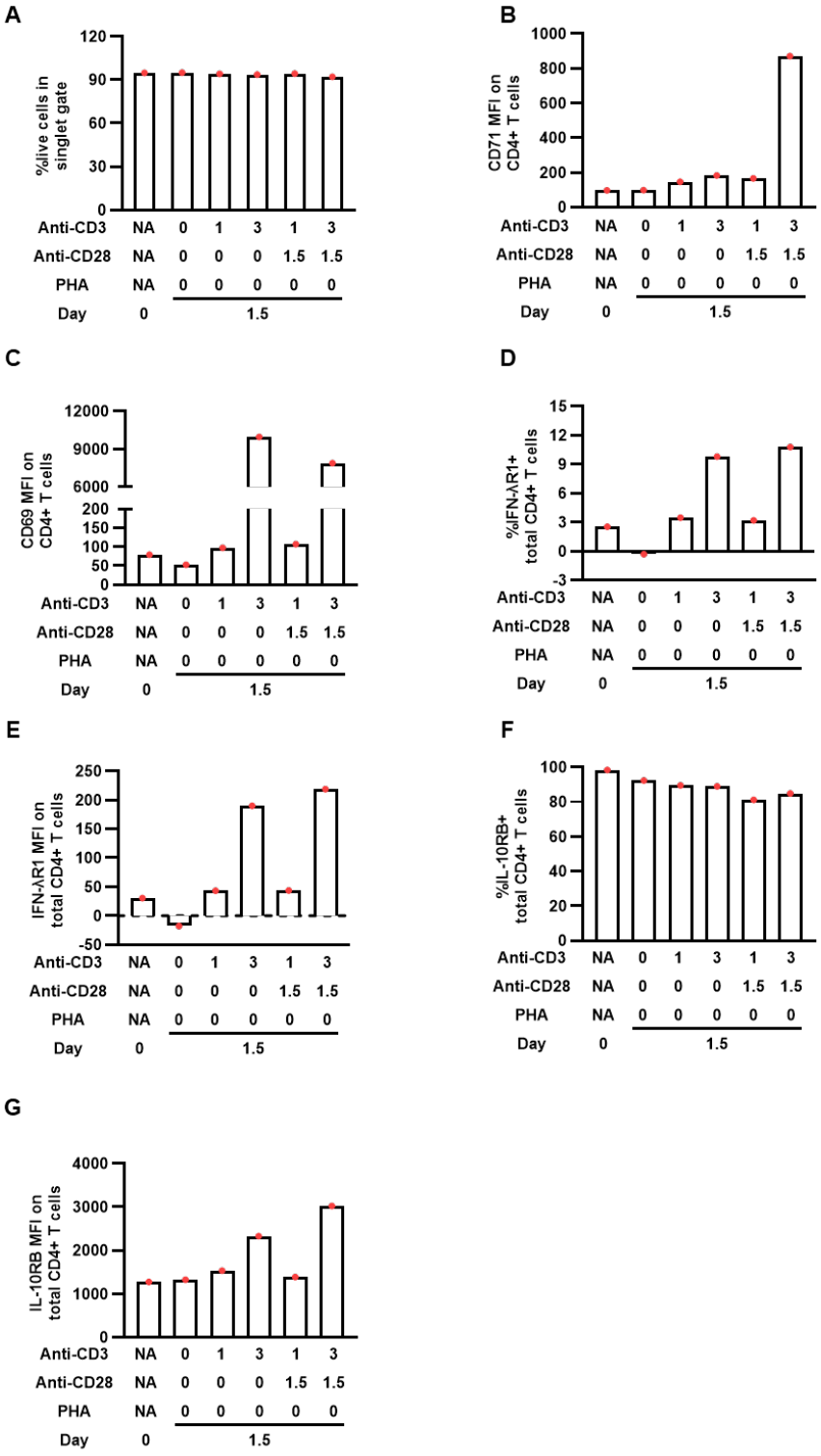

Figure 21. TCR stimulation upregulates IFN-λR1, and to a lesser extent IL-10RB, on the surface of purified CD4+ T cells.

(A) cell viabilities are shown in the percentage of Zombie AQUA negative staining cells in live cells. (B) CD71 MFI and (C) CD69 MFI on CD4+ T cell population under TCR stimulation

conditions with or without different concentrations of anti-CD3 (coated on the 96-well plate) and anti-CD28 (in cell culture media suspension) on Day 1.5. (D) The percentage of IFN-λR1+ CD8+ T cells and (E) IFN-λR1 on Day 1.5. (F) The percentage of IL-10RB+ CD8+ T cells and (G) IL-10RB on Day 1.5. For panels (A-G), the numbers listed under or in bracket "()" on the right of the graph indicate the concentration of the respective antibody or PHA, unit μg/mL. For (C-H), comparisons were made between the respective condition average and Day 1.5 control without anti-CD3, anti-CD28, and PHA (second column from the left in the respective panel). Statistical analyses could not be completed when only one donor recruited to date.

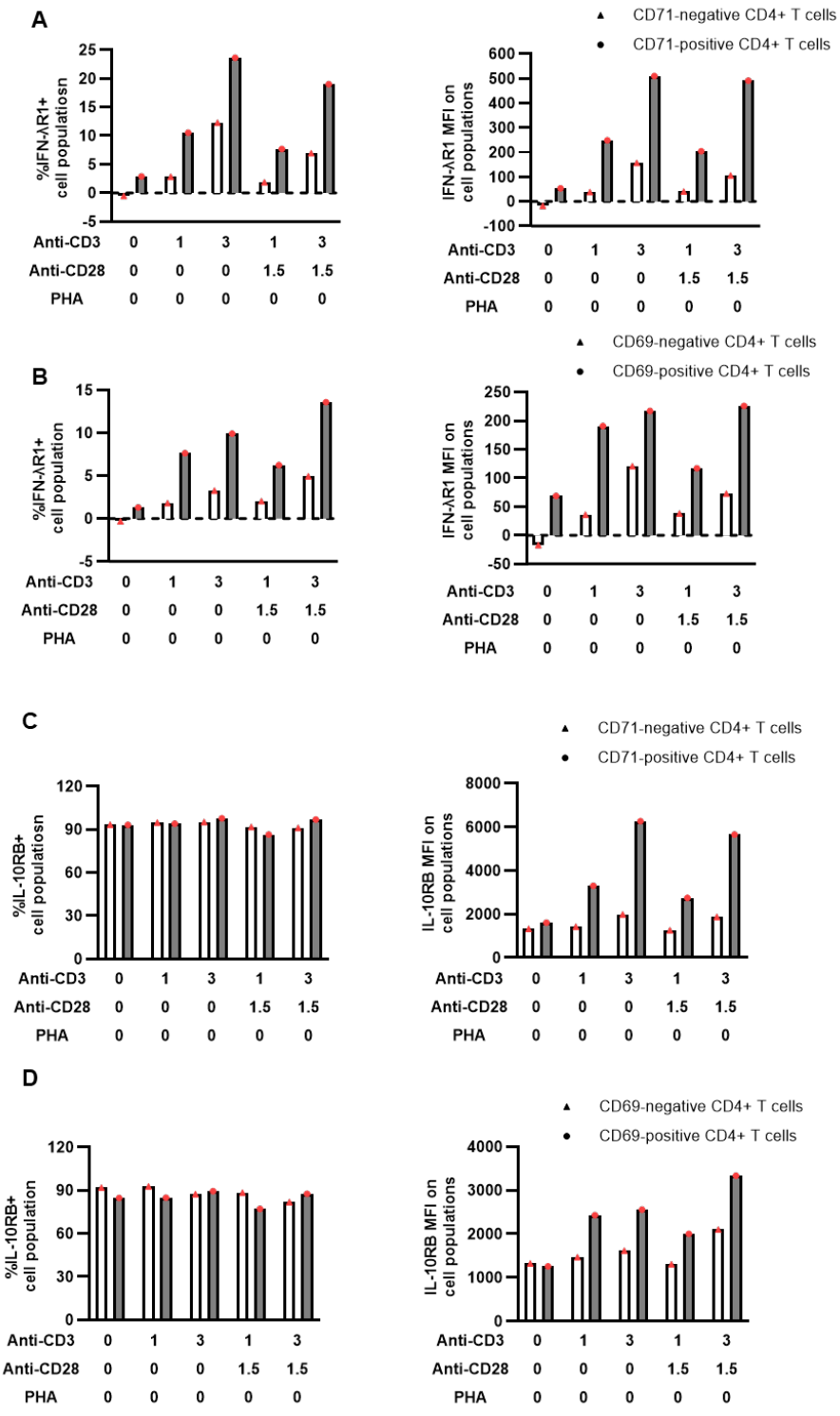

Figure 22. Higher IFN-λR1 levels, but not IL-10RB+%, were observed on CD71+ and CD69+ CD4+ T cell populations post TCR-stimulation.

(A) IFN-λR1+% and (B) IFN-λR1 MFI on CD71+ and CD71- CD4+ T cells after 1.5-day TCR stimulation. (C) IFN-λR1+% and (D) IFN-λR1 MFI on CD62L+ and CDCD62L- CD4+ T cells

after 1.5-day TCR stimulation. (E) IL-10RB+% and (F) IL-10RB MFI on CD62L+ and CD62L- CD8+ T cells after 1-day TCR stimulation. Each colour of dots in the column graph represents a different healthy donor. The table below the x-axis indicates the concentration of anti-CD3, anti-CD28, or PHA, unit μg/mL. IFN-λR1+% and IFN-λR1 MFI of FMO were subtracted from respective actual staining to calculate actual IFN-λR1+% and IFN-λR1 MFI. Statistical analyses could not be completed when only one donor recruited to date.

3.1.4 Investigate the molecular mechanisms downstream of TCR signalling that regulates IFN-λR1 on the human T cell surface.

Hypothesis: ZAP70, PI3K, and calcineurin contribute to the upregulation of IFN-λR1 levels and IFN-λR1+% on the human T cell surface by TCR stimulation.

Next, I aimed to uncover the cell signalling events required for the upregulation of IFN-λR1 by TCR stimulation to occur. To reveal that, we used several TCR inhibitors known to target signalling pathways downstream of the TCR. ZAP180013, sp600125, Duvelisib, and FK506 are known to inhibit ZAP70, JNK, PI3K, and calcineurin, respectively. [198-201] A summary of these four inhibitors and their targets is included in **Figure 23**.

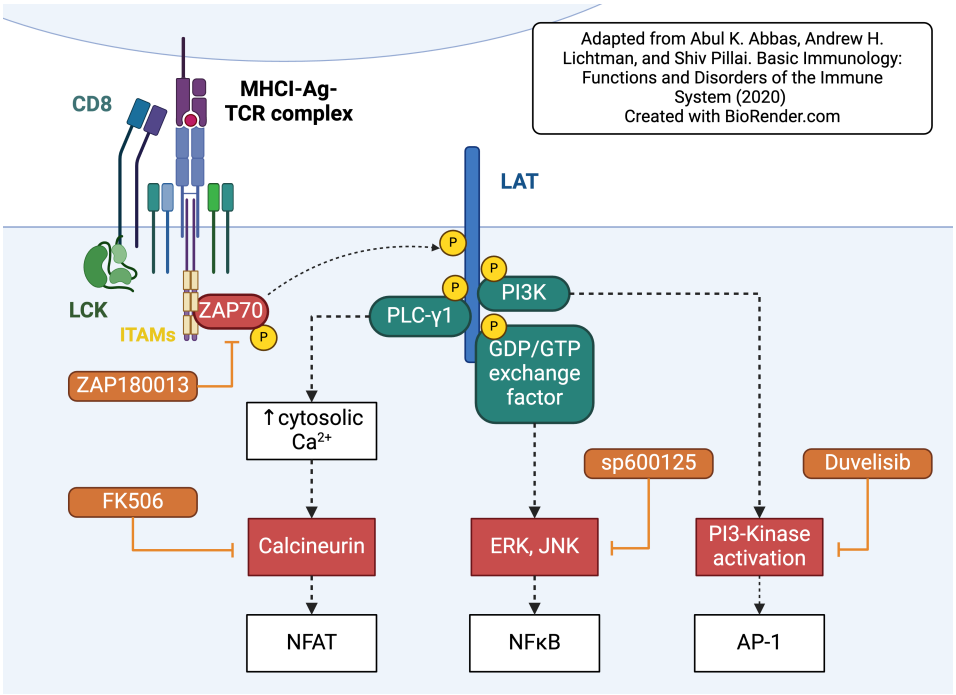

Figure 23. Selected TCR signalling inhibitors and their targets.

ZAP180013, FK506, sp600125, and Duvelisib were used to inhibit ZAP70, calcineurin, JNK, and PI3-Kinase downstream of TCR stimulation.

ZAP70 inhibitor ZAP180013 stock was stored in dimethyl sulfoxide (DMSO) and then diluted using complete RPMI 1640 media to its designated concentrations. Therefore, we used DMSO diluted in complete RPMI 1640 media with a dilution factor matching ZAP70 to treat anti-CD3 (0.3 μg/mL)-stimulated PBMCs as our control. **Figure 24A** showed that ZAP180013, at 0.2 and 2 μM, did not influence the viability of PBMCs. Adding ZAP-70 inhibitor ZAP180013 at 0.2 and 2 μM reduced CD71 MFI from ~170 to 100 and 60 (**Figure 24B**), respectively, indicating a lower magnitude of activation. The same trend was seen in CD8+ T cells (**Figure 24C**). IFN-λR1+% CD4+ T cell decreased from 13% to 10% (**Figure 24B).** For CD4+ T cells, adding ZAP180013 at 2 μM, the percentage of IFN-λR1-positive cells and MFI of IFN-λR1 both reduced by 3% and 150, respectively (**Figure 24D and 24F**). For CD8+ T cells, 2 μM ZAP180013 decreased IFN-λR1+% by 6% and 150, respectively (**Figure 24E and 24G**).

Duvelisib, a PI3K inhibitor, did not significantly influence cell survival; viable cell percentages in PBMCs treated with 0.03 and 0.3 μM Duvelisib were above 94% post-culturing (**Figure 25A**). Similar to ZAP180013, Duvelisib downregulated CD71 MFI in both CD4+ (by 71%) and CD8+ T cells (by 84%) (at 0.3 μM) (**Figure 25B and 25C**). In both CD4+ and CD8+ T cells, the more concentrated Duvelisib inhibited the levels of IFN-λR1 on the cell surface compared to the DMSO-treated anti-CD3-stimulated PBMCs (**Figure 25D-G**).

sp600125 treatment did not induce a reduction in cell viability in anti-CD3-treated PBMCs (**Figure 26A**). It inhibited the CD71 level on the T cell surface during TCR stimulation (**Figures 26B-C**) without strongly influencing the percentage of CD4+ and CD8+ T cells expressing IFN-λR1 on the cell surface (**Figures 26D-E**). Simultaneously, IFN-λR1 MFI was downregulated by sp600125 for a mild magnitude, indicating JNK might be dispensable for the TCR-regulated IFN-λR1 (**Figures 26D-G**).

NFAT was examined last. As discussed in the Introduction section, calcineurin serves as the crucial phosphatase that dephosphorylates and activates NFAT. FK506 functions through binding FK506-binding protein; the complex formed can inhibit calcineurin activity and, therefore, inhibit NFAT activities.[202] No FK506-induced cell death was observed at 0.1μM and 1 μM (**Figure 27A**). FK506 inhibited CD71 levels on CD4+ (65.5%) and CD8+ T cell (69.9%) surfaces (**Figure 27B-C**). The magnitude it downregulates IFN-λR1 is different in CD4+ and CD8+ T cells; the

upregulation of IFN-λR1 levels on CD8+ T cells was more resistant to NFAT blockade by FK506 (**Figure 27D-G**).

Based on those observations, we concluded that ZAP70, PI3K, and NFAT contribute to the TCR stimulation-induced upregulation of IFN-λR1 on the T cell surface. We admit the limited number of donors for this experiment, and repeats will be needed to confirm the trend we observed.

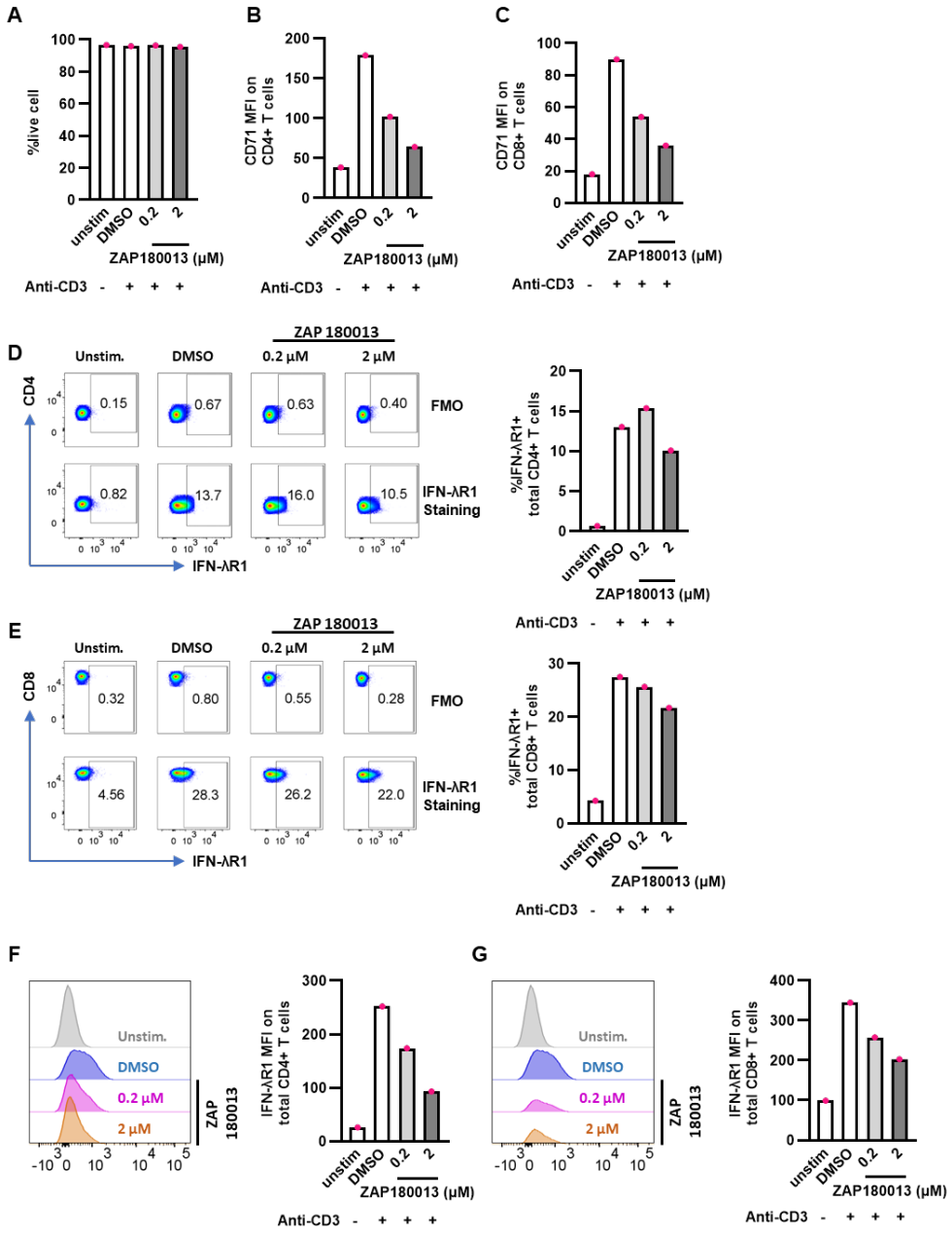

Figure 24. ZAP70 contributed to the upregulation of IFN-λR1 by TCR stimulation.

(A) Cell viability checks are shown in the percentage of live cells, using Zombie AQUA staining and flow cytometry. CD71 MFI in (B) CD4+ and (C) CD8+ T cells. (D) The percentage of IFN-λR1+ CD4+ T cells and (F) IFN-λR1 MFI on CD4+ T cells. (E) The percentage of IFN-λR1+ CD4+ T cells and (G) IFN-λR1 MFI on CD4+ T cells. For all conditions except the unstimulated conditions, whole PBMCs were cultured in wells pre-coated with 0.3 μg/mL anti-CD3 for 20 hours. For (A-G), comparisons were made between the respective condition and DMSO control (noted "DMSO"), which matches the DMSO (carrier for stock ZAP180013 stock) concentration to 2μM ZAP180013. Statistical analyses could not be completed when only one donor recruited to date.

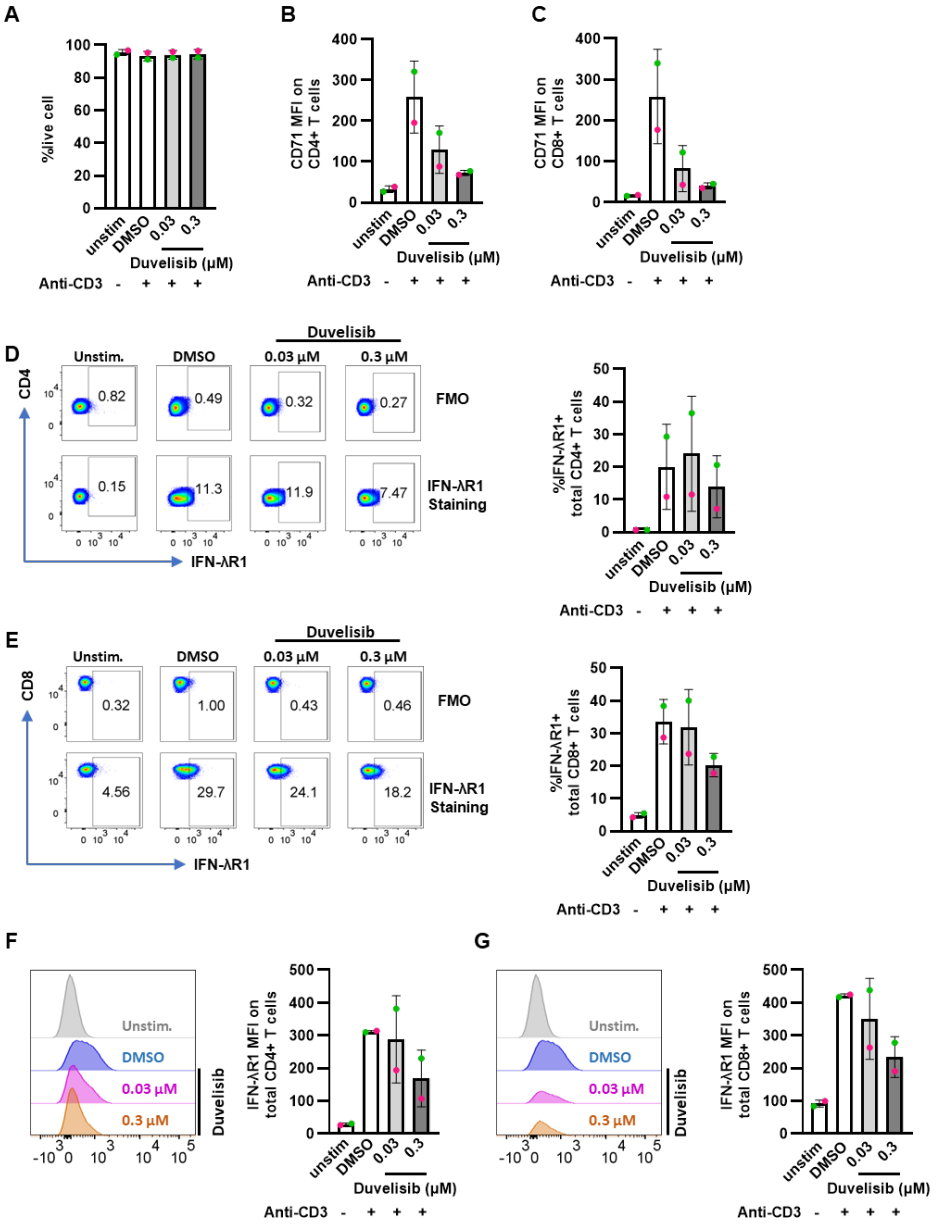

Figure 25. PI3K played a role in the upregulation of IFN-λR1 by TCR stimulation.

(A) Cell viability checks are shown in the percentage of live cells, using Zombie AQUA staining and flow cytometry. CD71 MFI in (B) CD4+ and (C) CD8+ T cells. (D) The percentage of IFN-λR1+ CD4+ T cells and (F) IFN-λR1 MFI on CD4+ T cells. (E) The percentage of IFN-λR1+ CD4+ T cells and (G) IFN-λR1 MFI on CD4+ T cells. For all conditions except the unstimulated conditions, whole PBMCs were cultured in wells pre-coated with 0.3 μg/mL anti-CD3 for 20 hours. For (A-G), comparisons were made between the respective condition and DMSO control (noted "DMSO"), which matches the DMSO (carrier for stock Duvelisib) concentration to 0.3 μM Duvelisib. Statistical analyses could not be completed when only two donors recruited to date.

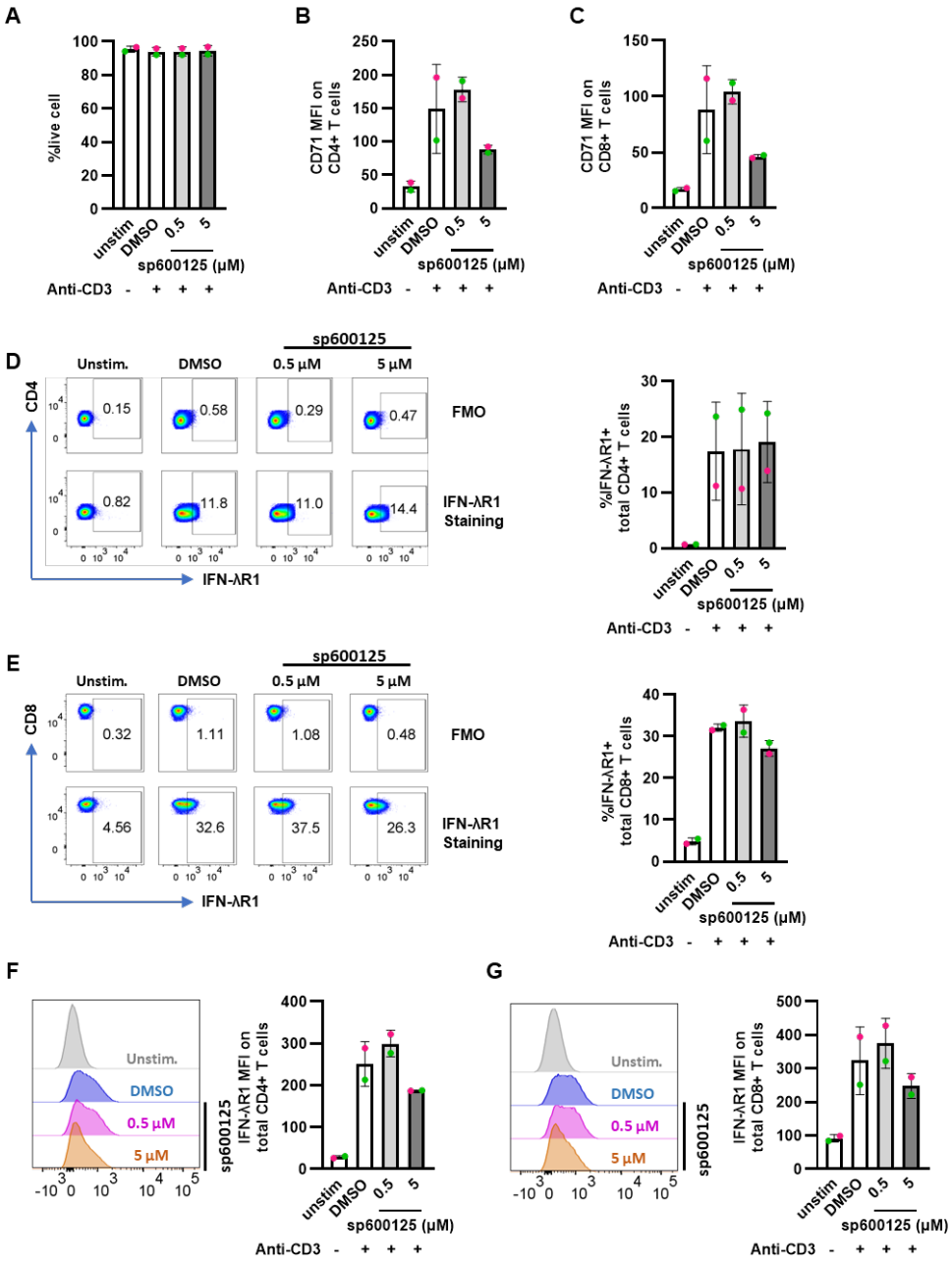

Figure 26. JNK did not contribute to the upregulation of IFN-λR1 by TCR stimulation.

(A) Cell viability checks are shown in the percentage of live cells, using Zombie AQUA staining and flow cytometry. CD71 MFI in (B) CD4+ and (C) CD8+ T cells. (D) The percentage of IFN-λR1+ CD4+ T cells and (F) IFN-λR1 MFI on CD4+ T cells. (E) The percentage of IFN-λR1+ CD4+ T cells and (G) IFN-λR1 MFI on CD4+ T cells. For all conditions except the unstimulated conditions, whole PBMCs were cultured in wells pre-coated with 0.3 μg/mL anti-CD3 for 20 hours. For (A-G), comparisons were made between the respective condition and DMSO control (noted "DMSO"), which matches the DMSO (carrier for sp600125 stock) concentration to the higher drug dose. Statistical analyses could not be completed when only two donors recruited to date.

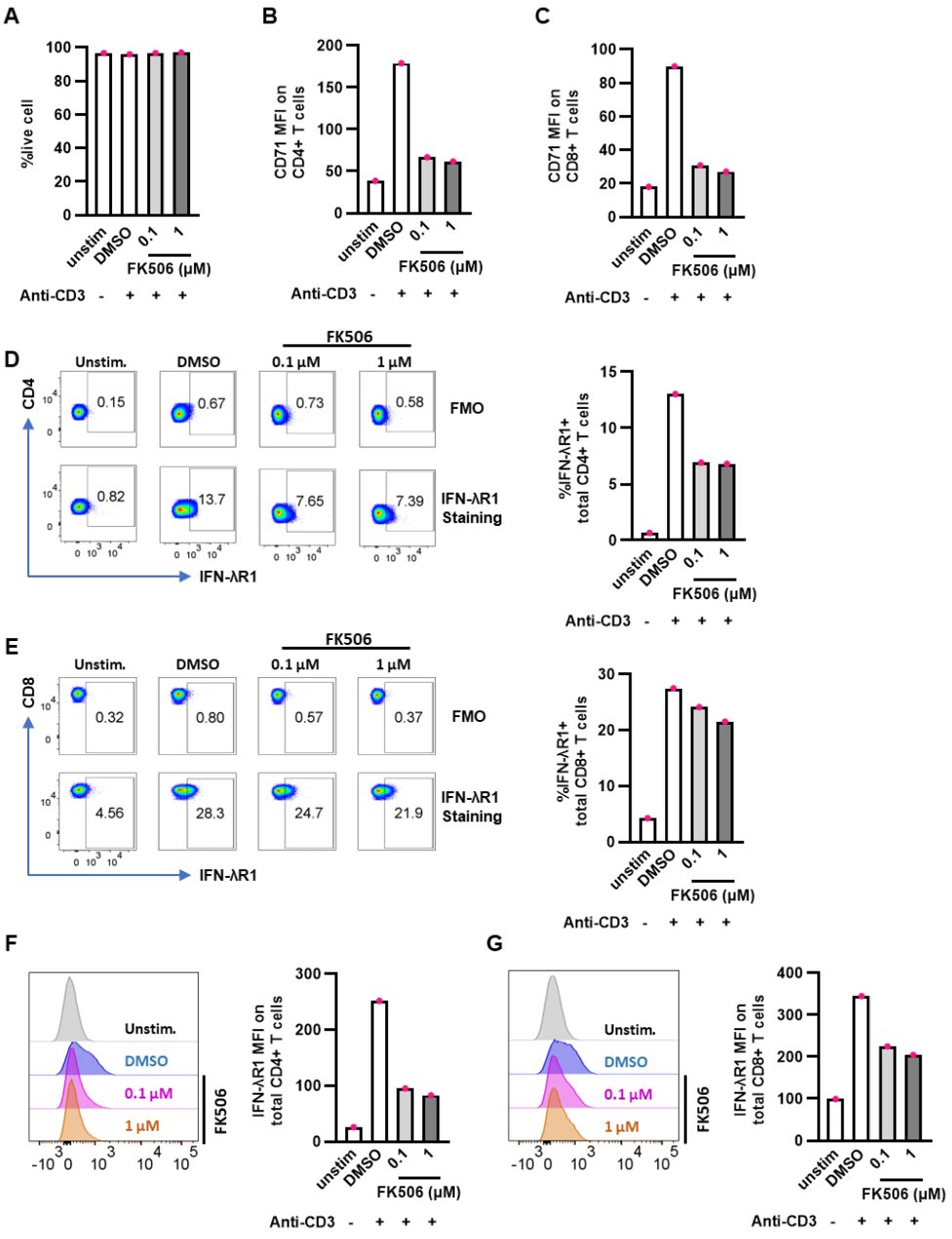

Figure 27. NFAT contributed to the upregulation of IFN-λR1 by TCR stimulation especially in CD4+ T cells.

(A) Cell viability checks are shown in the percentage of live cells, using Zombie AQUA staining and flow cytometry. CD71 MFI in (B) CD4+ and (C) CD8+ T cells. (D) The percentage of IFN-λR1+ CD4+ T cells and (F) IFN-λR1 MFI on CD4+ T cells. (E) The percentage of IFN-λR1+ CD4+ T cells and (G) IFN-λR1 MFI on CD4+ T cells. For all conditions except the unstimulated conditions, whole PBMCs were cultured in wells pre-coated with 0.3 μg/mL anti-CD3 for 20 hours. For (A-G), comparisons were made between the respective condition and DMSO (carrier for FK506) control (noted "DMSO"), which matches the DMSO concentration to the higher drug dose. Statistical analyses could not be completed when only one donor recruited to date.

3.2 Aim 2: Investigating the Regulatory Effect of IFN-λ3 on Polarization and Cytokine Production of CD4+ T Cell Lineages (Th1, Th2).

3.2.1 Investigate the Effect of IFN-λ3 on Th1 and Th2 Cytokine Production in Whole PBMCs Context.

Hypothesis: IFN-λ3 directly downregulates Th2 cytokine production (IL-13) but upregulates Th1 cytokine production (IFN-γ) in human PBMCs stimulated with anti-CD3 and anti-CD28.

Previously, it has been shown that IFN-λs can indirectly downregulate Th2 cytokines in various mouse airway hypersensitivity models through DCs, NK cells, T regs, and epithelial cells while upregulating Th1 cytokine production.[183-189,203] However, the distribution of IFN-λR1 on immune cells is different between mice and humans; specifically, data have shown mice T cells do not express detectable IFN-λR1 on the surface.[168,169] It is not known whether IFN-λ3 can directly regulate Th2 cytokines in humans during Th1 and Th2 polarization with anti-CD3 and anti-CD28 stimulation. I have shown in Aim 1 that at steady state, less than 1% of naïve CD4+ T cells express IFN-λR1 on the cell surface. TCR stimulation, which is a crucial prerequisite of CD4+ T cell polarization, increases the levels of IFN-λR1 by 20-fold. This upregulation in IFN-λR1 level provided CD4+ T cells with the potential to respond more potently to IFN-λ3 in humans. We hypothesize that IFN-λ3 can directly inhibit human Th2 cytokine while promote Th1 cytokine production when purified CD4+ T cells are stimulated *in vitro*.

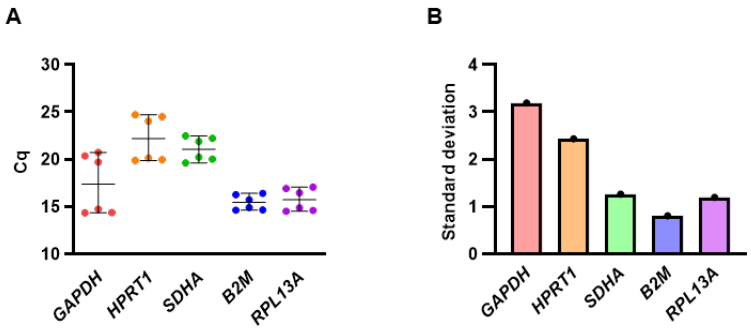

Figure 28. *B2M* and *RPL13A* were the most stable reference genes across the stimulation conditions tested.

Reference gene *GAPDH*, *HPRT1*, *SDHA*, *B2M*, and *RPL13A* were compared using cDNA prepared from CD4+ T cell RNA post-stimulation using Dynabeads, Stemcell ImmunoCult activator, or anti-CD3 with anti-CD28. (A) Cq value from qPCR results for various reference gene candidates. (B) Standard deviation was calculated for each reference gene across different stimulation conditions.

Using enriched CD4+ T cells kindly provided by Dr. Thomas Murooka (University of Manitoba), we started by testing different reference gene candidates for use in RT-qPCR assays (*GAPDH*. *HPRT1*, *SDHA*, *B2M*, and *RPL13A*). Among the five tested, *B2M* had the lowest standard deviation and fluctuation in unstimulated or stimulated CD4+ T cells. (**Figure 28A and 28B**) We also used GeNorm (https://genorm.cmgg.be/) to compare these reference gene candidates and confirmed that *B2M* was the most stable reference gene among them.

Next, we examined whether IFN-λ3 regulates Th1 and Th2 cytokine at mRNA and protein levels in whole PBMCs. We measure *IL13* transcripts and IL-13 in cell supernatant to represent Th2 cytokines; as a typical Th2 cytokine, IL-13 contributes to airway mucus overproduction and hyperresponsiveness.[204] Using qPCR and ELISA, we showed that in the absence of TCR stimulation, IFN-λ3 does not alter CD4+ T cell *IL13* transcripts or production levels (data not shown and **Figure 29C**). When treated with IFN-λ3, PHA-stimulated PBMCs had a 30% decreased level of *IL13* transcripts compared to stimulation-only control and a lower level of IL-13 secretion in supernatant (**Figure 29A and 29D**). The inhibitory effects of IFN-λ3 on PBMCs IL-13 at both mRNA and protein levels were seen in anti-CD3 and anti-CD28 stimulation context with significance ($p < 0.05$) (**Figure 29B** and **29E**).

Next, we tested if IFN-λ3 regulates Th1 cell cytokine levels in whole PBMCs +/- TCR stimulation. Upon PHA or anti-CD3 and anti-CD28 stimulation, IFN-λ3 did not alter the level of *IFNG* transcript and IFN-γ secretion (**Figure 30A-B, 30D-E**). In unstimulated PBMC, we did not observe a detectable level of IFN-γ in cell supernatant, and *IFNG* mRNA was low (data not shown and **Figure 31C**). To conclude, we observed that in whole PBMCs, IFN-λ3 can downregulate IL-13 at both the mRNA and protein levels in the context of anti-CD3 and anti-CD28 stimulation; however, IFN-λ3 did not alter the level of IFN-γ secretion and *IFNG* transcripts.

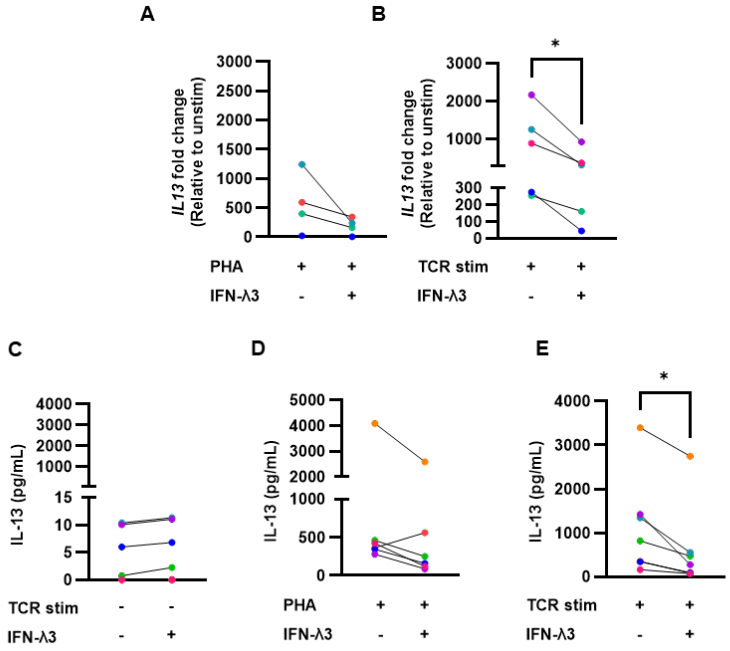

Figure 29. IFN-λ3 downregulated IL-13 at mRNA and protein levels in PBMCs upon anti-CD3 and anti-CD28 stimulation.

Fold induction of *IL13* from healthy donor whole PBMCs when stimulated with (A) PHA and (B) anti-CD3 and anti-CD28 ("TCR stim") (relative to unstimulated PBMCs without IFN-λ3 treatment, without PHA, without anti-CD3 and anti-CD28 stimulation, ("unstim") normalized to reference gene *B2M*). (C-E) IL-13 secretion in the cell culture supernatant from healthy donor whole PBMCs. (C) PBMCs unstimulated control +/- IFN-λ3 without TCR anti-CD3 and anti-CD28 stimulation, (D) stimulated with PHA, (E) stimulated with plate-bound anti-CD3 (1.5 µg/mL) with anti-CD28 (4.47 µg/mL, soluble) in media (noted as "TCR stim") +/- IFN-λ3 (100 ng/mL) for 48 hours. Paired t-test. All comparisons not marked with a star(s) "*" indicate no significant differences; *, $p < 0.05$.

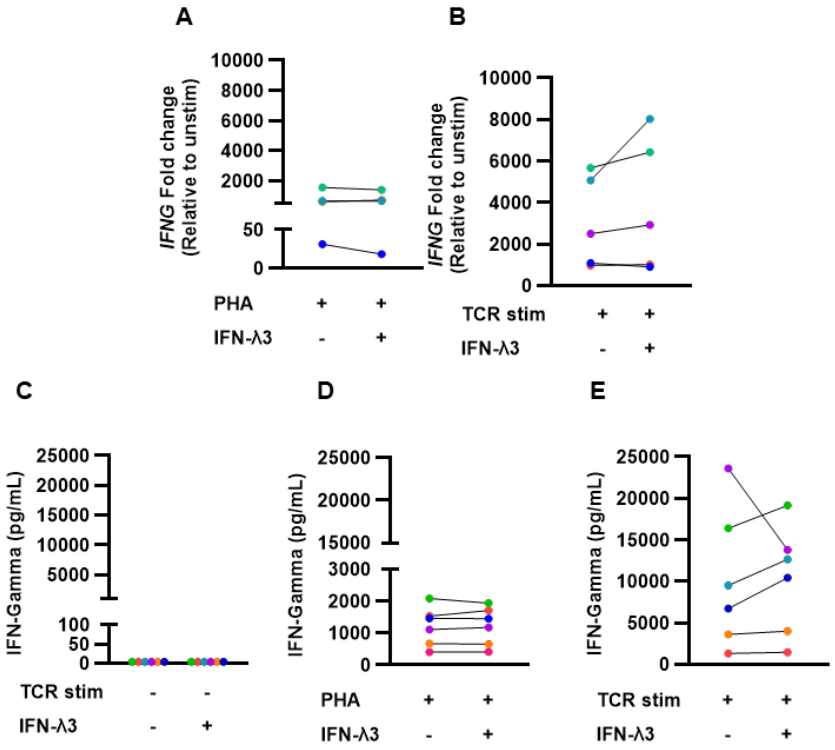

Figure 30. IFN-λ3 did not alter IFN-γ at the mRNA and protein levels in TCR or PHA-stimulated PBMCs.

Fold induction of *IFNG* from healthy donor whole PBMCs when stimulated with (A) PHA and (B) anti-CD3 and anti-CD28 ("TCR stim") (relative to unstimulated PBMCs without IFN-λ3 treatment, without PHA, without anti-CD3 and anti-CD28 stimulation, ("unstim") normalized to reference gene *B2M*). (C-E) IFN-γ secretion in the cell culture supernatant from healthy donor whole PBMCs. (C) PBMCs unstimulated control +/- IFN-λ3 without TCR anti-CD3 and anti-CD28 stimulation, (D) stimulated with PHA, (E) stimulated with plate-bound anti-CD3 (1.5 µg/mL) with anti-CD28 (4.47 µg/mL, soluble) in media (noted as "TCR stim") +/- IFN-λ3 (100 ng/mL) for 48 hours. Paired t-test. All comparisons not marked with a star(s) "*" indicate no significant differences. n=3 or 4 or 6.

3.2.2 Investigate the Effect of IFN-λ3 on Th1 and Th2 Cytokine Production During Naïve CD4+ T Cell Polarization.

Hypothesis: IFN-λ3 downregulates Th2 cytokine (IL-13, IL-4) but upregulates Th1 Cytokine (IFN-γ) production during naïve CD4+ T cell polarization.

Now that we know that IFN-λ3 can downregulate IL-13 at both mRNA and protein levels in the whole PBMC context, we wonder if this regulation is directly imposed on T cells. To address

that, we used purified naïve CD4+ T cells and studied the effect of IFN-λ3 on those cells upon Th0, Th1, and Th2 polarization conditions.

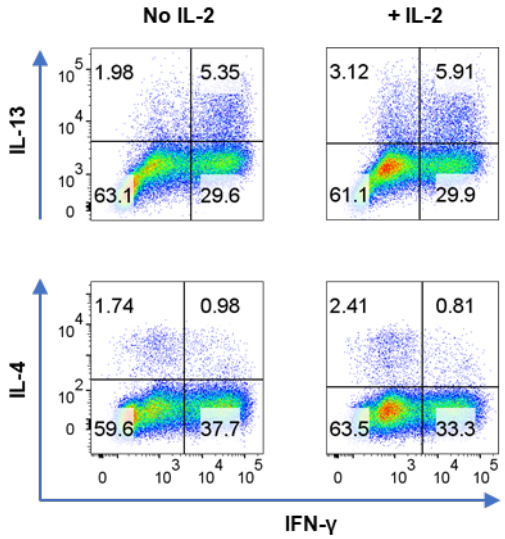

Figure 31. IL-2 addition did not alter IFN-γ production during Th1 polarization from naïve CD4+ T cells.

Cells were treated with plate-bound anti-CD3 (2.5 µg/mL) and anti-CD28 (1.5 µg/mL) and supplemented with IL-12 (5 ng/mL) and anti-IL-4 (5 µg/mL) for 6 days. Cells collected were stained and analyzed by flow cytometry. Statistical analyses could not be completed when only one donor recruited to date.

First, we needed to confirm our Th1 cell polarization protocols were effective. It is known that IL-2 contributes to CD4+ T cell proliferation and contributes to Th2 cell polarization;[107] Two Th1 polarization conditions were tested to investigate whether IL-2 promotes Th1 polarization. Comparing naïve CD4+ T cells (purity 92.7% by Zombie AQUA dye and flow cytometry, data not shown) polarized with Th1 polarizing cocktail (1.5 µg/mL anti-CD28, 5 ng/mL IL-12 and 5 µg/mL anti-IL-4), the addition of IL-2 did not alter IFN-γ+IL-13-% or IFN-γ+IL-4-% cells. (**Figure 31**)

Several protocols have been published to optimize the Th2 polarization condition. Some of them used soluble anti-CD3 to crosslink TCR and provide stimulation signalling, while others used immobilized anti-CD3 bound to cell culture plates.[205-210] We examined whether the form of anti-CD3 (plate bound vs. soluble in cell suspension) differs in Th2 cell polarization induction. The side scatter (SSC) vs. forward scatter (FSC) plot shows naïve CD4+ T cells treated with plate-

bound anti-CD3 with Th2 polarizing cocktail (0.5 μg/mL anti-CD28, 20 ng/mL IL-4, 5 μg/mL anti-IFN-γ, and 50 IU IL-2) had bigger size and more granular content, indicated by FSC and SSC, respectively (**Figure 32A**). IL-13+% in naïve CD4+ T cells treated with plate-bound anti-CD3 and soluble anti-CD3 were 10.9% and 0.74%, respectively (**Figure 32B**). IL-4+% was also much higher in immobilized anti-CD3-treated cells than in soluble anti-CD3-treated cells (**Figure 32B**). In terms of IL-13 and IL-4 production, intracellular flow staining showed plate-bound anti-CD3 induced 8-fold and 13-fold more IL-13+% and IL-4+% cells, compared to cells that had the same treatment with soluble anti-CD3. (**Figure 32B**) Anti-CD3 and anti-CD28 with Th2 polarizing environment induced more IL-13+% and IL-4+% than the Stemcell activator (an antibody cocktail containing anti-CD3 and anti-CD28) (**Figure 32C**). Anti-CD28 at 0.5 μg/mL and 1.5 μg/mL did not show a difference in inducing IL-13 and IL-4 production in the Th2-polarizing cocktail. Therefore, we selected plate-bound anti-CD3 and soluble anti-CD28 for the remaining experiments.

All naïve CD4+ T cell magnetic negative isolations led to purities of naïve CD4+ T cells of greater than 93%. I established the following gating strategy to quantify IFN-γ+ CD4+ T cells (Th1), including IFN-γ and zombie AQUA, to detect IFN-γ+ cells (**Figure 33A**). A viability check on day 6 showed that about 80% of cells were alive across different polarization conditions and IFN-λ3 treatment (**Figure 33B** and **33C**). In the Th0 condition, our preliminary data showed that IFN-λ3 decreased the percentage of cells that produced detectable IFN-γ and IFN-γ MFI. In the Th1 polarizing condition, IFN-λ3 did not induce a change in IFN-γ MFI or IFN-γ-positive cell percentage. (**Figure 33D** and **33E**)

The gating strategy sample is shown in **Figure 34A**. Next, I tested how IFN-λ3 regulates Th2 polarizing conditions, although at first, the same time point as Th1 (day 6) only led to 3.54% IL-4+ cells (**Figure 34B-D**), and both IL-4 and IL-13 levels went up at day 9, so I increased the differentiation time to 9 days. In contrast to Th1, 9 days of Th2 differentiation led to a drop in viability to around 60% (**Figure 34B**). The addition of IFN-λ3 downregulated IL-13 in both percentages of cells expressing IL-13 and IL-13 MFI (**Figure 34C-D**). We also observed a decrease in another Th2 cytokine, IL-4, in IFN-λ3 treated cells (**Figure 34C-D**). In conclusion, IFN-λ3 downregulated the production of Th2 cytokines represented by IL-13 and IL-4 and did not alter the levels of Th1 cytokines such as IFN-γ.

We are also curious if IFN-λ3 regulates other CD4+ T cell cytokines in addition to typical Th1 and Th2 cytokines during TCR stimulation. Our qPCR data showed that IFN-λ3 did not alter *IL2* and *TNF* transcript levels in the whole PBMC context when unstimulated, stimulated with PHA, or with anti-CD3 and anti-CD28 (**Figure 35A-D**).

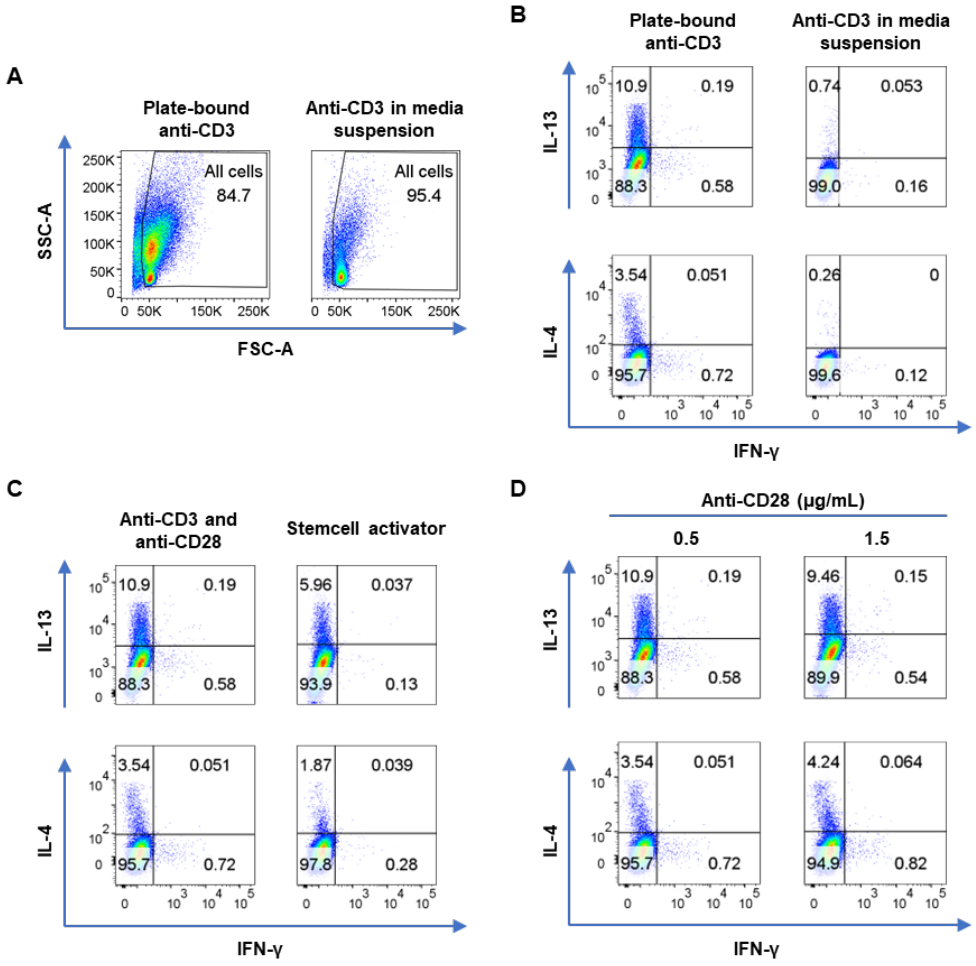

Figure 32. Plate-bound anti-CD3 with anti-CD28 promotes greater Th2 cytokine production during naïve CD4+ T cell polarization compared to soluble anti-CD3.

(A) side-scatter area vs. forward-scatter area of all cell gate of (B) IL-13, IL-4, and IFN-γ production when naïve CD4+ T cells were polarized with plate-bound anti-CD3 and anti-CD3 in cell suspension (both at 2 µg/mL). IL-13, IL-4, and IFN-γ production when (C) plate-bound anti-CD3 and anti-CD28 and Stemcell activator (D) anti-CD28 with indicated concentration (noted on top of the panel) in media suspension were provided during Th2 polarization in naïve CD4+ T cells. (A-D), all conditions were supplemented with anti-IFN-γ (5 µg/mL) and IL-4 (10 ng/mL). Cytokines and antibodies were added on day 0 and replenished on Day 3 and cells were incubated and collected for flow staining on Day 6. Statistical analyses could not be completed when only one donor recruited to date.

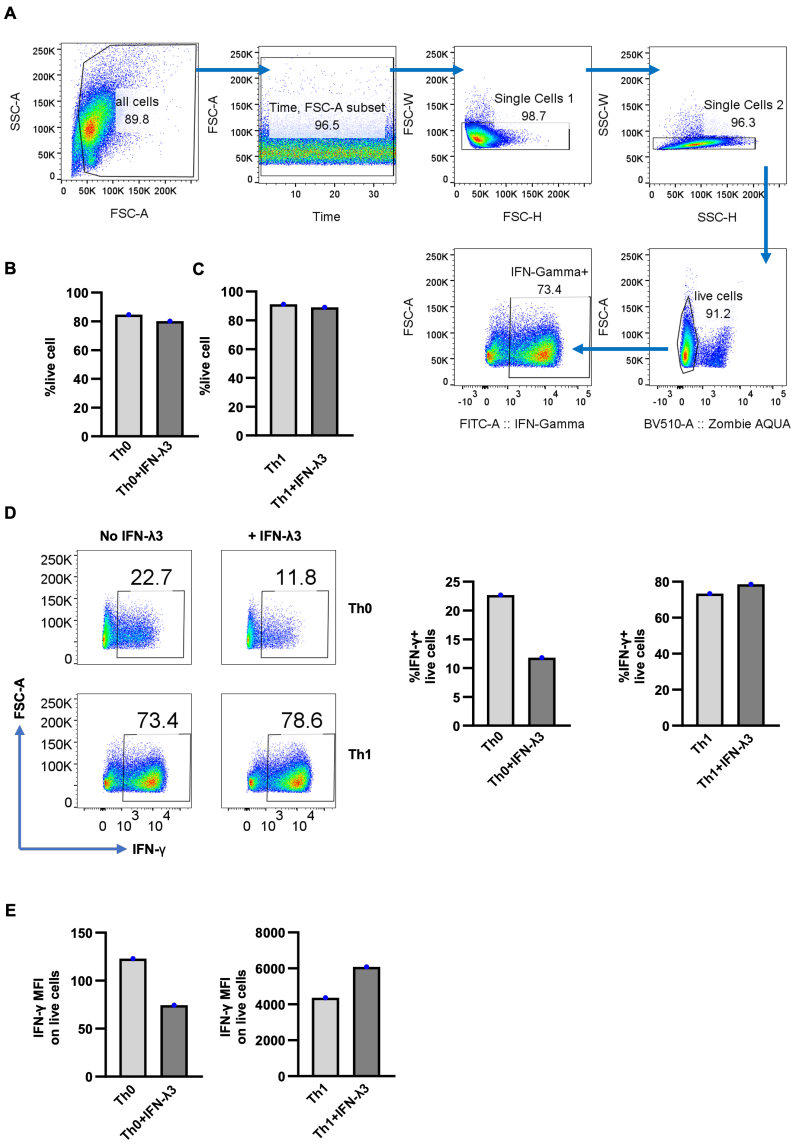

Figure 33. IFN-λ3 decreased IFN-γ production during Th0, but not Th1 polarization.

IFN-γ production in naïve CD4+ T cells treated with Th0 (2 µg/mL anti-CD3 precoated on wells, 1.5 µg/mL anti-CD28) or Th1 polarization condition (2 µg/mL anti-CD3 precoated, 1.5 µg/mL anti-CD28, 5 ng/mL IL-12, and 5 µg/mL anti-IL-4. IFN-λ3 was added to a final concentration of 100 ng/mL where applicable. For both Th0 and Th1 conditions, cells were incubated for 6 days with cytokines, antibodies, and IFN-λ3 added on day 0 and added again on day 3, and cells were incubated and collected for flow staining on Day 6. (A) Gating strategy for IFN-γ-positive cells. Cell viability is evaluated by the percentage of cells alive in Th0 (B) and Th1 (C) polarization conditions, with or without IFN-λ3. (D) The percentage of respective cells that are IFN-γ-positive in respective conditions and (E) IFN-γ MFI in respective conditions. Statistical analyses could not be completed when only one donor recruited to date.

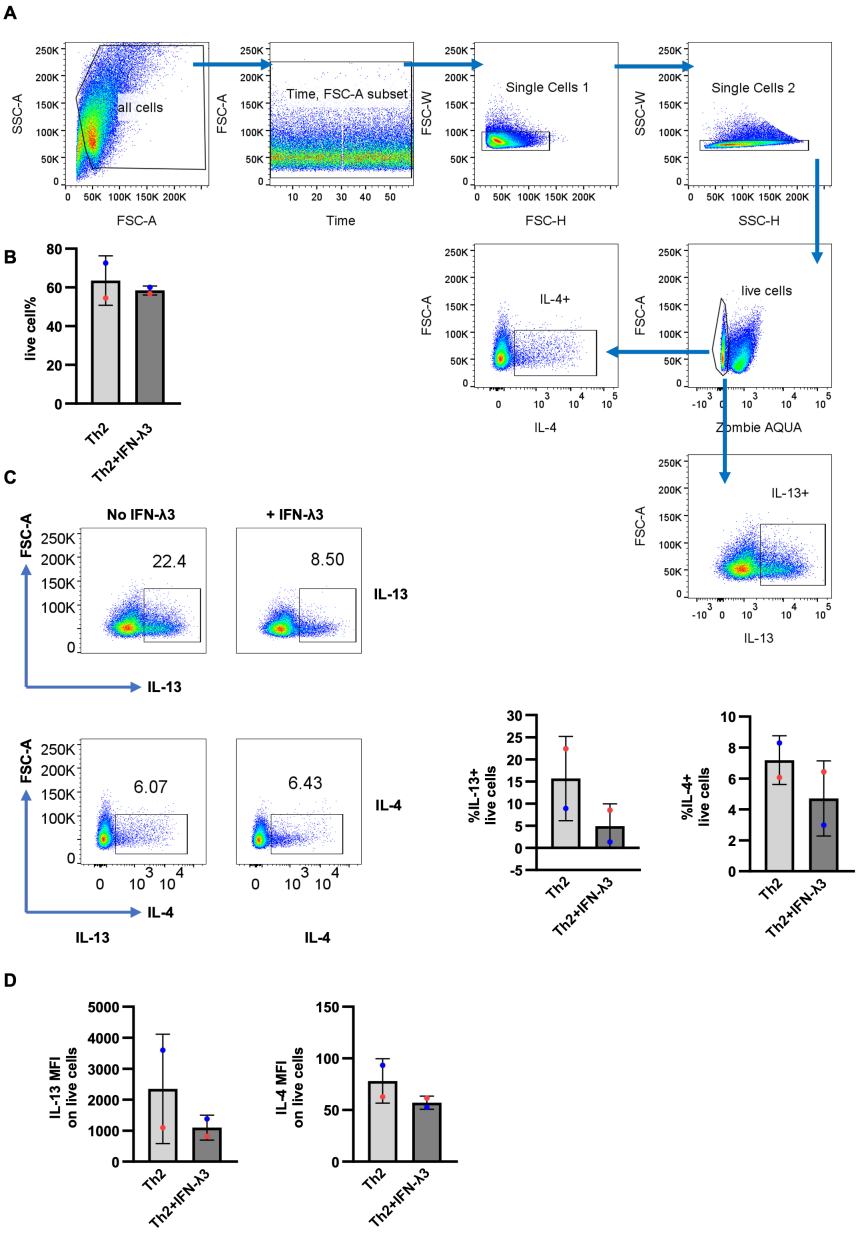

Figure 34. IFN-λ3 decreased IL-13 production during Th0 and Th1 polarization.

IL-13 production in naïve CD4+ T cells treated with Th2 polarization condition (2 µg/mL anti-CD3 0.5 µg/mL anti-CD28, 20 ng/mL IL-4, 5 µg/mL anti-IFN-γ, and 50 IU IL-2) on Day 9. IFN-λ3 was added to a final concentration of 100 ng/mL where applicable. For Th2 polarization conditions, cells were incubated for 6 days with cytokines, antibodies. Cytokines, antibodies, and IFN-λ3 added on day 0, and added to media again on day 3. (A) Gating strategy for quantifying IL-13-positive cells (representative of two experiments). (B) Cell viability is evaluated by the percentage of cells alive in Th2 polarization conditions, with or without IFN-λ3. (C) The percentage of respective cells that are IL-13-positive in respective conditions and (D) IL-13 MFI in respective conditions. Statistical analyses could not be completed when only two donors recruited to date.

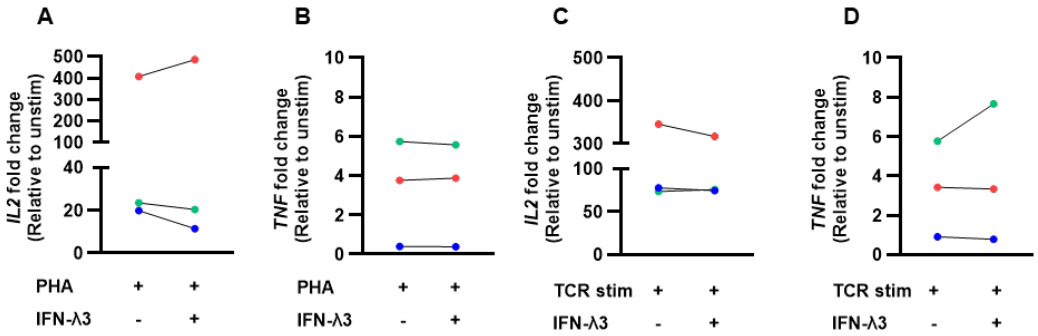

Figure 35. IFN-λ3 did not regulate *IL2* and *TNF* in PHA and TCR-stimulated PBMCs at mRNA levels.

(A, C) fold induction of *IL2*; and (B, D) fold induction of *TNF* from healthy donor whole PBMCs. (A-D) all relative to unstimulated PBMCs without IFN-λ3 treatment, without PHA, without anti-CD3 and anti-CD28 stimulation ("unstim"). *B2M* was used as the reference gene in the fold induction calculation. (A-B) stimulated with PHA, and (C-D) plate-bound anti-CD3 (1.5 μg/mL) with anti-CD28 (4.47 μg/mL) in media (noted as "TCR stim") with or without IFN-λ3 (100 ng/mL) for 48 hours. Paired t-test (A-D). t-test. All comparisons not marked with a star(s) "*" indicate no significant differences. n=3.

3.3 Aim 3: To Profile the Effect of IFN-λ3 on the Transcriptome of CD8+ T cells at Baseline and during TCR Stimulation.

3.3.1 To Investigate the Function of IFN-λ3 on CD8+ T Cells without TCR Stimulation.

Hypothesis: Without TCR stimulation, IFN-λ3 alone improves antiviral functions through upregulation of ISGs in human CD8+ T cells.

We investigated the direct effect of IFN-λ3 on purified CD8+ T cells. Coto-Llerena *et al.* showed that at low plate-bound anti-CD3 concentration (0.1 μg/mL), IFN-λ4 upregulated IFN-γ production by CD8+ T cells, and this upregulation is not observed in the absence of anti-CD3 or when anti-CD3 is provided at a higher dose.[161] Other than that study, little is known about the effect of IFN-λs on human CD8+ T cells. To reveal the overall impact of IFN-λ3 on CD8+ T cells, we treated purified CD8+ T cells from healthy donors with or without IFN-λ3 and with or without anti-CD3 and anti-CD28 stimulation for 20 hours, isolated RNA, and performed RNA sequencing on these samples. To reduce the bias introduced by the sex and age of donors, the demographic of 5 donors recruited for this study included males and females with an age range from 20 to 56. Using flow cytometry and the indicated gating strategy (**Figure 36A**), we showed that the putative CD8+ T cell we isolated from PBMCs had a purity higher than 92.7% before being cultured

(**Figure 36B**). With the help of Dr. Hemshekhar Mahadevappa (from Dr. Neeloffer Mookherjee's Lab), we also measured the RNA Integrity Number (RIN) for randomly selected four of our samples using a Bioanalyzer, which represents the degradation states of the RNA sample; the RIN for samples we obtained were from 8.4 to 9.1. All of the samples tested on Bioanalyzer had the key 18S and 28S RNA fragments (**Figure 37**).

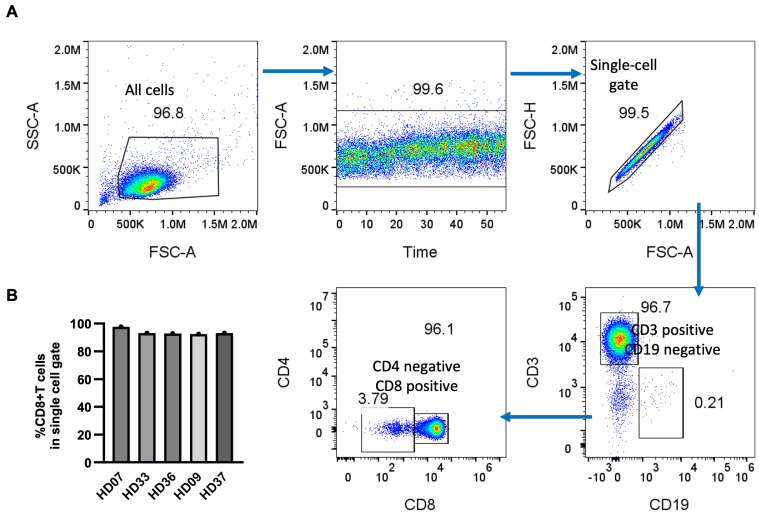

Figure 36. RNA sequencing sample purity check.

(A) Gating strategy example for CD8+ T cell purity check. The gating strategy is a representative of five different experiments. (B) The percentage of cells that are CD3+, CD19-, CD4-, and CD8+ in single cell gate for each donor. HD07, HD33, HD36, HD09, and HD37 were different donors.

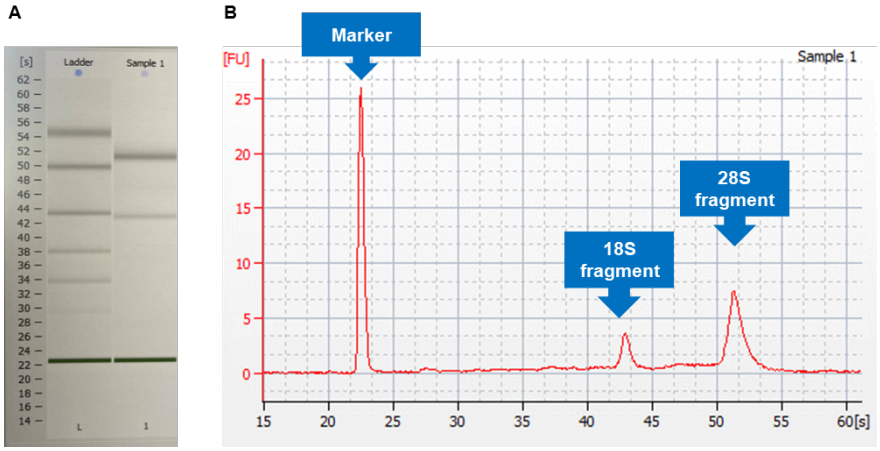

Figure 37. Bioanalyzer gel image and RNA integrity analysis output example for one sample out of twenty samples run for RNA sequencing.

(A) A Bioanalyzer gel image showing RNA samples and the ladder. (B) A representative electropherogram of the RNA sample.

It is known that type I and type III IFNs induce ISGs in cells[136,211], therefore, we confirmed the function of IFN-λ3 by measuring the fold-induction of two ISGs, *IFIT1* and *IFI44*, using RT-qPCR. Our data showed that IFN-λ3 promoted the fold change in *IFIT1* regardless of the presence or absence of anti-CD3 and anti-CD28 (**Figure 37A-B**). IFN-λ3 also enhanced *IFI44* fold change under unstimulated and TCR-stimulated conditions (**Figure 37C-D**).

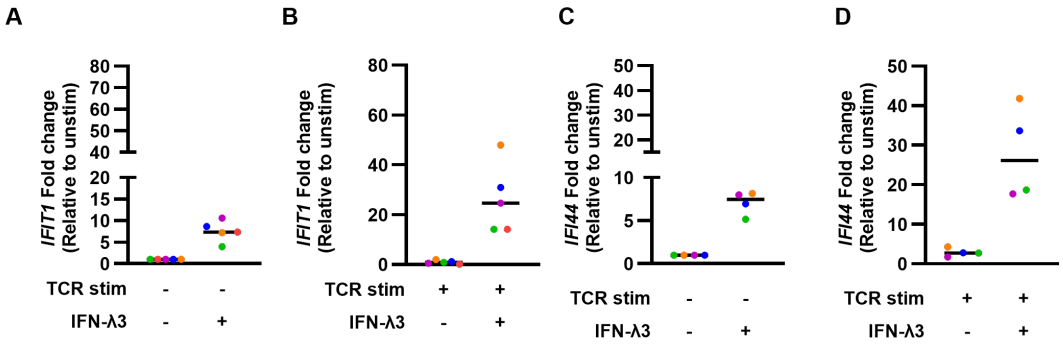

Figure 38. Screening of ISGs to ensure IFN-λ3 stimulated purified CD8+ T cells.

(A-B) Fold induction of *IFIT1* +/- TCR stimulation +/- IFN-λ3. (C-D) Fold induction of *IFI44* +/- TCR stimulation +/- IFN-λ3. (A-D) All relative to purified CD8+ T cells without IFN-λ3 treatment without anti-CD3 and anti-CD28 stimulation ("unstim"). *B2M* was used as the reference gene in the fold induction calculation. All TCR-stimulation represents that CD8+ T cells were stimulated with plate-bound anti-CD3 (3 μg/mL) and anti-CD28 (4.47 μg/mL) in media (noted as "TCR stim") +/-IFN-λ3 (100 ng/mL) for 20 hours. (A-B) n=5. (C-D) n=4.

Using samples analyzed above, we next sent our samples for RNA sequencing analysis to have an unbiased approach to hopefully uncover more than antiviral ISGs regulated by IFN-λ3 in CD8+ T cells. Our RNA sequencing data showed that compared to the unstimulated control, purified CD8+ T cells exposed to IFN-λ3 treatment had, in total, 366 genes upregulated, and 274 genes downregulated ($p < 0.05$). The higher expression of genes involved in cell signalling (i.e. *AKT1, NFKB1, CAMKK2, MAP3K7*), anti-viral response (i.e. *IFI44*, *IRF9, IRF7, Mx1*), cell survival (i.e. *AREL1-218*), cell proliferation and migration (i.e. *CEMIP*). The reduced expression of genes was related to processes such as gene silencing (i.e. *EHMT2*), cell metabolism (i.e. *MTHFR*), RNA degradation (i.e. *ERMARD*), and transcription initiation (i.e. KAT6B) (**Table 9**) (**Figure 39**). We also compared the *IFIT1* fold change from IFN-λ3-treated sample using *B2M* as reference gene over no IFN-λ3 treated sample from RT-qPCR, and the output of RNA sequencing;

when treated with IFN-λ3 without TCR stimulation, *IFIT1* fold change from RT-qPCR and RNA sequencing was 6.6 (**Figure 38A**) and 5.98, respectively.

Then, we investigated further at the pathway level how IFN-λ3 influenced CD8+ T cells. Gene Set Enrichment Analysis (GSEA) helps determine how a set of genes related to a certain pathway is regulated as a group and normalized by the number of genes in that group. In GSEA pathway analysis, as expected, the pathways upregulated by IFN-λ3 include response to viruses and symbionts and IFN-α and IFN-γ responses. IFN-γ also activates the TYK2-JAK-STAT pathways for their signalling.[212] We also observed that the positive regulation of canonical and non-canonical NF-κB signalling was upregulated in IFN-λ3-treated CD8+ T cells. Among 39 genes that got upregulated by IFN-λ3 in the absence of TCR stimulation in purified CD8+ T cells that are involved in NF-κB signalling, there were some genes functioning in translation regulation (*EIF2AK2*, *SPHK1*), NF-κB signalling induction (*IFI35*, *TLR7, TRIM56*), phosphorylation of p65 unit of NFκB (*LGALS9*), acetylation of p65 unit of NFκB (*NMI*). Some of the downregulated pathways in IFN-λ3-treated CD8+ T cells were related to protein synthesis and translation elongation, which indicates a slower overall protein synthesis in these cells compared to non-IFN-λ3-treated cells. (**Figure 40A**) After grouping the regulated pathways, we saw the most up-regulated group of pathways in IFN-λ3-treated cells being the antiviral response and effector function responses; there were some other up-regulated pathways but to a lesser magnitude, such as TNF production, cell-mediated antiviral immunity, and T cell protein tyrosine phosphatase (PTP) (**Figure 40B**). In contrast to Lck, which is an Src family PTK initiating TCR signalling by phosphorylating their substrates, PTP acts as one of the most important regulation mechanisms of TCR signalling via dephosphorylation. The effects of PTP are dependent on the dephosphorylation site and context. Therefore, further functional assays (i.e. CD8+ T cell cytotoxicity assay) are required to confirm the exact regulation mechanism that IFN-λ3 upregulated.

Table 9. Top 15 up-and down-regulated genes in CD8+ T cells stimulated with IFN-λ3 vs. unstimulated control (by log2Fold change).

Upregulated genes				
Gene name	Gene description	p-value	p-adj	$\log_2$ (Fold change)
AREL1-218	apoptosis resistant E3 ubiquitin protein ligase 1	4.24E-09	1.76E-06	24.5869
NSD1-222	nuclear receptor binding SET domain protein 1	1.95E-10	1.21E-07	23.3924
CHAMP1	chromosome alignment maintaining phosphoprotein 1	2.27E-08	7.76E-06	23.3744
SH3BP2	SH3 domain binding protein 2	2.40E-08	8.07E-06	23.3339
OBSCN	obscurin, cytoskeletal calmodulin and titin-interacting RhoGEF	3.03E-08	9.66E-06	23.1647
TMEM104	transmembrane protein 104	5.97E-08	1.73E-05	22.6625
TOM1L2	target of myb1 like 2 membrane trafficking protein	7.60E-08	2.11E-05	22.4826
CEMIP	cell migration inducing hyaluronidase 1	7.93E-08	2.18E-05	22.4526
IGLV1-44	Immunoglobulin Lambda Variable 1-44	7.99E-08	2.19E-05	22.4471
SMARCA2	SWI/SNF related, matrix associated, actin dependent regulator of chromatin, subfamily a, member 2	1.73E-11	1.33E-08	22.3391
ADAR/IFI4	adenosine deaminase RNA specific	9.29E-08	2.52E-05	22.3311
EHMT2	euchromatic histone lysine methyltransferase 2	3.83E-12	3.30E-09	22.3151
HNRNPK	heterogeneous nuclear ribonucleoprotein K	4.80E-09	1.95E-06	22.1880
YES1	YES proto-oncogene 1, Src family tyrosine kinase	1.24E-11	9.88E-09	22.1698
NOLC1	nucleolar and coiled-body phosphoprotein 1	3.87E-12	3.30E-09	22.1543
Down-regulated genes				
Gene name	Gene description	p-value	p-adj	log2 (Fold change)
EHMT2	euchromatic histone lysine methyltransferase 2	7.86E-15	1.08E-11	-25.38777355
RGPD6	RANBP2-like and GRIP domain containing 8	1.84E-11	1.40E-08	-25.02940483
RSBN1	round spermatid basic protein 1	3.61E-09	1.51E-06	-24.67451297
SNAPC4	small nuclear RNA activating complex polypeptide 4	3.36E-21	1.35E-17	-24.41463944
VPS13C	vacuolar protein sorting 13 homolog C	7.32E-09	2.87E-06	-24.18382589
MTHFR	methylenetetrahydrofolate reductase	8.34E-09	3.24E-06	-24.09223927
RAD21	RAD21 cohesin complex component	1.67E-30	1.27E-26	-23.97624142
TMEM106B	transmembrane protein 106B	7.83E-17	1.67E-13	-23.95882964
ERMARD	ER membrane associated RNA degradation	1.40E-08	5.20E-06	-23.72428923
NAT10	N-acetyltransferase 10	8.82E-09	3.37E-06	-23.6920
MPP7	membrane palmitoylated protein 7	1.48E-08	5.41E-06	-23.68410513
EFTUD2	elongation factor Tu GTP binding domain containing 2	1.66E-45	1.14E-40	-23.6691448
PLEKHG4	pleckstrin homology and RhoGEF domain containing G4	3.53E-10	1.99E-07	-23.52780181
KAT6B	lysine acetyltransferase 6B	2.74E-10	1.63E-07	-23.51948797
SFI1	SFI1 centrin binding protein	4.60E-15	7.15E-12	-23.51874703

The top 50 (significant $p < 0.05$) genes from RNA-Seq analysis is shown, along with fold change (purified CD8+ T cells with IFN-λ3 (100 ng/mL) treatment over no IFN-λ3 treatment) for 20 hours, *p*-value for differential expression, and *q* (false discovery rate value) based on the Benjamini-Hochberg method for multiple *p*-value correction).

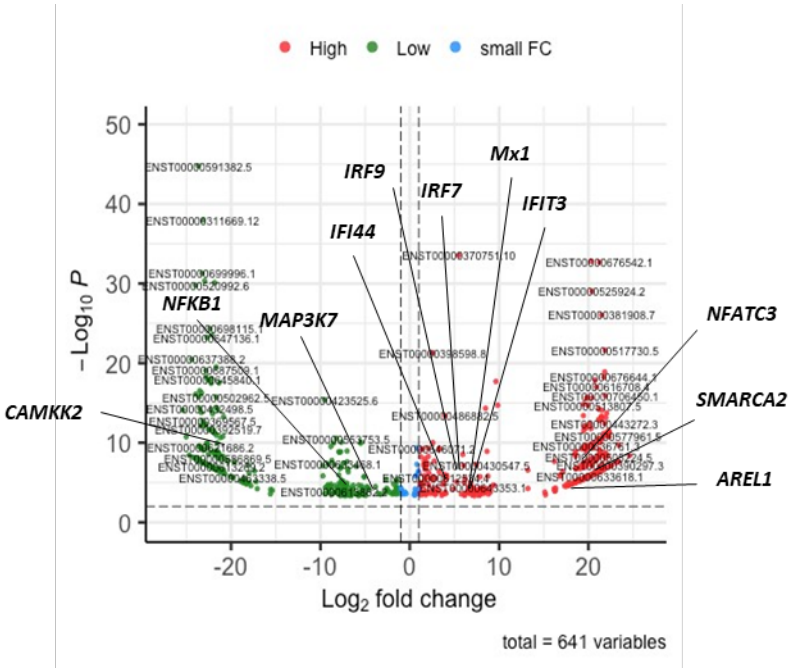

Figure 39. Volcano plot of the differentially expressed genes from human purified CD8+ T cells +/- IFN-λ3.

Volcano plot comparing transcriptome of enriched human CD8+ T cell with or without IFN-λ3 (100 ng/mL) after 20-hour cell culture. Red dots and green dots represent genes with a higher and lower fold change detected in IFN-λ3-treated CD8+ T cells compared to samples that were not treated with IFN-λ3, respectively. $p < 0.05$.

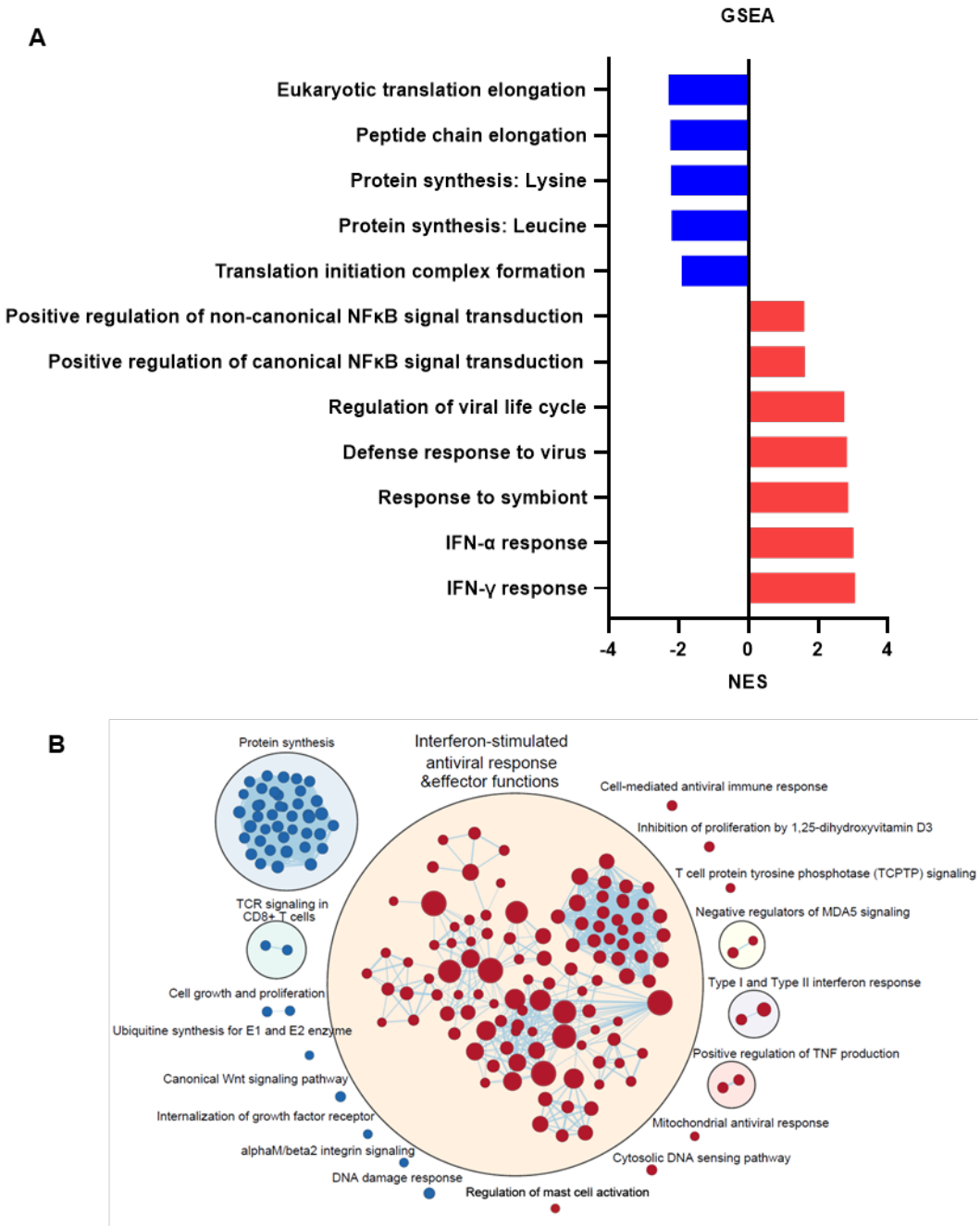

Figure 40. IFN-λ3 upregulated anti-viral response and downregulated protein synthesis in CD8+ T cells.

(A) GSEA showing the KEGG and Hallmark pathways that are enriched or depleted in enriched CD8+ T cell treated with IFN-λ3 (100 ng/mL) compared to no IFN-λ3 treatment and cultured for 20 hours ($p < 0.05$, NES > 1 or < -1, the false discovery rate (FDR) < 0.05. The color of bar in blue and red indicates the given pathway is less active or more active in IFN-λ3 treated samples compared to samples were not treated with IFN-λ3, respectively. (B) Pathway analysis visualized using Cytoscape showing pathways grouped by their relevance to cell activities. The color of nodes in blue and red indicate the given pathway is less active or more active in IFN-

λ3 treated samples compared to samples were not treated with IFN-λ3, respectively. The size of the nodes reflects the magnitude of pathway activity levels difference between IFN-λ3-treated samples compared to samples that were not treated with IFN-λ3. The blue thin lines (edges) connecting different circles indicate the crosstalk between pathways.

3.3.2 To Study the Impact of IFN-λ3 on CD8+ T Cells with TCR-Activation.

Hypothesis: IFN-λ3 enhances TCR activation but downregulates overall protein synthesis-related genes in CD8+ T cells.

When comparing the TCR-stimulated CD8+ T cells, IFN-λ3 treatment upregulated 288 genes and down-regulated 177 genes ($p < 0.05$). Some of the upregulated genes are related to transcription activation, gene silencing, DNA repair and cell-cycle progression (i.e. *KAT6B*), positive regulation of transcription (i.e. *SMARCA2*), fatty acid metabolism (i.e. *ACACB*), NFAT signalling (i.e. *CAMKK2*, *NFATC3*), MAPK signalling (i.e. *MAP4K1*, *MKNK1*, *MAPKAP1*). As expected, IFN-λ3 also induced upregulation in ISGs (i.e. *IFI44*, *IFIT1*, *MX1*) (**Table 10**, **Figure 41**).

When examining the pathways upregulated by IFN-λ3 in TCR-stimulated CD8+ T cells, GSEA showed that besides expected defence responses to virus and symbiont, and IFN-γ response, the positive regulation of canonical and non-canonical NF-κB signal transduction was observed again. However, there were more genes (146 genes) related to NF-κB signalling enhanced by IFN-λ3 in the context of TCR stimulation than no TCR stimulation. Some of the core genes include *IFIT5*, *LGALS9*, *TRIM25*, *BST2*, and *TNFSF10*. Interestingly, another pathway promoted by IFN-λ3 was the positive regulation of IL-10 production (**Figure 42A**), with core enriched genes such as LGALS9, ISG15, CD274, and *HSPD1*. In grouped pathways, we observed that the majority of pathways that were upregulated by IFN-λ3 were involved in antiviral immunity. Protein synthesis at the mRNA level was also decreased (**Figure 42B**). It is possible that additional TCR-related pathways would have been altered by IFN-λ3 if we had tittered down the potency of TCR stimulation. Overall, it is clear IFN-λ3 directly influenced the CD8+ T cell transcriptome, although the majority of genes examined in more detail thus far are clearly related to antiviral immunity.

Table 10. Top 15 up-and down-regulated genes in purified CD8+ T cells with TCR-stimulation and IFN-λ3 vs. TCR only (by log2Fold change).

Upregulated genes				
Gene name	Gene description	*p*-value	*p*-adj	$\log_2$ Fold change
OBSCN	obscurin, cytoskeletal calmodulin and titin-interacting RhoGEF	8.71E-24	5.95E-20	42.05124
ARFGAP1	ADP ribosylation factor GTPase activating protein 1	8.73E-18	2.42E-14	35.92501
OAS2	2'-5'-oligoadenylate synthetase 2	1.64E-17	4.00E-14	35.6159
FCHSD2	FCH and double SH3 domains 2	1.94E-21	1.02E-17	34.86546
NELL2	neural EGFL like 2	1.60E-15	2.60E-12	33.32781
TMEM104	transmembrane protein 104	6.71E-14	7.51E-11	31.33915
NLRX1	NLR family member X1	3.58E-13	3.60E-10	30.42005
TBC1D1	TBC1 domain family member 1	7.09E-13	6.54E-10	30.0172
CTNNB1	catenin beta 1	5.89E-12	4.57E-09	28.80249
TOM1L2	target of myb1 like 2 membrane trafficking protein	2.75E-11	1.82E-08	27.9124
BCOR	BCL6 corepressor	4.97E-13	4.85E-10	26.38442
ARHGEF1	Rho guanine nucleotide exchange factor 1	7.83E-10	3.96E-07	25.71403
IFIT2	interferon induced protein with tetratricopeptide repeats 2	5.39E-16	1.02E-12	25.27636
TAP2	transporter 2, ATP binding cassette subfamily B member	1.74E-10	1.03E-07	25.24525
HNRNPDL	heterogeneous nuclear ribonucleoprotein D like	1.91E-10	1.12E-07	24.95188
Down-regulated genes				
Gene name	Gene description	*p*-value	*p*-adj	$\log_2$ Fold change
TCF12	transcription factor 12	2.40E-18	8.21E-15	-36.5406
WWOX	WW domain containing oxidoreductase	1.31E-16	2.80E-13	-34.6155
CPEB2	cytoplasmic polyadenylation element binding protein 2	2.67E-15	3.97E-12	-33.0777
ARMCX3	armadillo repeat containing X-linked 3	1.07E-14	1.33E-11	-32.3785
SMARCA4	SWI/SNF related, matrix associated, actin dependent regulator of chromatin, subfamily a, member 4	2.93E-13	3.12E-10	-30.5417
STRADA	STE20-related kinase adaptor alpha	2.14E-12	1.83E-09	-29.3878
CHAMP1	chromosome alignment maintaining phosphoprotein 1	3.97E-11	2.53E-08	-27.6297
DCAF11	DDB1 and CUL4 associated factor 11	4.57E-17	1.04E-13	-25.3443
OSBPL8	oxysterol binding protein like 8	8.85E-12	6.38E-09	-24.3439
RING1	ring finger protein 1	1.29E-11	8.89E-09	-24.3069
NOP2	NOP2 nucleolar protein	5.90E-13	5.60E-10	-24.2063
SPTAN1	spectrin alpha, non-erythrocytic 1	2.13E-28	4.85E-24	-24.1652
B3GALT4	beta-1,3-galactosyltransferase 4	1.62E-16	3.35E-13	-23.6693
GPR68	G protein-coupled receptor 68	1.55E-18	5.56E-15	-23.5057
MAP9	microtubule associated protein 9	3.57E-13	3.60E-10	-23.4905

The top 50 (significant $p < 0.05$) genes from RNA-Seq analysis is shown, along with fold change (purified CD8+ T cells stimulated with plate-bound anti-CD3 (3 μg/mL) and anti-CD28 (1.5 μg/mL) in media with IFN-λ3 (100 ng/mL) treatment over no IFN-λ3 treatment) for 20 hours, raw *p*-value for differential expression, and *q* (false discovery rate value) based on the Benjamini-Hochberg method for multiple *p*-value correction).

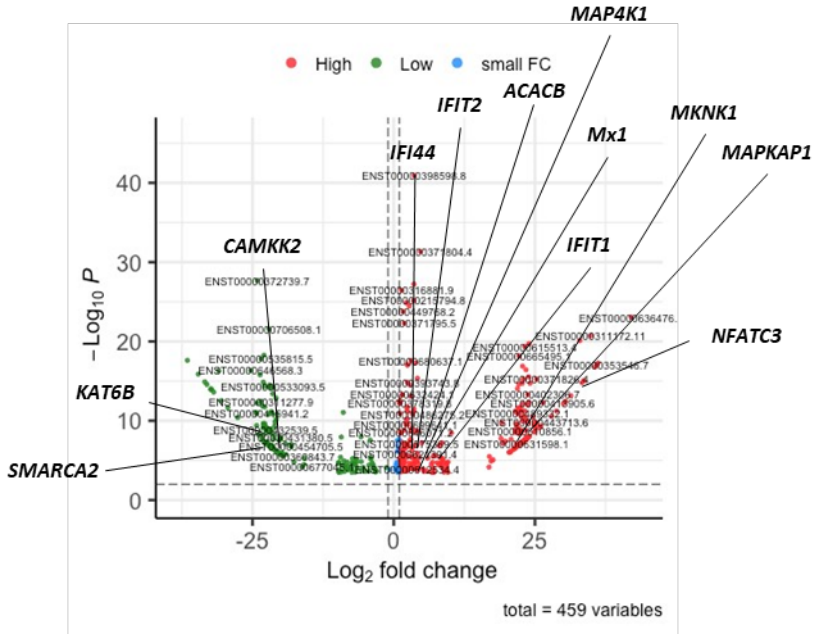

Figure 41. Volcano plot of the differentially expressed genes from human purified TCR-stimulated CD8+ T cells +/- IFN-λ3.

Volcano plot comparing transcriptome of enriched human CD8+ T cell with or without IFN-λ3 (100 ng/mL) after 20-hour cell culture with plate-bound anti-CD3 (3 μg/mL) and anti-CD28 in media (1.5 μg/mL) ("TCR stimulation"). Red dots and green dots represent genes with a higher and lower fold changes detected in IFN-λ3-treated TCR-stimulated CD8+ T cells compared to samples treated with TCR-stimulation but not treated with IFN-λ3, respectively. $p < 0.05$.

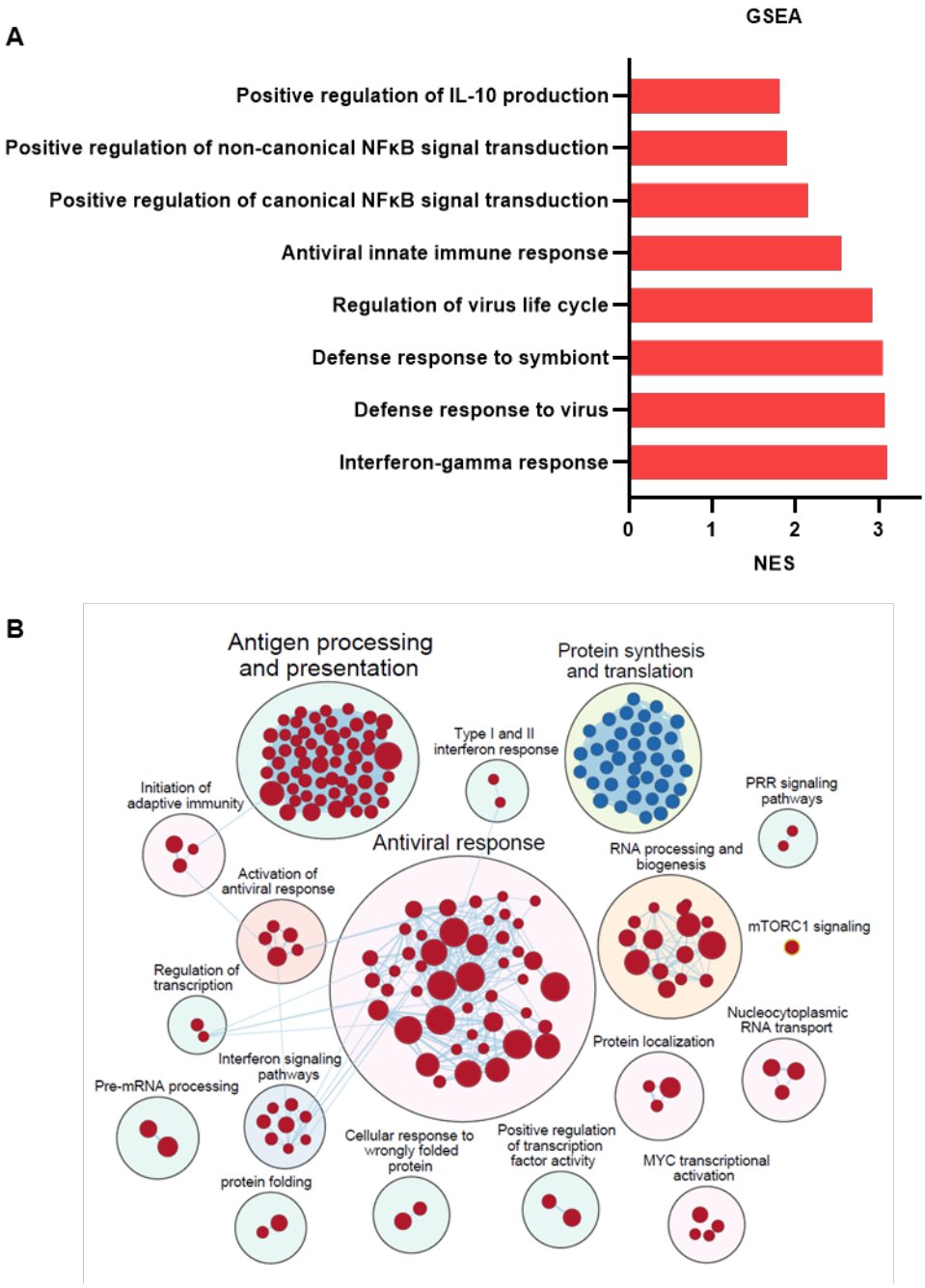

Figure 42. IFN-λ3 upregulated anti-viral response and downregulated protein synthesis in TCR-stimulated CD8+ T cells.

(A) GSEA showing the KEGG and Hallmark pathways selected enriched or depleted in enriched CD8+ T cell treated with plate-bound anti-CD3 (3 μg/mL) and anti-CD28 in media (1.5 μg/mL) ("TCR stimulation"), and with IFN-λ3 (100 ng/mL) compared to no IFN-λ3 treatment and cultured for 20 hours ($p < 0.05$, NES > 1 or < -1, FDR < 0.05. The color of bar in red indicates the given pathway is more active in IFN-λ3 treated and TCR-stimulated samples compared to samples were not treated with IFN-λ3 but with TCR stimulation, respectively. (B) Pathway

analysis visualized using Cytoscape and grouped by their relevance to cell activities. The nodes in blue and red indicate the given pathway is less active or more active in IFN-λ3 treated samples compared to samples were not treated with IFN-λ3 that are both treated with TCR stimulation, respectively. The size of nodes reflect the magnitude of pathway activity between IFN-λ3-treated samples compared to samples that were not treated with IFN-λ3. The blue thin lines (edges) connecting different circles indicate the crosstalk between pathways.

CHAPTER 4. DISCUSSION, CONCLUSIONS, AND LIMITATION

4.1 Discussion

4.1.1 The Distributions of IFN-λR1 on Immune Cells

The quantification of IFN-λR1 at the cell surface is essential for investigating the biology of type III IFNs, yet the study of this receptor has heavily relied on mRNA-levels until recently. The newly identified IFN-λR1 antibodies our group published were able to differentiate IFN-λR1 protein levels first in various cell lines,[197] but my thesis project went deeper into understanding how IFN-λR1 levels differ within T cell subsets at baseline and after different activation.

For the first time, using the newly identified antibody, we examined the protein level of IFN-λR1 on various subsets of CD4+ and CD8+ T cells. We showed that within whole PBMCs, CD4+ T cells express lower IFN-λR1 (IFN-λR1+% and IFN-λR1 MFI) on the cell surface compared to CD8+ T cells.

In CD4+ and CD8+ T cells, we observed that IFN-λR1 levels were the lowest on naïve cell surface, compared to T_{CM}, T_{EM}, and T_{EMRA} subsets at steady state. In CD8+ T cells, over 20% of T_{EM} cells had IFN-λR1 on the surface, followed by T_{CM} and T_{EMRA} cells that were IFN-λR1+. Meanwhile, only a small proportion of naïve T cells express IFN-λR1 on the cell surface. IFN-λR1 MFI was also the lowest on naïve CD4+ T cells compared to memory populations. Naïve CD4+ T cells were the population with the lowest IFN-λR1 expression (MFI and IFN-λR1+%) compared to T_{EM}, T_{CM}, and T_{EMRA} CD4+ T cell populations. Consistent with our observation at protein levels, Schmiedel *et al*. also showed that the *IFNLR1* mRNA level in memory CD4+ T cells is higher compared to naïve cells.[213] (data available from v23.proteinatlas.org, https://www.proteinatlas.org/ENSG00000185436-IFNLR1/immune+cell)

A critical difference between memory and naïve T cells is less concentrated antigens can activate those memory T cells; in other words, naïve T cells exhibit a higher activation threshold but lower effector cytokine productivity than memory T cells.[214] In addition, memory T cells, such as T_{CM} (at a lower extent), T_{EM}, and T_{EMRA} T cells, can quickly produce effector molecules upon re-stimulations, while naïve T cells do not readily produce effector cytokines or realize effector functions.[215,216] At the gene level, researchers have shown that memory and naïve T cells have distinct gene expression signatures: memory T cells have increased levels of transcripts involving cell migration, adhesion, intracellular signalling, and cell survival genes, whereas naïve T cells

have more transcripts involving in inhibitory cytokine (i.e. TGF-β) sensing.[217,218] At the epigenetic level, it has been shown that memory T cells and naïve T cells have distinct chromatin accessibility landscapes, which partially explains the function disparity in memory and naïve T cells.[219] The differential expression of *IFNLR1* across different cell types is related to the methylation of the *IFNLR1* gene.[220] Specifically, histone deacetylase inhibition enhances *IFNLR1* expression by providing the transcription activators with higher accessibility at the *IFNLR1* promoter.[221] Potentially in memory and naïve T cells, the chromatin methylation state and accessibility of *IFNLR1* promoter difference in these two populations may play a role in the distinct IFN-λR1 levels we observed.

We observed that almost all CD4+ and CD8+ T cells express IL-10RB on the cell surface. However, the high level of IL-10RB does not directly provide T cells with the capacity to respond to IL-22, IL-26, and IFN-λs readily, which all include IL-10RB as a part of their receptor; this is because each of these cytokines needs to bind to its unique α receptor component, which is IL-22R, IL-20R1, and IFN-λR1, for signalling initiation.[222-224] In addition, TYK2 associated with the IL-10RB component of IFN-λR is not essential for type III IFN signalling in some cell types, as IFN-λ showed a comparable inhibition effect on vesicular stomatitis virus infections in wild-type and TYK2 KO HAP1 cells (a chronic myeloid leukemia cell line).[177] These facts further illustrate the complexity of IFN-λR biology.

4.1.2 TCR Stimulation Upregulates Cell Surface IFN-λR1

CD8+ T cells, even though they had higher levels of IFN-λR1 at the steady state, had an even higher increase in IFN-λR1+% upon TCR stimulation. Our observation at the protein level aligned with the previous mRNA data published by our group, which showed that *IFNLR1* transcript levels in CD4+ T cells increase upon stimulation using anti-CD3 and anti-CD28.[141] In addition, we showed a significantly positive association between cell surface IFN-λR1 levels (MFI) and activation marker CD71 MFI. Importantly, our data demonstrates that TCR stimulation of purified T cells also leads to IFN-λR1 upregulation, which indicates other cells are not required. The maximal effect in this preliminary data was only half though, so more experiments are needed to determine if any other cell types could promote IFN-λR1 expression indirectly.

The timing or length of activation could also influence IFN-λR1 levels. We observed IFN-λR1 levels increasing as early as twenty hours post-stimulation, although we have not checked

earlier time points yet. It is possible that the increase of IFN-λR1 on the T cell surface in a very short period of time would not require *de novo* protein synthesis. A putative mechanism is that IFN-λR1 is already made and stored in intracellular vesicles, and TCR stimulation promotes the transportation of IFN-λR to the plasma membrane, so this remains to be tested.

We also examined the IFN-λR1 levels 72-hour post-stimulation. Compared to Day 1, even though the IFN-λR1+% in CD4+ and CD8+ T cells within PBMCs did not further increase, IFN-λR1 MFI went up when cells were stimulated with anti-CD3 alone, anti-CD3 with anti-CD28, and PHA. That observation leads to another question: whether the IFN-λR1 level (MFI) can further increase after 3-day TCR stimulation, and how long time it can remain at this high level. The endocytosis machinery of IFN-αR may provide us with some enlightenment. At a steady state when the IFN ligands are absent, IFN-αR1, which is the low-affinity receptor component for IFN-αR, remains in equilibrium on the plasma membrane between endocytosis, which internalizes IFN-αR1 and sorting back, which transports IFN-αR1 back to the cell surface. Upon ligand binding, the IFN-α-IFN-αR complex gets endocytosed, IFN-αR1 gets ubiquitinated and shuttled to the lysosome for degradation, while IFN-αR2, the high-affinity component of IFN-αR, gets transported back to the plasma membrane and ready for the next round of ligand-binding signalling initiation.[225] This receptor degradation-recycling machinery relies on the binding of ligands to the receptor. It is not known if IFN-λR1 is recycled or degraded upon ligand interaction, but this is an area of research in our lab. At the mRNA level, the published data from our group showed that in CD4+ T cells within PBMCs, IFN-λ3 induced higher fold induction of ISGs after 3-day stimulation with anti-CD3 and anti-CD28 for 3 days, compared to the non-TCR stimulation control, indicating the increase in responsiveness of CD4+ T cells post TCR-stimulation. Now that we have seen the upregulation of IFN-λR1 at the protein level on the T cell surface, the next step is to investigate if the T cells with higher IFN-λR1 on their surface, are more responsive to IFN-λs stimulation, compared to the cells that did not undergo TCR stimulation.

Anti-CD28 itself did not alter the IFN-λR1 levels (MFI) or % IFN-λR1 + CD4+ or CD8+ T cells. Instead, anti-CD28 enhanced IFN-λR1+%, and IFN-λR1 MFI significantly on CD4+ T and CD8+ T cells, when anti-CD3 was provided at 0.3 μg/mL simultaneously, indicating that anti-CD28 can amplify the effect of anti-CD3 stimulation on IFN-λR1 upregulation. Still, it is not essential for the IFN-λR1 upregulation. Downstream of CD28 signalling involves the

phosphorylation of mTOR and IκB, and both contribute to the activation of NF-κB.[56] It is also known that anti-CD28 promotes NFAT signalling through the inhibition of NFAT repressor.[56]

4.1.3 TCR Stimulation Upregulates Cell Surface IL-10RB Level on Day 3

Our observations revealed that TCR stimulation with anti-CD3 and anti-CD28 did not alter the percentage of IL-10RB+ CD4+ and CD8+ T cells. However, IL-10RB MFI in CD4+ and CD8+ T cells increased by 2-fold on day 3 compared to day 1, whereas there was not a significant upregulation in IL-10RB MFI on day 1 compared to day 0 in all three cell TCR-stimulation conditions. This significant increase in IL-10RB expression (MFI) on the cell surface is prominent, considering the IL-10RB MFI at steady state was already at a very high level. As discussed above, the IL-10RB subunit serves as the low-affinity receptor component for IL-22, IL-26, and IFN-λs.[98,222,224] However, the increase in its level likely provides T cells with a lower threshold for receptor-ligand binding dynamic and a higher sensitivity to those cytokines. In addition, IL-10RB is essential for IL-10 signalling.[226] Given the well-known anti-inflammatory properties of IL-10,[227] it is likely that these T cells stimulated with TCR also have a higher sensitivity to IL-10, which helps to control the immune response and reduce the chance of causing excessive damage.

In terms of different stimulation methods, we observed that PHA did not upregulate the MFI of IL-10RB on the cell surface as anti-CD3, even though the flow cytometry showed that CD71 MFI was upregulated by PHA stimulation. PHA-induced T cell stimulation differs from TCR stimulation in that it is independent of the redox status of the cell.[228] Previous studies also showed that PHA differs from mitogen and anti-CD3 cell stimulation by calcium mobilization, where PHA cell stimulation does not rely on the intracellular calcium channel.[228] This indicates that the Ca^{2+} flux induced by TCR stimulation using anti-CD3 and CD28 is likely playing an important role in regulating the cell surface IFN-λR1.

4.1.4 The Mechanisms that TCR Stimulation Upregulate Cell Surface IFN-λR1 level

To determine which TCR signalling pathway(s) were required for the upregulation of IFN-λR1, we used several pathway-specific inhibitors. ZAP70 is required for TCR signalling as it helps phosphorylate ITAMs in the endoplasmic tail of the TCR.[9,32] Using ZAP180013, we preliminarily showed that ZAP70 is essential for IFN-λR1 upregulation by TCR stimulation. As ZAP70 serves as the core element of antigen-specific T cell activation, it is likely that antigen-specific T cell stimulation is one of the key mechanisms regulating IFN-λR1 on the cell surface. Next, we used

duvelisib (PI3K inhibitor), sp600125 (JNK inhibitor), and FK506 (calcineurin inhibitor) to further evaluate the dependence of IFN-λR1 regulation on specific TCR stimulation downstream pathways. Calcineurin is an essential phosphatase that activates NFAT via dephosphorylation. As the treatment with respective inhibitors downregulated the MFI of activation marker CD71 as well as IFN-λR1+% and IFN-λR1 MFI on CD4+ and CD8+ T cells, we showed that PI3K and NFAT pathways were all involved in the TCR-mediated IFN-λR1 increase on both CD4+ and CD8+ T cell surface. Our data showed that anti-CD28 stimulation also contributes to IFN-λR1 increase on the T cell surface. Anti-CD28 also induces the PI3K pathway, which confirms the importance of the PI3K pathway in IFN-λR1 regulation. According to our preliminary data, JNK was not essential for TCR-dependent IFN-λR1 regulation, but all experiments must be repeated with 3 more healthy donors before statistical analyses are completed.

4.1.5 The Potential Regulation Effect of Type III IFNs on CD4+ T cells and Potential Mechanisms

Several studies have shown that IFN-λs can regulate Th2 responses in mice, specifically, down-regulate Th2 cytokines in mice in the gastrointestinal tract and respiratory tract.[184-187,203,229] We did not observe a regulation effect of IFN-λ3 on IFN-γ+% cells in Th1 polarization; however, consistent with previous studies in mice, IFN-λ3 downregulated the IL-13+% and IL-4+% cells during Th2 polarization, although additional donors must be tested. During the differentiation of Th2 cells, the Th2 locus, which contains both *IL13* and *IL4* genes, goes through epigenetic changes, followed by the binding of GATA-3 and STAT6 to promote the expression of *IL13* and *IL4*.[115] IFN-λ3 may regulate *GATA3* expression in T cells and reduce the induction of Th2 cytokines. We also showed that in human whole PBMCs and Th2 cell polarizing conditions, IFN-λ3 downregulated the production of IL-13 but decreased IL-4 production very mildly. Our observation was consistent with a previous study; IFN-λ1 preferentially decreased *IL13* mRNA, IL-13 protein secretion, and the number of IL-13%+ CD4+ T cells, but did not consistently downregulate those parameters for IL-4. IL-13 was originally considered to have overlapping functions with IL-4; later studies showed that IL-13 is essential in controlling certain diseases where IL-4 is not, such as *N. brasiliensis*.[230] In humans and mice, IL-13 and IL-4 genes are found adjacent to each other, and it is proposed that a gene duplication generated them during evolution.[231] The differential regulation effects of IFN-λ3 we observed indicate the complexity of this regulation mechanism.

Illustrated previously in the Introduction section, IFN-λs are also capable of regulating Th2 responses in mouse via DCs-dependent indirect mechanism.[184] My results showed that Th2 cell cytokine production, such as IL-13, can be directly downregulated by IFN-λ3 during human naïve CD4+ T cell polarization and whole PBMCs stimulation. That indicates a potential of using IFN-λ3 as a future therapeutic to dampen excessive Th2 cytokines in treating Th2-high endotype asthma. However, further study is required to confirm the effect of IFN-λ3 in the human system in the airway in vivo, although we know from antiviral clinical trials that IFN-λ treatment in vivo is safe for both short and long-term treatments.[143,144,232] Whether IFN-λ therapy would have side effects in a person suffering from Th2-high endotype asthma is not known. IFN-λ3 also showed its functioning in indirectly regulating type 2 immune responses via downregulating Th2-promoting epithelial cytokines TSLP and IL-33, implicated in more severe Th2-high asthma.[120] Studies are building at least in mice that IFN-λs can interact with several types of immune cells to reduce Th2-high airway hypersensitivity from different angles, but much more work is needed to understand the immunoregulatory pathways in humans including fully characterizing other Th types promoting immunopathology including Th17 cells.

4.1.6 The Potential Regulation Effect of Type III IFNs on CD8+ T cells and Potential Mechanisms

Previous studies showed that the immune-regulation effect of IFN-α is dependent on the temporal relationship between the IFN-α and TCR signalling. IFN-α and promotes T cell activation when IFN-α coincides or is provided slightly later than TCR signalling; meanwhile, IFN-α showed anti-proliferation and pro-apoptosis functions when IFN-α signalling occurs much before TCR stimulation.[233] That observation indicates a fine-tuned regulation mechanism in the immune system: any given cell can integrate extracellular signals spatially and temporally, and those together determine the fate of that cell. Type III IFNs and type I IFNs have a lot in common in their downstream pathway; therefore, the regulatory effect of type III IFNs may also be dependent on the temporal factor. When profiling the macro effects of IFN-λ3 on CD8+ T cells with and without TCR stimulation, we treated the cells with IFN-λ3 to coincide with anti-CD3 and anti-CD28. So, pre-treating CD8+ T cells with IFN-λ3 or adding IFN-λ3 post-TCR stimulation and then testing for CD8+ T cells' cytokine production and surface activation markers are what I would have done next to elucidate the temporal factor on the regulation effect of IFN-λ3 on CD8+ T cells. In addition, I would consider using less concentrated anti-CD3 and anti-CD28 to stimulate CD8+

T cells to study the potential function of IFN-λ3 as Signal 3 at conditions with less potent TCR stimulation.

The MAPK pathway is crucial in regulating T-cell activities. Previous studies showed that MAPK pathways are also essential for IFN-λ signalling in the various cell lines from epithelial cells and immune cells.[137,179,180] As MAPK signalling is also essential in TCR signalling in CD4+ and CD8+ T cells, IFN-λ likely promotes T cell antiviral functions by enhancing MAPK signalling. Our RNA sequencing result showed IFN-λ3 upregulated NF-κB signalling pathways in CD8+ T cells, which has not been studied in great detail in the past. Further investigation is required to show if this upregulation of NF-κB pathway pose an effect on specific human CD8+ T cell functions.

As expected, IFN-λ3 stimulation of purified human CD8+ T cells led to a significant upregulation of antiviral ISGs. Our RNA sequencing data revealed that IFN-λ3 induced upregulation of MAPK-related genes like *MAP3K7* and *MAP4K1*, as well as the NF-κB pathway in CD8+ T cells in the contexts with and without TCR stimulation. It is likely that in CD8+T cells specifically, IFN-λ3 signalling downstream elements crosstalk with CD8+ internal cell signalling at the steady state and during TCR stimulation, with MAPK and NF-κB being two of the crucial transfer hubs. We also observed that in TCR-stimulated CD8+ T cells, IFN-λ3 upregulated IL-10 production pathways. Two populations of CD8+ T cells were identified in the context of coronavirus-induced acute viral encephalitis: IL-10+CD8+ T cells and IL-10-CD8+ T cells. [234] The IL-10+CD8+ T cell, strikingly, with increased levels of activation marker (CD69, KLRG-1, and CD127) and a higher expression of inflammatory cytokines production profile (IL-1β and perforin) compared to their IL-10- counterpart, also release a higher level of IL-10, offering protective functions. They also showed that the IL-10 production in these hyperactivated IL-10+CD8+ T cells relies on ERK1/2 and p38 MAPK pathways.[234] As has been shown before, IFN-λ3 upregulates the phosphorylation of ERK, JNK, and p38; IFN-λ3 can likely help generate this IL-10+ CD8+ T cell phenotype.[180,181] In the future, we could use ELISA and flow cytometry to analyze IFN-λ3-treated CD8+T cells to see the impact of IFN-λ3 on IL-10 production in these cells.

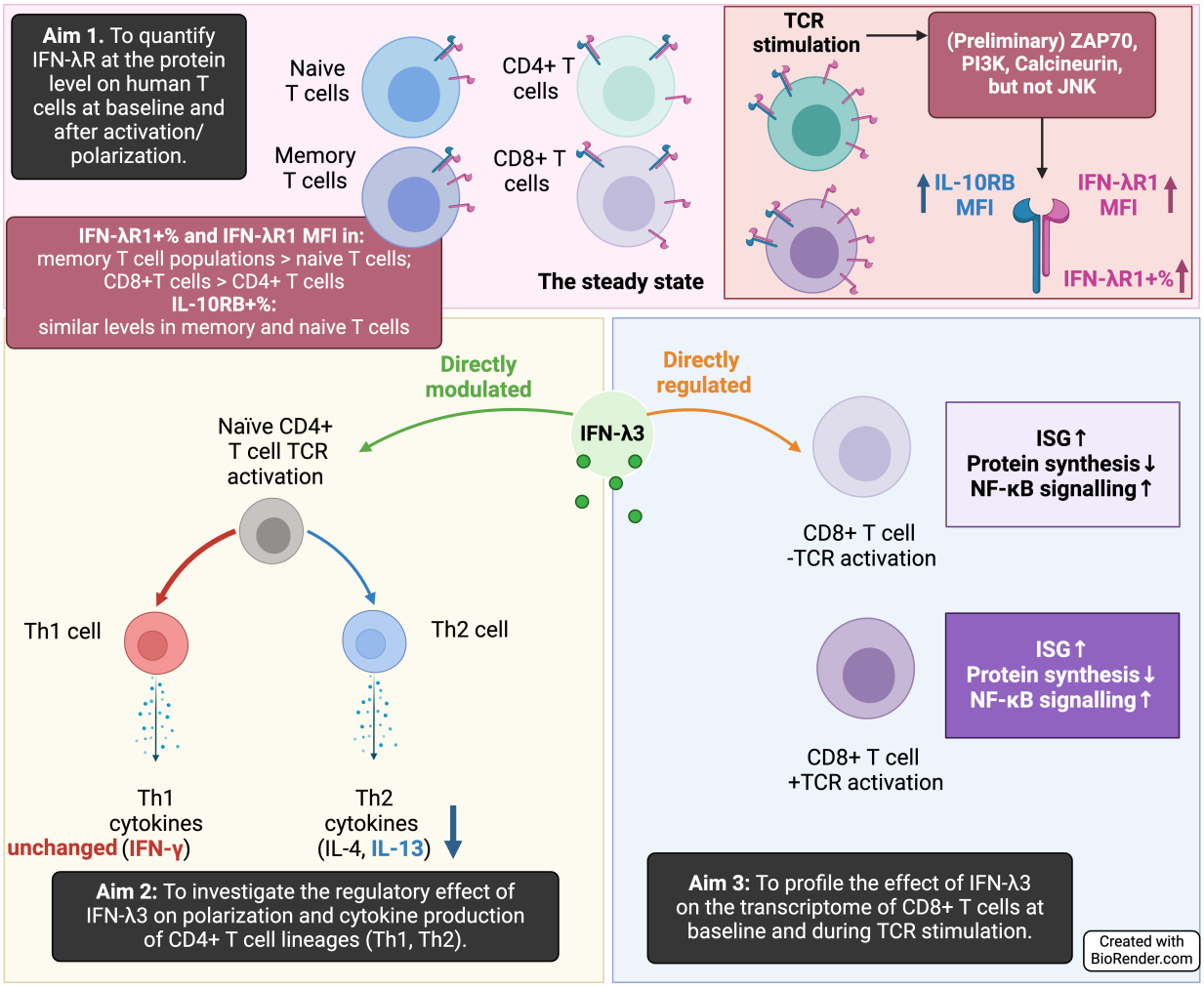

Figure 43. Graphic summary of the results of this dissertation.

4.2 Limitations of the Study

Most experiments in this study were conducted using primary human cells *in vitro*; studies using animal models would be difficult as murine T cells do not express IFN-λR1. In addition, PBMCs represent circulating immune cells, so comparing my results with T cells at different tissue sites could reveal differential patterns of regulation, whether in the steady state or during an infection or other chronic conditions. For the PBMC study, we used CD71 as an activation marker; other conventional T cell activation markers could be used to confirm the trend we observed, such as OX40 and HLA-DR. Some experiments included in this dissertation were only conducted on 1 or 2 donors. Therefore, more donors are required to be analyzed to confirm the trends and association observed from the preliminary data and complete my statistical analyses. In this project, we examined the levels and the percentage of IFN-λR1 and IL-10RB on human T cells up to day

3 under the condition of TCR stimulation. At the same time, Th1 and Th2 polarization took 6 and 9 days, respectively. It is likely the IFN-λR expression on the T cell surface changes after 6 and 9 days of TCR stimulation with respective Th1 and Th2 polarization cocktails; therefore, we need to fully measure IFN-λR1 and IL-10RB over the course and during different polarization conditions. It is also essential to test in a future study if the upregulation of IFN-λR1 on the T cell surface by TCR stimulation also enhances the responsiveness of these cells to IFN-λ3. When profiling the universal effect of IFN-λ3 on CD8+ T cells with or without TCR stimulation, other factors may be considered, such as the type and the strength of TCR stimulation, the age, and sexes of donors with variability noted among our RNA sequencing analysis with 5 donors in total. Any RNA sequencing results should be confirmed at the protein level for top pathway hits for the influence of IFN-λ3 on CD8+ T cells. In some cases, the influence of cytokines is dependent on the phosphorylation state of downstream signalling proteins rather than their abundance; the phosphorylation profile can further help identify the effect of IFN-λ3 on CD8+ T cells.

CHAPTER 5. FUTURE DIRECTIONS OF THIS DISSERTATION PROJECT

5.1 Confirming the Direct Effects of TCR Stimulation on IFN-λR levels on CD4+ and CD8+ T cells and the Underlying Mechanisms

Our data suggested that anti-CD3 and anti-CD28 directly promoted the IFN-λR1 levels on purified CD4+ T cells without the presence of other cell types; using TCR signalling inhibitors, our study also showed that JNK, PI3K, and NFAT pathways downstream of TCR signalling contribute to the upregulation of IFN-λR1 observed on the cell surface. However, more repeats are required to confirm the involvement of those pathways in IFN-λR1 regulation. When repeating, we can add different inhibitors at the same time to investigate the synergetic effects of those pathways on IFN-λR1 regulation. To get an even deeper understanding of these pathways, we could check the phosphorylation profile of different TCR stimulation and examine more molecular intermediates, such as ZAP70, LAT, ERK, and NFAT.

5.2 Examining the IFN-λ Responsiveness of TCR Stimulated T Cells

We predict that the levels of IFN-λR1 on the cell surface should correlate with the responsiveness of IFN-λ of that cell. But we have not confirmed this yet in this project. Now that we have the newly identified IFN-λR1 flow antibody, we would culture enriched CD4+ and CD8+ T cells in duplicate with or without anti-CD3 and anti-CD28 for 1.5 days. After stimulation, we would stimulate the cells with or without IFN-λ for 30 minutes and quantify phosphorylated STAT1 as an indicator of IFN-λ signalling within IFN-λR+ cells using flow cytometry. Additionally, a longer stimulation could be done to look at ISG fold induction via RT-qPCR.

5.3 Accessing the Direct Impact of TCR-stimulation on Cell Surface IFN-λR Level on T Cells over Longer Time Courses and on Other Cell Types with TCR, Such as NK T Cells and γδ T Cells

We showed that on both IFN-λR+% and IFN-λR MFI was increased by TCR stimulation on day 3, and for the next step, we can examine the IFN-λR on the cell surface under conditions with longer TCR stimulation. The effect of Th1 and Th2 polarizing cytokines on IFN-λR1 and IL-10RB can also be studied using flow cytometry after polarizing CD4+ T cells. This study shows that IFN-λR1 regulation by TCR stimulation is dependent on CD3 signalling. Whether TCR stimulation affects IFN-LR1 levels on γδ T cells has not been tested, although at baseline IFNLR1 mRNA is detectable in γδ T cells .[213,235] (data available from v23.proteinatlas.org,

https://www.proteinatlas.org/ENSG00000185436-IFNLR1/immune+cell) This would also be possible through the study of NK T Cells.

5.4 Examining the Effect of IFN-λ3 on T reg, Th17, and Other Th Subset Polarization

First, my Th1 and Th2 polarizations need to be expanded to more donors. Next, I think with so little known about IFN-λ3 interactions with human T cells, it would be important to study if IFN-λs regulate the polarization of naïve CD4+ T cells to induced regulatory T cells (iT reg) and Th17 cells. IFN-β, which is a type I IFN, is widely accepted as a treatment for multiple sclerosis (MS). Kavrochorianou *et al*. showed the protective role of IFN-β signalling by revealing that IFN-β promotes the IL-10- and IFN-γ-producing CD4+ T cells, dampening Th17 responses in the acute phase of MS in mice.[236] We have already finished optimizing the polarization conditions for human Th17 cells, and the next step is to repeat the culture assays +/- IFN-λ3 addition.

5.5 Examining the Effects of IFN-λ3 on Unstimulated and TCR-stimulated CD8+T Cells

Using RNA sequencing analyses, we showed that IFN-λ3 modulated multiple pathways, although the majority were related to antiviral activity. As mRNA levels do not always correlate with protein levels, we want to confirm various results using flow cytometry and/or Western blot. We also want to expand our CD8+ T cell assays to include functional readouts such as proliferation and degranulation and ensure the timing and potency of TCR stimulation is now considered.

CHAPTER 6. REFERENCES

1. Abbas AK. Basic immunology: functions and disorders of the immune system. In: Lichtman AH, Pillai S, Baker DL, eds. Sixth edition. ed.
2. Kondo M. Lymphoid and myeloid lineage commitment in multipotent hematopoietic progenitors. Immunol Rev 2010;238(1):37-46. (In eng). DOI: 10.1111/j.1600-065X.2010.00963.x.
3. Nemeth MJ, Bodine DM. Regulation of hematopoiesis and the hematopoietic stem cell niche by Wnt signaling pathways. Cell Res 2007;17(9):746-58. (In eng). DOI: 10.1038/cr.2007.69.
4. Scimone ML, Aifantis I, Apostolou I, von Boehmer H, von Andrian UH. A multistep adhesion cascade for lymphoid progenitor cell homing to the thymus. Proc Natl Acad Sci U S A 2006;103(18):7006-11. (In eng). DOI: 10.1073/pnas.0602024103.
5. Aldrich CJ, Hammer RE, Jones-Youngblood S, et al. Negative and positive selection of antigen-specific cytotoxic T lymphocytes affected by the alpha 3 domain of MHC I molecules. Nature 1991;352(6337):718-21. (In eng). DOI: 10.1038/352718a0.
6. Harryvan TJ, de Lange S, Hawinkels L, Verdegaal EME. The ABCs of Antigen Presentation by Stromal Non-Professional Antigen-Presenting Cells. Int J Mol Sci 2021;23(1) (In eng). DOI: 10.3390/ijms23010137.
7. Li D, Wu M. Pattern recognition receptors in health and diseases. Signal Transduct Target Ther 2021;6(1):291. (In eng).
8. Ma CY, Marioni JC, Griffiths GM, Richard AC. Stimulation strength controls the rate of initiation but not the molecular organisation of TCR-induced signalling. Elife 2020;9 (In eng). DOI: 10.7554/eLife.53948.
9. Hwang JR, Byeon Y, Kim D, Park SG. Recent insights of T cell receptor-mediated signaling pathways for T cell activation and development. Exp Mol Med 2020;52(5):750-761. (In eng). DOI: 10.1038/s12276-020-0435-8.
10. Huppa JB, Davis MM. T-cell-antigen recognition and the immunological synapse. Nat Rev Immunol 2003;3(12):973-83. (In eng). DOI: 10.1038/nri1245.
11. Huang J, Brameshuber M, Zeng X, et al. A single peptide-major histocompatibility complex ligand triggers digital cytokine secretion in CD4(+) T cells. Immunity 2013;39(5):846-57. (In eng). DOI: 10.1016/j.immuni.2013.08.036.
12. Yang W, Pan W, Chen S, et al. Dynamic regulation of CD28 conformation and signaling by charged lipids and ions. Nat Struct Mol Biol 2017;24(12):1081-1092. (In eng). DOI: 10.1038/nsmb.3489.
13. Gmünder H, Lesslauer W. A 45-kDa human T-cell membrane glycoprotein functions in the regulation of cell proliferative responses. Eur J Biochem 1984;142(1):153-60. (In eng). DOI: 10.1111/j.1432-1033.1984.tb08263.x.
14. Sharpe AH. Mechanisms of costimulation. Immunol Rev 2009;229(1):5-11. (In eng). DOI: 10.1111/j.1600-065X.2009.00784.x.
15. Weiss L, Whitmarsh AJ, Yang DD, Rincón M, Davis RJ, Flavell RA. Regulation of c-Jun NH(2)-terminal kinase (Jnk) gene expression during T cell activation. J Exp Med 2000;191(1):139-46. (In eng). DOI: 10.1084/jem.191.1.139.
16. Schmidt CS, Mescher MF. Peptide antigen priming of naive, but not memory, CD8 T cells requires a third signal that can be provided by IL-12. J Immunol 2002;168(11):5521-9. (In eng). DOI: 10.4049/jimmunol.168.11.5521.
17. Curtsinger JM, Lins DC, Mescher MF. Signal 3 determines tolerance versus full activation of naive CD8 T cells: dissociating proliferation and development of effector function. J Exp Med 2003;197(9):1141-51. (In eng). DOI: 10.1084/jem.20021910.
18. Wilson DC, Matthews S, Yap GS. IL-12 signaling drives CD8+ T cell IFN-gamma production and differentiation of KLRG1+ effector subpopulations during Toxoplasma gondii Infection. J Immunol 2008;180(9):5935-45. (In eng). DOI: 10.4049/jimmunol.180.9.5935.

19. Pape KA, Khoruts A, Mondino A, Jenkins MK. Inflammatory cytokines enhance the in vivo clonal expansion and differentiation of antigen-activated CD4+ T cells. J Immunol 1997;159(2):591-8. (In eng).
20. Ben-Sasson SZ, Hu-Li J, Quiel J, et al. IL-1 acts directly on CD4 T cells to enhance their antigen-driven expansion and differentiation. Proc Natl Acad Sci U S A 2009;106(17):7119-24. (In eng). DOI: 10.1073/pnas.0902745106.
21. Sckisel GD, Bouchlaka MN, Monjazeb AM, et al. Out-of-Sequence Signal 3 Paralyzes Primary CD4(+) T-Cell-Dependent Immunity. Immunity 2015;43(2):240-50. (In eng). DOI: 10.1016/j.immuni.2015.06.023.
22. Corthay A. A three-cell model for activation of naïve T helper cells. Scand J Immunol 2006;64(2):93-6. (In eng). DOI: 10.1111/j.1365-3083.2006.01782.x.
23. Willcox CR, Mohammed F, Willcox BE. The distinct MHC-unrestricted immunobiology of innate-like and adaptive-like human γδ T cell subsets-Nature's CAR-T cells. Immunol Rev 2020;298(1):25-46. (In eng). DOI: 10.1111/imr.12928.
24. Cambier JC, Johnson SA. Differential binding activity of ARH1/TAM motifs. Immunol Lett 1995;44(2-3):77-80. (In eng). DOI: 10.1016/0165-2478(94)00196-x.
25. Wange RL, Samelson LE. Complex complexes: signaling at the TCR. Immunity 1996;5(3):197-205. (In eng). DOI: 10.1016/s1074-7613(00)80315-5.
26. Irving BA, Chan AC, Weiss A. Functional characterization of a signal transducing motif present in the T cell antigen receptor zeta chain. J Exp Med 1993;177(4):1093-103. (In eng). DOI: 10.1084/jem.177.4.1093.
27. Bromann PA, Korkaya H, Courtneidge SA. The interplay between Src family kinases and receptor tyrosine kinases. Oncogene 2004;23(48):7957-68. (In eng). DOI: 10.1038/sj.onc.1208079.
28. Parsons SJ, Parsons JT. Src family kinases, key regulators of signal transduction. Oncogene 2004;23(48):7906-9. (In eng). DOI: 10.1038/sj.onc.1208160.
29. Nika K, Soldani C, Salek M, et al. Constitutively active Lck kinase in T cells drives antigen receptor signal transduction. Immunity 2010;32(6):766-77. (In eng). DOI: 10.1016/j.immuni.2010.05.011.
30. Rossy J, Williamson DJ, Gaus K. How does the kinase Lck phosphorylate the T cell receptor? Spatial organization as a regulatory mechanism. Front Immunol 2012;3:167. (In eng). DOI: 10.3389/fimmu.2012.00167.
31. van Oers NS, Killeen N, Weiss A. Lck regulates the tyrosine phosphorylation of the T cell receptor subunits and ZAP-70 in murine thymocytes. J Exp Med 1996;183(3):1053-62. (In eng). DOI: 10.1084/jem.183.3.1053.
32. Chan AC, Dalton M, Johnson R, et al. Activation of ZAP-70 kinase activity by phosphorylation of tyrosine 493 is required for lymphocyte antigen receptor function. Embo j 1995;14(11):2499-508. (In eng). DOI: 10.1002/j.1460-2075.1995.tb07247.x.
33. Horkova V, Drobek A, Paprckova D, et al. Unique roles of co-receptor-bound LCK in helper and cytotoxic T cells. Nat Immunol 2023;24(1):174-185. (In eng). DOI: 10.1038/s41590-022-01366-0.
34. Horejsí V, Zhang W, Schraven B. Transmembrane adaptor proteins: organizers of immunoreceptor signalling. Nat Rev Immunol 2004;4(8):603-16. (In eng). DOI: 10.1038/nri1414.
35. Kalia V, Sarkar S. Regulation of Effector and Memory CD8 T Cell Differentiation by IL-2-A Balancing Act. Front Immunol 2018;9:2987. (In eng). DOI: 10.3389/fimmu.2018.02987.
36. Boyman O, Sprent J. The role of interleukin-2 during homeostasis and activation of the immune system. Nat Rev Immunol 2012;12(3):180-90. (In eng). DOI: 10.1038/nri3156.
37. Crabtree GR. Contingent genetic regulatory events in T lymphocyte activation. Science 1989;243(4889):355-61. (In eng). DOI: 10.1126/science.2783497.

38. Lin A, Minden A, Martinetto H, et al. Identification of a dual specificity kinase that activates the Jun kinases and p38-Mpk2. Science 1995;268(5208):286-90. (In eng). DOI: 10.1126/science.7716521.
39. Moriguchi T, Toyoshima F, Masuyama N, Hanafusa H, Gotoh Y, Nishida E. A novel SAPK/JNK kinase, MKK7, stimulated by TNFalpha and cellular stresses. Embo j 1997;16(23):7045-53. (In eng). DOI: 10.1093/emboj/16.23.7045.
40. Whitmarsh AJ, Davis RJ. Transcription factor AP-1 regulation by mitogen-activated protein kinase signal transduction pathways. J Mol Med (Berl) 1996;74(10):589-607. (In eng). DOI: 10.1007/s001090050063.
41. Ullman KS, Northrop JP, Admon A, Crabtree GR. Jun family members are controlled by a calcium-regulated, cyclosporin A-sensitive signaling pathway in activated T lymphocytes. Genes Dev 1993;7(2):188-96. (In eng). DOI: 10.1101/gad.7.2.188.
42. Su B, Jacinto E, Hibi M, Kallunki T, Karin M, Ben-Neriah Y. JNK is involved in signal integration during costimulation of T lymphocytes. Cell 1994;77(5):727-36. (In eng). DOI: 10.1016/0092-8674(94)90056-6.
43. Johansen KH, Golec DP, Thomsen JH, Schwartzberg PL, Okkenhaug K. PI3K in T Cell Adhesion and Trafficking. Front Immunol 2021;12:708908. (In eng). DOI: 10.3389/fimmu.2021.708908.
44. Mair I, Zandee SEJ, Toor IS, et al. A Context-Dependent Role for αv Integrins in Regulatory T Cell Accumulation at Sites of Inflammation. Front Immunol 2018;9:264. (In eng). DOI: 10.3389/fimmu.2018.00264.
45. Baekkevold ES, Yamanaka T, Palframan RT, et al. The CCR7 ligand elc (CCL19) is transcytosed in high endothelial venules and mediates T cell recruitment. J Exp Med 2001;193(9):1105-12. (In eng). DOI: 10.1084/jem.193.9.1105.
46. Bilanges B, Posor Y, Vanhaesebroeck B. PI3K isoforms in cell signalling and vesicle trafficking. Nat Rev Mol Cell Biol 2019;20(9):515-534. (In eng). DOI: 10.1038/s41580-019-0129-z.
47. Macian F. NFAT proteins: key regulators of T-cell development and function. Nat Rev Immunol 2005;5(6):472-84. (In eng). DOI: 10.1038/nri1632.
48. Aguado E, Arbulo-Echevarria MM. Slow phosphor-Y-LAT-ion for TCR ligand discrimination. Nat Immunol 2019;20(11):1420-1422. (In eng). DOI: 10.1038/s41590-019-0522-y.
49. Wülfing C, Sjaastad MD, Davis MM. Visualizing the dynamics of T cell activation: intracellular adhesion molecule 1 migrates rapidly to the T cell/B cell interface and acts to sustain calcium levels. Proc Natl Acad Sci U S A 1998;95(11):6302-7. (In eng). DOI: 10.1073/pnas.95.11.6302.
50. Zanoni I, Granucci F. Regulation and dysregulation of innate immunity by NFAT signaling downstream of pattern recognition receptors (PRRs). Eur J Immunol 2012;42(8):1924-31. (In eng). DOI: 10.1002/eji.201242580.
51. Mognol GP, Carneiro FR, Robbs BK, Faget DV, Viola JP. Cell cycle and apoptosis regulation by NFAT transcription factors: new roles for an old player. Cell Death Dis 2016;7(4):e2199. (In eng). DOI: 10.1038/cddis.2016.97.
52. Gilmore TD. NF-kappa B, KBF1, dorsal, and related matters. Cell 1990;62(5):841-3. (In eng). DOI: 10.1016/0092-8674(90)90257-f.
53. Gerondakis S, Fulford TS, Messina NL, Grumont RJ. NF-κB control of T cell development. Nat Immunol 2014;15(1):15-25. (In eng). DOI: 10.1038/ni.2785.
54. Lindstein T, June CH, Ledbetter JA, Stella G, Thompson CB. Regulation of lymphokine messenger RNA stability by a surface-mediated T cell activation pathway. Science 1989;244(4902):339-43. (In eng). DOI: 10.1126/science.2540528.
55. Fraser JD, Irving BA, Crabtree GR, Weiss A. Regulation of interleukin-2 gene enhancer activity by the T cell accessory molecule CD28. Science 1991;251(4991):313-6. (In eng). DOI: 10.1126/science.1846244.
56. Boomer JS, Green JM. An enigmatic tail of CD28 signaling. Cold Spring Harb Perspect Biol 2010;2(8):a002436. (In eng). DOI: 10.1101/cshperspect.a002436.

57. Prlic M, Williams MA, Bevan MJ. Requirements for CD8 T-cell priming, memory generation and maintenance. Curr Opin Immunol 2007;19(3):315-9. (In eng). DOI: 10.1016/j.coi.2007.04.010.
58. D'Cruz LM, Rubinstein MP, Goldrath AW. Surviving the crash: transitioning from effector to memory CD8+ T cell. Semin Immunol 2009;21(2):92-8. (In eng). DOI: 10.1016/j.smim.2009.02.002.
59. Collins DR, Urbach JM, Racenet ZJ, et al. Functional impairment of HIV-specific CD8(+) T cells precedes aborted spontaneous control of viremia. Immunity 2021;54(10):2372-2384.e7. (In eng). DOI: 10.1016/j.immuni.2021.08.007.
60. Guo L, Liu X, Su X. The role of TEMRA cell-mediated immune senescence in the development and treatment of HIV disease. Front Immunol 2023;14:1284293. (In eng). DOI: 10.3389/fimmu.2023.1284293.
61. Ahmed R, Bevan MJ, Reiner SL, Fearon DT. The precursors of memory: models and controversies. Nat Rev Immunol 2009;9(9):662-8. (In eng). DOI: 10.1038/nri2619.
62. Chang JT, Wherry EJ, Goldrath AW. Molecular regulation of effector and memory T cell differentiation. Nat Immunol 2014;15(12):1104-15. (In eng). DOI: 10.1038/ni.3031.
63. Jandus C, Usatorre AM, Viganò S, Zhang L, Romero P. The Vast Universe of T Cell Diversity: Subsets of Memory Cells and Their Differentiation. Methods Mol Biol 2017;1514:1-17. (In eng). DOI: 10.1007/978-1-4939-6548-9_1.
64. Gehad A, Teague JE, Matos TR, et al. A primary role for human central memory cells in tissue immunosurveillance. Blood Adv 2018;2(3):292-298. (In eng). DOI: 10.1182/bloodadvances.2017011346.
65. Pakpour N, Zaph C, Scott P. The central memory CD4+ T cell population generated during Leishmania major infection requires IL-12 to produce IFN-gamma. J Immunol 2008;180(12):8299-305. (In eng). DOI: 10.4049/jimmunol.180.12.8299.
66. Gray JI, Westerhof LM, MacLeod MKL. The roles of resident, central and effector memory CD4 T-cells in protective immunity following infection or vaccination. Immunology 2018;154(4):574-81. (In eng). DOI: 10.1111/imm.12929.
67. Hale JS, Youngblood B, Latner DR, et al. Distinct memory CD4+ T cells with commitment to T follicular helper- and T helper 1-cell lineages are generated after acute viral infection. Immunity 2013;38(4):805-17. (In eng). DOI: 10.1016/j.immuni.2013.02.020.
68. Farber DL, Yudanin NA, Restifo NP. Human memory T cells: generation, compartmentalization and homeostasis. Nat Rev Immunol 2014;14(1):24-35. (In eng). DOI: 10.1038/nri3567.
69. Mustelin T, Coggeshall KM, Altman A. Rapid activation of the T-cell tyrosine protein kinase pp56lck by the CD45 phosphotyrosine phosphatase. Proc Natl Acad Sci U S A 1989;86(16):6302-6. (In eng). DOI: 10.1073/pnas.86.16.6302.
70. ten Dam GB, Zilch CF, Wallace D, et al. Regulation of alternative splicing of CD45 by antagonistic effects of SR protein splicing factors. J Immunol 2000;164(10):5287-95. (In eng). DOI: 10.4049/jimmunol.164.10.5287.
71. Tian Y, Babor M, Lane J, et al. Unique phenotypes and clonal expansions of human CD4 effector memory T cells re-expressing CD45RA. Nat Commun 2017;8(1):1473. (In eng). DOI: 10.1038/s41467-017-01728-5.
72. Ladell K, Hellerstein MK, Cesar D, Busch R, Boban D, McCune JM. Central memory CD8+ T cells appear to have a shorter lifespan and reduced abundance as a function of HIV disease progression. J Immunol 2008;180(12):7907-18. (In eng). DOI: 10.4049/jimmunol.180.12.7907.
73. Geginat J, Lanzavecchia A, Sallusto F. Proliferation and differentiation potential of human CD8+ memory T-cell subsets in response to antigen or homeostatic cytokines. Blood 2003;101(11):4260-6. (In eng). DOI: 10.1182/blood-2002-11-3577.
74. Marsee DK, Pinkus GS, Yu H. CD71 (transferrin receptor): an effective marker for erythroid precursors in bone marrow biopsy specimens. Am J Clin Pathol 2010;134(3):429-35. (In eng). DOI: 10.1309/ajcpcrk3moaoj6at.

75. Schuurman HJ, van Wichen D, de Weger RA. Expression of activation antigens on thymocytes in the 'common thymocyte' stage of differentiation. Thymus 1989;14(1-3):43-53. (In eng).
76. Motamedi M, Xu L, Elahi S. Correlation of transferrin receptor (CD71) with Ki67 expression on stimulated human and mouse T cells: The kinetics of expression of T cell activation markers. J Immunol Methods 2016;437:43-52. (In eng). DOI: 10.1016/j.jim.2016.08.002.
77. Mohammed RN, Watson HA, Vigar M, et al. L-selectin Is Essential for Delivery of Activated CD8(+) T Cells to Virus-Infected Organs for Protective Immunity. Cell Rep 2016;14(4):760-771. (In eng). DOI: 10.1016/j.celrep.2015.12.090.
78. Watson HA, Durairaj RRP, Ohme J, et al. L-Selectin Enhanced T Cells Improve the Efficacy of Cancer Immunotherapy. Front Immunol 2019;10:1321. (In eng). DOI: 10.3389/fimmu.2019.01321.
79. Chao CC, Jensen R, Dailey MO. Mechanisms of L-selectin regulation by activated T cells. J Immunol 1997;159(4):1686-94. (In eng).
80. Berard M, Tough DF. Qualitative differences between naïve and memory T cells. Immunology 2002;106(2):127-38. (In eng). DOI: 10.1046/j.1365-2567.2002.01447.x.
81. Cibrián D, Sánchez-Madrid F. CD69: from activation marker to metabolic gatekeeper. Eur J Immunol 2017;47(6):946-953. (In eng). DOI: 10.1002/eji.201646837.
82. Vazquez BN, Laguna T, Carabana J, Krangel MS, Lauzurica P. CD69 gene is differentially regulated in T and B cells by evolutionarily conserved promoter-distal elements. J Immunol 2009;183(10):6513-21. (In eng). DOI: 10.4049/jimmunol.0900839.
83. Martín P, Gómez M, Lamana A, et al. The leukocyte activation antigen CD69 limits allergic asthma and skin contact hypersensitivity. J Allergy Clin Immunol 2010;126(2):355-65, 365.e1-3. (In eng). DOI: 10.1016/j.jaci.2010.05.010.
84. Toscano MA, Bianco GA, Ilarregui JM, et al. Differential glycosylation of TH1, TH2 and TH-17 effector cells selectively regulates susceptibility to cell death. Nat Immunol 2007;8(8):825-34. (In eng). DOI: 10.1038/ni1482.
85. Lin CR, Wei TY, Tsai HY, Wu YT, Wu PY, Chen ST. Glycosylation-dependent interaction between CD69 and S100A8/S100A9 complex is required for regulatory T-cell differentiation. Faseb j 2015;29(12):5006-17. (In eng). DOI: 10.1096/fj.15-273987.
86. Vignali DA, Collison LW, Workman CJ. How regulatory T cells work. Nat Rev Immunol 2008;8(7):523-32. (In eng). DOI: 10.1038/nri2343.
87. Yu L, Yang F, Zhang F, et al. CD69 enhances immunosuppressive function of regulatory T-cells and attenuates colitis by prompting IL-10 production. Cell Death Dis 2018;9(9):905. (In eng). DOI: 10.1038/s41419-018-0927-9.
88. Baeyens AAL, Schwab SR. Finding a Way Out: S1P Signaling and Immune Cell Migration. Annu Rev Immunol 2020;38:759-784. (In eng). DOI: 10.1146/annurev-immunol-081519-083952.
89. Hunter MC, Teijeira A, Halin C. T Cell Trafficking through Lymphatic Vessels. Front Immunol 2016;7:613. (In eng). DOI: 10.3389/fimmu.2016.00613.
90. Bankovich AJ, Shiow LR, Cyster JG. CD69 suppresses sphingosine 1-phosophate receptor-1 (S1P1) function through interaction with membrane helix 4. J Biol Chem 2010;285(29):22328-37. (In eng). DOI: 10.1074/jbc.M110.123299.
91. Shiow LR, Rosen DB, Brdicková N, et al. CD69 acts downstream of interferon-alpha/beta to inhibit S1P1 and lymphocyte egress from lymphoid organs. Nature 2006;440(7083):540-4. (In eng). DOI: 10.1038/nature04606.
92. Matloubian M, Lo CG, Cinamon G, et al. Lymphocyte egress from thymus and peripheral lymphoid organs is dependent on S1P receptor 1. Nature 2004;427(6972):355-60. (In eng). DOI: 10.1038/nature02284.
93. Pham TH, Okada T, Matloubian M, Lo CG, Cyster JG. S1P1 receptor signaling overrides retention mediated by G alpha i-coupled receptors to promote T cell egress. Immunity 2008;28(1):122-33. (In eng). DOI: 10.1016/j.immuni.2007.11.017.

94. Lambrecht BN, Pauwels RA, Fazekas De St Groth B. Induction of rapid T cell activation, division, and recirculation by intratracheal injection of dendritic cells in a TCR transgenic model. J Immunol 2000;164(6):2937-46. (In eng). DOI: 10.4049/jimmunol.164.6.2937.
95. Mosmann TR, Cherwinski H, Bond MW, Giedlin MA, Coffman RL. Two types of murine helper T cell clone. I. Definition according to profiles of lymphokine activities and secreted proteins. J Immunol 1986;136(7):2348-57. (In eng).
96. Annunziato F, Cosmi L, Liotta F, Maggi E, Romagnani S. Human Th1 dichotomy: origin, phenotype and biologic activities. Immunology 2014;144(3):343-51. (In eng).
97. Maggi L, Santarlasci V, Capone M, et al. Distinctive features of classic and nonclassic (Th17 derived) human Th1 cells. Eur J Immunol 2012;42(12):3180-8. (In eng). DOI: 10.1002/eji.201242648.
98. Ouyang W, Kolls JK, Zheng Y. The biological functions of T helper 17 cell effector cytokines in inflammation. Immunity 2008;28(4):454-67. (In eng). DOI: 10.1016/j.immuni.2008.03.004.
99. Desai BB, Quinn PM, Wolitzky AG, Mongini PK, Chizzonite R, Gately MK. IL-12 receptor. II. Distribution and regulation of receptor expression. J Immunol 1992;148(10):3125-32. (In eng).
100. Nakanishi K, Yoshimoto T, Tsutsui H, Okamura H. Interleukin-18 regulates both Th1 and Th2 responses. Annu Rev Immunol 2001;19:423-74. (In eng). DOI: 10.1146/annurev.immunol.19.1.423.
101. Parronchi P, De Carli M, Manetti R, et al. IL-4 and IFN (alpha and gamma) exert opposite regulatory effects on the development of cytolytic potential by Th1 or Th2 human T cell clones. J Immunol 1992;149(9):2977-83. (In eng).
102. Brombacher F, Kastelein RA, Alber G. Novel IL-12 family members shed light on the orchestration of Th1 responses. Trends Immunol 2003;24(4):207-12. (In eng). DOI: 10.1016/s1471-4906(03)00067-x.
103. Brogdon JL, Leitenberg D, Bottomly K. The potency of TCR signaling differentially regulates NFATc/p activity and early IL-4 transcription in naive CD4+ T cells. J Immunol 2002;168(8):3825-32. (In eng). DOI: 10.4049/jimmunol.168.8.3825.
104. Constant S, Pfeiffer C, Woodard A, Pasqualini T, Bottomly K. Extent of T cell receptor ligation can determine the functional differentiation of naive CD4+ T cells. J Exp Med 1995;182(5):1591-6. (In eng). DOI: 10.1084/jem.182.5.1591.
105. Presky DH, Minetti LJ, Gillessen S, et al. Analysis of the multiple interactions between IL-12 and the high affinity IL-12 receptor complex. J Immunol 1998;160(5):2174-9. (In eng).
106. van Panhuys N, Klauschen F, Germain RN. T-cell-receptor-dependent signal intensity dominantly controls CD4(+) T cell polarization In Vivo. Immunity 2014;41(1):63-74. (In eng). DOI: 10.1016/j.immuni.2014.06.003.
107. Walker JA, McKenzie ANJ. T(H)2 cell development and function. Nat Rev Immunol 2018;18(2):121-133. (In eng). DOI: 10.1038/nri.2017.118.
108. Langenhorst D, Haack S, Göb S, et al. CD28 Costimulation of T Helper 1 Cells Enhances Cytokine Release In Vivo. Front Immunol 2018;9:1060. (In eng). DOI: 10.3389/fimmu.2018.01060.
109. Aquino-López A, Senyukov VV, Vlasic Z, Kleinerman ES, Lee DA. Interferon Gamma Induces Changes in Natural Killer (NK) Cell Ligand Expression and Alters NK Cell-Mediated Lysis of Pediatric Cancer Cell Lines. Front Immunol 2017;8:391. (In eng). DOI: 10.3389/fimmu.2017.00391.
110. Luo P, Wang P, Xu J, et al. Immunomodulatory role of T helper cells in rheumatoid arthritis : a comprehensive research review. Bone Joint Res 2022;11(7):426-438. (In eng).
111. Romagnani S. Th1/Th2 cells. Inflamm Bowel Dis 1999;5(4):285-94. (In eng). DOI: 10.1097/00054725-199911000-00009.
112. Webb GJ, Hirschfield GM, Lane PJ. OX40, OX40L and Autoimmunity: a Comprehensive Review. Clin Rev Allergy Immunol 2016;50(3):312-32. (In eng). DOI: 10.1007/s12016-015-8498-3.

113. Kim S, Prout M, Ramshaw H, Lopez AF, LeGros G, Min B. Cutting edge: basophils are transiently recruited into the draining lymph nodes during helminth infection via IL-3, but infection-induced Th2 immunity can develop without basophil lymph node recruitment or IL-3. J Immunol 2010;184(3):1143-7. (In eng). DOI: 10.4049/jimmunol.0902447.
114. Van Dyken SJ, Nussbaum JC, Lee J, et al. A tissue checkpoint regulates type 2 immunity. Nat Immunol 2016;17(12):1381-1387. (In eng). DOI: 10.1038/ni.3582.
115. Bao K, Reinhardt RL. The differential expression of IL-4 and IL-13 and its impact on type-2 immunity. Cytokine 2015;75(1):25-37. (In eng). DOI: 10.1016/j.cyto.2015.05.008.
116. Chen F, Liu Z, Wu W, et al. An essential role for TH2-type responses in limiting acute tissue damage during experimental helminth infection. Nat Med 2012;18(2):260-6. (In eng). DOI: 10.1038/nm.2628.
117. Zheng WP, Flavell RA. Pillars Article: The Transcription Factor GATA-3 Is Necessary and Sufficient for Th2 Cytokine Gene Expression in CD4 T Cells. Cell. 1997. 89: 587-596. J Immunol 2016;196(11):4426-35. (In eng).
118. Zhu J, Yamane H, Cote-Sierra J, Guo L, Paul WE. GATA-3 promotes Th2 responses through three different mechanisms: induction of Th2 cytokine production, selective growth of Th2 cells and inhibition of Th1 cell-specific factors. Cell Res 2006;16(1):3-10. (In eng). DOI: 10.1038/sj.cr.7310002.
119. Cote-Sierra J, Foucras G, Guo L, et al. Interleukin 2 plays a central role in Th2 differentiation. Proc Natl Acad Sci U S A 2004;101(11):3880-5. (In eng). DOI: 10.1073/pnas.0400339101.
120. Hammad H, Lambrecht BN. The basic immunology of asthma. Cell 2021;184(6):1469-1485. DOI: 10.1016/j.cell.2021.02.016.
121. Le Floc'H A, Allinne J, Nagashima K, et al. Dual blockade of IL-4 and IL-13 with dupilumab, an IL-4Rα antibody, is required to broadly inhibit type 2 inflammation. Allergy 2020;75(5):1188-1204. DOI: 10.1111/all.14151.
122. Nemeth ZH, Bogdanovski DA, Barratt-Stopper P, Paglinco SR, Antonioli L, Rolandelli RH. Crohn's Disease and Ulcerative Colitis Show Unique Cytokine Profiles. Cureus 2017;9(4):e1177. (In eng). DOI: 10.7759/cureus.1177.
123. Mostafa DHD, Hemshekhar M, Piyadasa H, et al. Characterization of sex-related differences in allergen house dust mite-challenged airway inflammation, in two different strains of mice. Sci Rep 2022;12(1):20837. (In eng).
124. Heller F, Florian P, Bojarski C, et al. Interleukin-13 is the key effector Th2 cytokine in ulcerative colitis that affects epithelial tight junctions, apoptosis, and cell restitution. Gastroenterology 2005;129(2):550-64. (In eng). DOI: 10.1016/j.gastro.2005.05.002.
125. Cullen SP, Martin SJ. Mechanisms of granule-dependent killing. Cell Death Differ 2008;15(2):251-62. (In eng). DOI: 10.1038/sj.cdd.4402244.
126. Motyka B, Korbutt G, Pinkoski MJ, et al. Mannose 6-phosphate/insulin-like growth factor II receptor is a death receptor for granzyme B during cytotoxic T cell-induced apoptosis. Cell 2000;103(3):491-500. (In eng). DOI: 10.1016/s0092-8674(00)00140-9.
127. Waring P, Müllbacher A. Cell death induced by the Fas/Fas ligand pathway and its role in pathology. Immunol Cell Biol 1999;77(4):312-7. (In eng). DOI: 10.1046/j.1440-1711.1999.00837.x.
128. de Weerd NA, Nguyen T. The interferons and their receptors—distribution and regulation. Immunology & Cell Biology 2012;90(5):483-491. DOI: https://doi.org/10.1038/icb.2012.9.
129. Broggi A, Granucci F, Zanoni I. Type III interferons: Balancing tissue tolerance and resistance to pathogen invasion. J Exp Med 2020;217(1) (In eng). DOI: 10.1084/jem.20190295.
130. Sommereyns C, Paul S, Staeheli P, Michiels T. IFN-lambda (IFN-lambda) is expressed in a tissue-dependent fashion and primarily acts on epithelial cells in vivo. PLoS Pathog 2008;4(3):e1000017. (In eng). DOI: 10.1371/journal.ppat.1000017.

131. Kotenko SV, Gallagher G, Baurin VV, et al. IFN-lambdas mediate antiviral protection through a distinct class II cytokine receptor complex. Nat Immunol 2003;4(1):69-77. (In eng). DOI: 10.1038/ni875.
132. Sheppard P, Kindsvogel W, Xu W, et al. IL-28, IL-29 and their class II cytokine receptor IL-28R. Nat Immunol 2003;4(1):63-8. (In eng). DOI: 10.1038/ni873.
133. Manivasagam S, Klein RS. Type III Interferons: Emerging Roles in Autoimmunity. Front Immunol 2021;12:764062. (In eng). DOI: 10.3389/fimmu.2021.764062.
134. Hamming OJ, Terczyńska-Dyla E, Vieyres G, et al. Interferon lambda 4 signals via the IFNλ receptor to regulate antiviral activity against HCV and coronaviruses. Embo j 2013;32(23):3055-65. (In eng). DOI: 10.1038/emboj.2013.232.
135. Prokunina-Olsson L, Muchmore B, Tang W, et al. A variant upstream of IFNL3 (IL28B) creating a new interferon gene IFNL4 is associated with impaired clearance of hepatitis C virus. Nat Genet 2013;45(2):164-71. DOI: 10.1038/ng.2521.
136. Lazear HM, Nice TJ, Diamond MS. Interferon-λ: Immune Functions at Barrier Surfaces and Beyond. Immunity 2015;43(1):15-28. (In eng). DOI: 10.1016/j.immuni.2015.07.001.
137. Kotenko SV, Rivera A, Parker D, Durbin JE. Type III IFNs: Beyond antiviral protection. Semin Immunol 2019;43:101303. (In eng). DOI: 10.1016/j.smim.2019.101303.
138. Stanifer ML, Guo C, Doldan P, Boulant S. Importance of Type I and III Interferons at Respiratory and Intestinal Barrier Surfaces. Front Immunol 2020;11:608645. (In eng). DOI: 10.3389/fimmu.2020.608645.
139. Miner JJ, Platt DJ, Ghaznavi CM, et al. HSV-1 and Zika Virus but Not SARS-CoV-2 Replicate in the Human Cornea and Are Restricted by Corneal Type III Interferon. Cell Rep 2020;33(5):108339. (In eng). DOI: 10.1016/j.celrep.2020.108339.
140. Lazear HM, Daniels BP, Pinto AK, et al. Interferon-λ restricts West Nile virus neuroinvasion by tightening the blood-brain barrier. Sci Transl Med 2015;7(284):284ra59. (In eng). DOI: 10.1126/scitranslmed.aaa4304.
141. Santer DM, Minty GES, Golec DP, et al. Differential expression of interferon-lambda receptor 1 splice variants determines the magnitude of the antiviral response induced by interferon-lambda 3 in human immune cells. PLoS Pathog 2020;16(4):e1008515. (In eng). DOI: 10.1371/journal.ppat.1008515.
142. Nice TJ, Baldridge MT, McCune BT, et al. Interferon-λ cures persistent murine norovirus infection in the absence of adaptive immunity. Science 2015;347(6219):269-73. (In eng). DOI: 10.1126/science.1258100.
143. Santer DM, Li D, Ghosheh Y, et al. Interferon-λ treatment accelerates SARS-CoV-2 clearance despite age-related delays in the induction of T cell immunity. Nat Commun 2022;13(1):6992. (In eng). DOI: 10.1038/s41467-022-34709-4.
144. Phillips S, Mistry S, Riva A, et al. Peg-Interferon Lambda Treatment Induces Robust Innate and Adaptive Immunity in Chronic Hepatitis B Patients. Front Immunol 2017;8:621. (In eng). DOI: 10.3389/fimmu.2017.00621.
145. Hou W, Wang X, Ye L, et al. Lambda interferon inhibits human immunodeficiency virus type 1 infection of macrophages. J Virol 2009;83(8):3834-42. (In eng). DOI: 10.1128/jvi.01773-08.
146. Bierne H, Travier L, Mahlakõiv T, et al. Activation of type III interferon genes by pathogenic bacteria in infected epithelial cells and mouse placenta. PLoS One 2012;7(6):e39080. (In eng). DOI: 10.1371/journal.pone.0039080.
147. Cohen TS, Prince AS. Bacterial pathogens activate a common inflammatory pathway through IFNλ regulation of PDCD4. PLoS Pathog 2013;9(10):e1003682. (In eng). DOI: 10.1371/journal.ppat.1003682.
148. Love AC, Schwartz I, Petzke MM. Borrelia burgdorferi RNA induces type I and III interferons via Toll-like receptor 7 and contributes to production of NF-κB-dependent cytokines. Infect Immun 2014;82(6):2405-16. (In eng). DOI: 10.1128/iai.01617-14.

149. Pietilä TE, Latvala S, Osterlund P, Julkunen I. Inhibition of dynamin-dependent endocytosis interferes with type III IFN expression in bacteria-infected human monocyte-derived DCs. J Leukoc Biol 2010;88(4):665-74. (In eng). DOI: 10.1189/jlb.1009651.
150. Odendall C, Voak AA, Kagan JC. Type III IFNs Are Commonly Induced by Bacteria-Sensing TLRs and Reinforce Epithelial Barriers during Infection. J Immunol 2017;199(9):3270-3279. DOI: 10.4049/jimmunol.1700250.
151. Pires S, Parker D. IL-1β activation in response to Staphylococcus aureus lung infection requires inflammasome-dependent and independent mechanisms. Eur J Immunol 2018;48(10):1707-1716. (In eng). DOI: 10.1002/eji.201847556.
152. Ahn D, Wickersham M, Riquelme S, Prince A. The Effects of IFN-λ on Epithelial Barrier Function Contribute to Klebsiella pneumoniae ST258 Pneumonia. Am J Respir Cell Mol Biol 2019;60(2):158-166. (In eng). DOI: 10.1165/rcmb.2018-0021OC.
153. Espinosa V, Dutta O, McElrath C, et al. Type III interferon is a critical regulator of innate antifungal immunity. Sci Immunol 2017;2(16). DOI: 10.1126/sciimmunol.aan5357.
154. Barnas JL, Albrecht J, Meednu N, et al. B Cell Activation and Plasma Cell Differentiation Are Promoted by IFN-λ in Systemic Lupus Erythematosus. J Immunol 2021;207(11):2660-2672. (In eng). DOI: 10.4049/jimmunol.2100339.
155. Oke V, Brauner S, Larsson A, et al. IFN-λ1 with Th17 axis cytokines and IFN-α define different subsets in systemic lupus erythematosus (SLE). Arthritis Res Ther 2017;19(1):139. (In eng). DOI: 10.1186/s13075-017-1344-7.
156. Goel RR, Wang X, O'Neil LJ, et al. Interferon lambda promotes immune dysregulation and tissue inflammation in TLR7-induced lupus. Proc Natl Acad Sci U S A 2020;117(10):5409-5419. (In eng). DOI: 10.1073/pnas.1916897117.
157. Mendoza JL, Schneider WM, Hoffmann HH, et al. The IFN-λ-IFN-λR1-IL-10Rβ Complex Reveals Structural Features Underlying Type III IFN Functional Plasticity. Immunity 2017;46(3):379-392. (In eng). DOI: 10.1016/j.immuni.2017.02.017.
158. Le Bon A, Schiavoni G, D'Agostino G, Gresser I, Belardelli F, Tough DF. Type i interferons potently enhance humoral immunity and can promote isotype switching by stimulating dendritic cells in vivo. Immunity 2001;14(4):461-70. (In eng). DOI: 10.1016/s1074-7613(01)00126-1.
159. Kotenko SV, Langer JA. Full house: 12 receptors for 27 cytokines. Int Immunopharmacol 2004;4(5):593-608. (In eng). DOI: 10.1016/j.intimp.2004.01.003.
160. Lasfar A, Abushahba W, Balan M, Cohen-Solal KA. Interferon lambda: a new sword in cancer immunotherapy. Clin Dev Immunol 2011;2011:349575. (In eng). DOI: 10.1155/2011/349575.
161. Coto-Llerena M, Lepore M, Spagnuolo J, et al. Interferon lambda 4 can directly activate human CD19(+) B cells and CD8(+) T cells. Life Sci Alliance 2021;4(1) (In eng). DOI: 10.26508/lsa.201900612.
162. Ouyang W, Rutz S, Crellin NK, Valdez PA, Hymowitz SG. Regulation and functions of the IL-10 family of cytokines in inflammation and disease. Annu Rev Immunol 2011;29:71-109. (In eng). DOI: 10.1146/annurev-immunol-031210-101312.
163. Jordan WJ, Eskdale J, Boniotto M, Rodia M, Kellner D, Gallagher G. Modulation of the human cytokine response by interferon lambda-1 (IFN-lambda1/IL-29). Genes Immun 2007;8(1):13-20. (In eng). DOI: 10.1038/sj.gene.6364348.
164. Hernández PP, Mahlakoiv T, Yang I, et al. Interferon-λ and interleukin 22 act synergistically for the induction of interferon-stimulated genes and control of rotavirus infection. Nat Immunol 2015;16(7):698-707. (In eng). DOI: 10.1038/ni.3180.
165. Misumi I, Whitmire JK. IFN-λ exerts opposing effects on T cell responses depending on the chronicity of the virus infection. J Immunol 2014;192(8):3596-606. (In eng). DOI: 10.4049/jimmunol.1301705.
166. Lin JD, Feng N, Sen A, et al. Distinct Roles of Type I and Type III Interferons in Intestinal Immunity to Homologous and Heterologous Rotavirus Infections. PLoS Pathog 2016;12(4):e1005600. (In eng). DOI: 10.1371/journal.ppat.1005600.

167. Mahlakõiv T, Hernandez P, Gronke K, Diefenbach A, Staeheli P. Leukocyte-derived IFN-α/β and epithelial IFN-λ constitute a compartmentalized mucosal defense system that restricts enteric virus infections. PLoS Pathog 2015;11(4):e1004782. (In eng). DOI: 10.1371/journal.ppat.1004782.
168. Galani IE, Triantafyllia V, Eleminiadou EE, et al. Interferon-λ Mediates Non-redundant Front-Line Antiviral Protection against Influenza Virus Infection without Compromising Host Fitness. Immunity 2017;46(5):875-890.e6. (In eng). DOI: 10.1016/j.immuni.2017.04.025.
169. Broggi A, Tan Y, Granucci F, Zanoni I. IFN-λ suppresses intestinal inflammation by non-translational regulation of neutrophil function. Nat Immunol 2017;18(10):1084-1093. (In eng). DOI: 10.1038/ni.3821.
170. Hemann EA, Gale M, Jr., Savan R. Interferon Lambda Genetics and Biology in Regulation of Viral Control. Front Immunol 2017;8:1707. (In eng). DOI: 10.3389/fimmu.2017.01707.
171. Ank N, West H, Bartholdy C, Eriksson K, Thomsen AR, Paludan SR. Lambda interferon (IFN-lambda), a type III IFN, is induced by viruses and IFNs and displays potent antiviral activity against select virus infections in vivo. J Virol 2006;80(9):4501-9. (In eng). DOI: 10.1128/jvi.80.9.4501-4509.2006.
172. Ank N, Iversen MB, Bartholdy C, et al. An important role for type III interferon (IFN-lambda/IL-28) in TLR-induced antiviral activity. J Immunol 2008;180(4):2474-85. (In eng). DOI: 10.4049/jimmunol.180.4.2474.
173. Lasfar A, Lewis-Antes A, Smirnov SV, et al. Characterization of the mouse IFN-lambda ligand-receptor system: IFN-lambdas exhibit antitumor activity against B16 melanoma. Cancer Res 2006;66(8):4468-77. (In eng). DOI: 10.1158/0008-5472.Can-05-3653.
174. Megjugorac NJ, Gallagher GE, Gallagher G. Modulation of human plasmacytoid DC function by IFN-lambda1 (IL-29). J Leukoc Biol 2009;86(6):1359-63. (In eng). DOI: 10.1189/jlb.0509347.
175. Dai J, Megjugorac NJ, Gallagher GE, Yu RY, Gallagher G. IFN-lambda1 (IL-29) inhibits GATA3 expression and suppresses Th2 responses in human naive and memory T cells. Blood 2009;113(23):5829-38. (In eng). DOI: 10.1182/blood-2008-09-179507.
176. Stanifer ML, Pervolaraki K, Boulant S. Differential Regulation of Type I and Type III Interferon Signaling. Int J Mol Sci 2019;20(6) (In eng). DOI: 10.3390/ijms20061445.
177. Fuchs S, Kaiser-Labusch P, Bank J, et al. Tyrosine kinase 2 is not limiting human antiviral type III interferon responses. Eur J Immunol 2016;46(11):2639-2649. (In eng). DOI: 10.1002/eji.201646519.
178. Pervolaraki K, Stanifer ML, Münchau S, et al. Type I and Type III Interferons Display Different Dependency on Mitogen-Activated Protein Kinases to Mount an Antiviral State in the Human Gut. Front Immunol 2017;8:459. (In eng).
179. Zhou Z, Hamming OJ, Ank N, Paludan SR, Nielsen AL, Hartmann R. Type III interferon (IFN) induces a type I IFN-like response in a restricted subset of cells through signaling pathways involving both the Jak-STAT pathway and the mitogen-activated protein kinases. J Virol 2007;81(14):7749-58. (In eng).
180. Brand S, Beigel F, Olszak T, et al. IL-28A and IL-29 mediate antiproliferative and antiviral signals in intestinal epithelial cells and murine CMV infection increases colonic IL-28A expression. Am J Physiol Gastrointest Liver Physiol 2005;289(5):G960-8. (In eng). DOI: 10.1152/ajpgi.00126.2005.
181. Alase AA, El-Sherbiny YM, Vital EM, Tobin DJ, Turner NA, Wittmann M. IFNλ Stimulates MxA Production in Human Dermal Fibroblasts via a MAPK-Dependent STAT1-Independent Mechanism. J Invest Dermatol 2015;135(12):2935-2943. (In eng). DOI: 10.1038/jid.2015.317.
182. Lambrecht BN, Hammad H, Fahy JV. The Cytokines of Asthma. Immunity 2019;50(4):975-991. (In eng). DOI: 10.1016/j.immuni.2019.03.018.
183. Jordan WJ, Eskdale J, Srinivas S, et al. Human interferon lambda-1 (IFN-lambda1/IL-29) modulates the Th1/Th2 response. Genes Immun 2007;8(3):254-61. (In eng). DOI: 10.1038/sj.gene.6364382.

184. Koltsida O, Hausding M, Stavropoulos A, et al. IL-28A (IFN-λ2) modulates lung DC function to promote Th1 immune skewing and suppress allergic airway disease. EMBO Mol Med 2011;3(6):348-61. (In eng). DOI: 10.1002/emmm.201100142.
185. Li Y, Gao Q, Yuan X, et al. Adenovirus expressing IFN-λ1 (IL-29) attenuates allergic airway inflammation and airway hyperreactivity in experimental asthma. Int Immunopharmacol 2014;21(1):156-62. (In eng). DOI: 10.1016/j.intimp.2014.04.022.
186. Won J, Gil CH, Jo A, Kim HJ. Inhaled delivery of Interferon-lambda restricts epithelial-derived Th2 inflammation in allergic asthma. Cytokine 2019;119:32-36. (In eng). DOI: 10.1016/j.cyto.2019.02.010.
187. Won J, Jo A, Gil CH, Kim S, Shin H, Jik Kim H. Inhaled delivery of recombinant interferon-lambda restores allergic inflammation after development of asthma by controlling Th2- and Th17-cell-mediated immune responses. Int Immunopharmacol 2022;112:109180. (In eng). DOI: 10.1016/j.intimp.2022.109180.
188. Yan B, Chen F, Xu L, Wang Y, Wang X. Interleukin-28B dampens airway inflammation through up-regulation of natural killer cell-derived IFN-γ. Sci Rep 2017;7(1):3556. (In eng). DOI: 10.1038/s41598-017-03856-w.
189. Yan B, Gao J, Guo J, Yang D, Li D. Interleukin-28B dampens protease-induced lung inflammation via IL-25 and TSLP inhibition in epithelial cells. Sci Rep 2020;10(1):20973. (In eng). DOI: 10.1038/s41598-020-77844-y.
190. Mennechet FJ, Uzé G. Interferon-lambda-treated dendritic cells specifically induce proliferation of FOXP3-expressing suppressor T cells. Blood 2006;107(11):4417-23. (In eng). DOI: 10.1182/blood-2005-10-4129.
191. Egli A, Santer DM, O'Shea D, et al. IL-28B is a key regulator of B- and T-cell vaccine responses against influenza. PLoS Pathog 2014;10(12):e1004556. (In eng). DOI: 10.1371/journal.ppat.1004556.
192. Syedbasha M, Bonfiglio F, Linnik J, Stuehler C, Wüthrich D, Egli A. Interferon-λ Enhances the Differentiation of Naive B Cells into Plasmablasts via the mTORC1 Pathway. Cell Rep 2020;33(1):108211. (In eng). DOI: 10.1016/j.celrep.2020.108211.
193. de Groen RA, Groothuismink ZM, Liu BS, Boonstra A. IFN-λ is able to augment TLR-mediated activation and subsequent function of primary human B cells. J Leukoc Biol 2015;98(4):623-30. (In eng). DOI: 10.1189/jlb.3A0215-041RR.
194. de Groen RA, Boltjes A, Hou J, et al. IFN-λ-mediated IL-12 production in macrophages induces IFN-γ production in human NK cells. Eur J Immunol 2015;45(1):250-9. (In eng). DOI: 10.1002/eji.201444903.
195. Blazek K, Eames HL, Weiss M, et al. IFN-λ resolves inflammation via suppression of neutrophil infiltration and IL-1β production. J Exp Med 2015;212(6):845-53. (In eng). DOI: 10.1084/jem.20140995.
196. Santer DM, Minty GES, Mohamed A, et al. A novel method for detection of IFN-lambda 3 binding to cells for quantifying IFN-lambda receptor expression. J Immunol Methods 2017;445:15-22. (In eng). DOI: 10.1016/j.jim.2017.03.001.
197. de Weerd NA, Ogungbola O, Liu X, et al. Characterization of Monoclonal Antibodies to Measure Cell Surface Protein Levels of Human Interferon-Lambda Receptor 1. J Interferon Cytokine Res 2023 (In eng). DOI: 10.1089/jir.2023.0040.
198. Huang K, Liang Q, Zhou Y, et al. A Novel Allosteric Inhibitor of Phosphoglycerate Mutase 1 Suppresses Growth and Metastasis of Non-Small-Cell Lung Cancer. Cell Metab 2019;30(6):1107-1119.e8. (In eng). DOI: 10.1016/j.cmet.2019.09.014.
199. Funk CR, Wang S, Chen KZ, et al. PI3Kδ/γ inhibition promotes human CART cell epigenetic and metabolic reprogramming to enhance antitumor cytotoxicity. Blood 2022;139(4):523-537. (In eng). DOI: 10.1182/blood.2021011597.

200. Poli V, Di Gioia M, Sola-Visner M, et al. Inhibition of transcription factor NFAT activity in activated platelets enhances their aggregation and exacerbates gram-negative bacterial septicemia. Immunity 2022;55(2):224-236 e5. (In eng). DOI: 10.1016/j.immuni.2021.12.002.
201. Kim B, Kim HY, Lee WW. Zap70 Regulates TCR-Mediated Zip6 Activation at the Immunological Synapse. Front Immunol 2021;12:687367. (In eng). DOI: 10.3389/fimmu.2021.687367.
202. Thomson AW, Bonham CA, Zeevi A. Mode of action of tacrolimus (FK506): molecular and cellular mechanisms. Ther Drug Monit 1995;17(6):584-91. (In eng). DOI: 10.1097/00007691-199512000-00007.
203. He SH, Chen X, Song CH, et al. Interferon-λ mediates oral tolerance and inhibits antigen-specific, T-helper 2 cell-mediated inflammation in mouse intestine. Gastroenterology 2011;141(1):249-58, 258.e1-2. (In eng). DOI: 10.1053/j.gastro.2011.04.006.
204. Rael EL, Lockey RF. Interleukin-13 signaling and its role in asthma. World Allergy Organ J 2011;4(3):54-64. (In eng). DOI: 10.1097/WOX.0b013e31821188e0.
205. Annunziato F, Maggi L. Strategies for T Helper Cell Subset Differentiation from Naïve Precursors. Methods Mol Biol 2017;1514:127-137. (In eng). DOI: 10.1007/978-1-4939-6548-9_11.
206. Huber JP, Ramos HJ, Gill MA, Farrar JD. Cutting edge: Type I IFN reverses human Th2 commitment and stability by suppressing GATA3. J Immunol 2010;185(2):813-7. (In eng). DOI: 10.4049/jimmunol.1000469.
207. Sen P, Andrabi SBA, Buchacher T, et al. Quantitative genome-scale metabolic modeling of human CD4(+) T cell differentiation reveals subset-specific regulation of glycosphingolipid pathways. Cell Rep 2021;37(6):109973. (In eng). DOI: 10.1016/j.celrep.2021.109973.
208. Hawkins RD, Larjo A, Tripathi SK, et al. Global chromatin state analysis reveals lineage-specific enhancers during the initiation of human T helper 1 and T helper 2 cell polarization. Immunity 2013;38(6):1271-84. (In eng). DOI: 10.1016/j.immuni.2013.05.011.
209. Elo LL, Järvenpää H, Tuomela S, et al. Genome-wide profiling of interleukin-4 and STAT6 transcription factor regulation of human Th2 cell programming. Immunity 2010;32(6):852-62. (In eng). DOI: 10.1016/j.immuni.2010.06.011.
210. Blom L, Poulsen LK. In vitro Th1 and Th2 cell polarization is severely influenced by the initial ratio of naïve and memory CD4+ T cells. J Immunol Methods 2013;397(1-2):55-60. (In eng). DOI: 10.1016/j.jim.2013.08.008.
211. Rich HE, Antos D, Melton NR, Alcorn JF, Manni ML. Insights Into Type I and III Interferons in Asthma and Exacerbations. Front Immunol 2020;11:574027. (In eng). DOI: 10.3389/fimmu.2020.574027.
212. Ivashkiv LB. IFNγ: signalling, epigenetics and roles in immunity, metabolism, disease and cancer immunotherapy. Nat Rev Immunol 2018;18(9):545-558. (In eng). DOI: 10.1038/s41577-018-0029-z.
213. Schmiedel BJ, Singh D, Madrigal A, et al. Impact of Genetic Polymorphisms on Human Immune Cell Gene Expression. Cell 2018;175(6):1701-1715.e16. (In eng). DOI: 10.1016/j.cell.2018.10.022.
214. Farber DL. Biochemical signaling pathways for memory T cell recall. Semin Immunol 2009;21(2):84-91. (In eng). DOI: 10.1016/j.smim.2009.02.003.
215. Maecker HT, McCoy JP, Nussenblatt R. Standardizing immunophenotyping for the Human Immunology Project. Nat Rev Immunol 2012;12(3):191-200. (In eng). DOI: 10.1038/nri3158.
216. Pulko V, Davies JS, Martinez C, et al. Human memory T cells with a naive phenotype accumulate with aging and respond to persistent viruses. Nat Immunol 2016;17(8):966-75. (In eng). DOI: 10.1038/ni.3483.
217. Newman DK, Fu G, McOlash L, et al. Frontline Science: PECAM-1 (CD31) expression in naïve and memory, but not acutely activated, CD8(+) T cells. J Leukoc Biol 2018;104(5):883-893. (In eng).

218. Glinos DA, Soskic B, Williams C, et al. Genomic profiling of T-cell activation suggests increased sensitivity of memory T cells to CD28 costimulation. Genes Immun 2020;21(6-8):390-408. (In eng). DOI: 10.1038/s41435-020-00118-0.
219. Tu WJ, Hardy K, Sutton CR, et al. Priming of transcriptional memory responses via the chromatin accessibility landscape in T cells. Sci Rep 2017;7:44825. (In eng). DOI: 10.1038/srep44825.
220. Arthur SE, Sorgeloos F, Hosmillo M, Goodfellow IG. Epigenetic Suppression of Interferon Lambda Receptor Expression Leads to Enhanced Human Norovirus Replication In Vitro. mBio 2019;10(5) (In eng). DOI: 10.1128/mBio.02155-19.
221. Ding S, Khoury-Hanold W, Iwasaki A, Robek MD. Epigenetic reprogramming of the type III interferon response potentiates antiviral activity and suppresses tumor growth. PLoS Biol 2014;12(1):e1001758. (In eng). DOI: 10.1371/journal.pbio.1001758.
222. Xie MH, Aggarwal S, Ho WH, et al. Interleukin (IL)-22, a novel human cytokine that signals through the interferon receptor-related proteins CRF2-4 and IL-22R. J Biol Chem 2000;275(40):31335-9. (In eng). DOI: 10.1074/jbc.M005304200.
223. Kotenko SV, Izotova LS, Mirochnitchenko OV, et al. Identification of the functional interleukin-22 (IL-22) receptor complex: the IL-10R2 chain (IL-10Rbeta) is a common chain of both the IL-10 and IL-22 (IL-10-related T cell-derived inducible factor, IL-TIF) receptor complexes. J Biol Chem 2001;276(4):2725-32. (In eng). DOI: 10.1074/jbc.M007837200.
224. Sheikh F, Baurin VV, Lewis-Antes A, et al. Cutting edge: IL-26 signals through a novel receptor complex composed of IL-20 receptor 1 and IL-10 receptor 2. J Immunol 2004;172(4):2006-10. (In eng). DOI: 10.4049/jimmunol.172.4.2006.
225. Zanin N, Viaris de Lesegno C, Lamaze C, Blouin CM. Interferon Receptor Trafficking and Signaling: Journey to the Cross Roads. Front Immunol 2020;11:615603. (In eng). DOI: 10.3389/fimmu.2020.615603.
226. Kotenko SV, Krause CD, Izotova LS, Pollack BP, Wu W, Pestka S. Identification and functional characterization of a second chain of the interleukin-10 receptor complex. Embo j 1997;16(19):5894-903. (In eng). DOI: 10.1093/emboj/16.19.5894.
227. Saraiva M, O'Garra A. The regulation of IL-10 production by immune cells. Nat Rev Immunol 2010;10(3):170-81. (In eng). DOI: 10.1038/nri2711.
228. Ren F, Chen X, Hesketh J, Gan F, Huang K. Selenium promotes T-cell response to TCR-stimulation and ConA, but not PHA in primary porcine splenocytes. PLoS One 2012;7(4):e35375. (In eng). DOI: 10.1371/journal.pone.0035375.
229. Won J, Jo A, Kim S, Shin H, Kim HJ. Distinct dampening of IL-33 following inhalation of interferon-lambda in the respiratory epithelium of in vivo asthma. Allergy 2024 (In eng). DOI: 10.1111/all.16010.
230. Wynn TA. IL-13 effector functions. Annu Rev Immunol 2003;21:425-56. (In eng). DOI: 10.1146/annurev.immunol.21.120601.141142.
231. McKenzie AN, Li X, Largaespada DA, et al. Structural comparison and chromosomal localization of the human and mouse IL-13 genes. J Immunol 1993;150(12):5436-44. (In eng).
232. Reis G, Moreira Silva EAS, Medeiros Silva DC, et al. Early Treatment with Pegylated Interferon Lambda for Covid-19. N Engl J Med 2023;388(6):518-528. (In eng). DOI: 10.1056/NEJMoa2209760.
233. Crouse J, Kalinke U, Oxenius A. Regulation of antiviral T cell responses by type I interferons. Nat Rev Immunol 2015;15(4):231-42. (In eng). DOI: 10.1038/nri3806.
234. Trandem K, Zhao J, Fleming E, Perlman S. Highly activated cytotoxic CD8 T cells express protective IL-10 at the peak of coronavirus-induced encephalitis. J Immunol 2011;186(6):3642-52. (In eng). DOI: 10.4049/jimmunol.1003292.
235. Monaco G, Lee B, Xu W, et al. RNA-Seq Signatures Normalized by mRNA Abundance Allow Absolute Deconvolution of Human Immune Cell Types. Cell Rep 2019;26(6):1627-1640.e7. (In eng). DOI: 10.1016/j.celrep.2019.01.041.

236. Kavrochorianou N, Evangelidou M, Markogiannaki M, Tovey M, Thyphronitis G, Haralambous S. IFNAR signaling directly modulates T lymphocyte activity, resulting in milder experimental autoimmune encephalomyelitis development. J Leukoc Biol 2016;99(1):175-88. (In eng). DOI: 10.1189/jlb.3A1214-598R.